

Editor-in-Chief B.E.Paton

Editorial board:

Yu.S.Borisov	V.F.Khorunov
A.Ya.Ishchenko	I.V.Krivtsun
B.V.Khitrovskaya	L.M.Lobanov
V.I.Kyrian	A.A.Mazur
S.I.Kuchuk	Yatsenko
Yu.N.Lankin	I.K.Pokhodnya
V.N.Lipodaev	V.D.Poznyakov
V.I.Makhnenko	K.A.Yushchenko
O.K.Nazarenko	A.T.Zelnichenko
I.A.Ryabtsev	

International editorial council:

N.P.Alyoshin	(Russia)
U.Diltey	(Germany)
Guan Qiao	(China)
D. von Hofe	(Germany)
V.I.Lysak	(Russia)
N.I.Nikiforov	(Russia)
B.E.Paton	(Ukraine)
Ya.Pilarczyk	(Poland)
G.A.Turichin	(Russia)
Zhang Yanmin	(China)
A.S.Zubchenko	(Russia)

Promotion group:

V.N.Lipodaev, V.I.Lokteva
A.T.Zelnichenko (exec. director)

Translators:

A.A.Fomin, O.S.Kurochko,
I.N.Kutianova, T.K.Vasilenko

Editor:

N.A.Dmitrieva
Electron gallery:
D.I.Sereda, T.Yu.Snegiryova

Address:

E.O. Paton Electric Welding Institute,
International Association «Welding»,
11, Bozhenko str., 03680, Kyiv, Ukraine
Tel.: (38044) 200 82 77
Fax: (38044) 200 81 45
E-mail: journal@paton.kiev.ua
http://www.nas.gov.ua/pwj
State Registration Certificate
KV 4790 of 09.01.2001

Subscriptions:

\$324, 12 issues per year,
postage and packaging included.
Back issues available.

All rights reserved.
This publication and each of the articles
contained herein are protected by copyright.
Permission to reproduce material contained in
this journal must be obtained in writing from
the Publisher.
Copies of individual articles may be obtained
from the Publisher.

CONTENTS

WELDING FACULTY of PSTU is 40	
<i>Gulakov S.V. and Shaferovsky V.A.</i> Specialist training at PSTU Welding Faculty	2
<i>Royanov V.A.</i> To the 65th Anniversary of the welding equipment and technology chair of the Priazovsky State Technical University	5
<i>Ivanov V.P. and Ivashchenko V.Yu.</i> Influence of hardfacing technology and heat treatment on structure and properties of metal deposited on carbon steel by LN-02Kh25N22AG4M2 strip electrode	7
<i>Stepnov K.K., Matvienko V.N. and Oldakovsky A.I.</i> Modification of medium-chromium deposited metal	10
<i>Malinov V.L.</i> Effect of manganese on structure and wear resistance of deposited metal of the low-carbon steel type	12
<i>Chejlyakh Ya.A. and Chigarev V.V.</i> Structure and properties of deposited wear-resistant Fe-Cr-Mn steel with a controllable content of metastable austenite	17
SCIENTIFIC AND TECHNICAL	
<i>Makhnenko V.I., Velikoivanenko E.A., Milenin A.S., Olejnik O.I., Rozynka G.F. and Pivtorak N.I.</i> Admissible pressure for filler of sealed sleeves used to repair main pipelines	22
<i>Neklyudov I.M., Bortz B.V. and Tkachenko V.I.</i> Features of formation of dissimilar metal joints in hot roll welding in vacuum	27
<i>Ryabtsev I.A., Kondratiev I.A., Osin V.V. and Gordan G.N.</i> Wear- and heat resistance of deposited metal of graphitized steel type	33
<i>Zaporozhets T.V., Gusak A.M. and Ustinov A.I.</i> Conditions of propagation of the SHS reaction front in nanolayered foils in contact with heat-conducting material	37
<i>Poklyatsky A.G.</i> Peculiarities of temperature distribution in thin-sheet aluminium alloy AMg5M in friction stir welding	42
BRIEF INFORMATION	
<i>Krivchikov S.Yu.</i> Development of the methods for elimination of deformation of crankshafts in wide-layer hardfacing	46
NEWS	
Seminar of the Society of Welders of Ukraine	49
Ukrainian-Polish Scientific-Technical Conference	51

Sincere greetings to lecturers, staff and students on the occasion of 65th anniversary of establishment of the Chair of Equipment and Technology of Welding Fabrication and 40th anniversary of the Welding Faculty of Priazovsky State Technical University (PSTU)!

Establishment of the Chair in 1946 and organizing the Welding Faculty at the end of 1971 were of great importance for training specialists on welding and related technologies for industrial enterprises of the South and South-East of Ukraine, primarily, Donbass region, as well as rapidly developing metallurgical and mechanical engineering giants in Mariupol, Kramatorsk, Kharkov and Lugansk. Over the 65 years the Chair has trained about 6000 specialists, many of which are leading major construction projects, enterprises, and are at the head of a number of higher educational establishments: 115 graduates of the Chair and Faculty became Candidates of Science, 10 are Doctors of Science and 11 are Professors. Over the last five years the Chair lecturers prepared 5 manuals approved by Ministry of Education and Science of Ukraine, and 6 monographs. Mariupol school of welders has gained recognition far beyond Ukraine.

During all these years the Chair of Equipment and Technology of Welding Fabrication and Welding Faculty have been in cooperation with leading scientific and training centers of Ukraine, China, Poland, Hungary, Slovakia, Czechia, Germany and have been actively involved in the work of International Association «Welding».

Published below is a selection of papers, which will allow the journal readers to get an idea about the directions and level of research, performed at PSTU.

*E.O. Paton Electric Welding Institute
Editorial Board and Editorial Office of the Journal*

SPECIALIST TRAINING AT PSTU WELDING FACULTY

S.V. GULAKOV and V.A. SHAFEROVSKY
Priazovsky State Technical University, Mariupol, Ukraine

Stage-by-stage improvement of the system of student training at the Welding Faculty of the University and features of their specialization are described. At present specialist training is performed under the conditions of multilevel system of higher education.

Keywords: *welding fabrication, higher education, specialist training, Bachelors, Specialists, Masters, curricula, module-rating system*

The first group of welding engineers graduated from Mariupol (Zhdanov) Metallurgical Institute in 1947. With each year the number of specialists graduating after different forms of training increased and by now it has risen to 5000 persons. Annual intake of applicants to the Welding Faculty was about 100 persons up to 1996.

In 1994 Mariupol Metallurgical Institute was transformed into Priazovsky State Technical University (PSTU) and certified to IV level of accreditation. From 1993 till 1997 PSTU Welding Faculty trained Bachelors in Welding in four specialities:

- 8.092301 «Equipment and technology of welding fabrication»;
- 8.092302 «Technological and metallurgical processes of welding»;
- 8.092303 «Automated electric welding processes and machines»;
- 8.092304 «Equipment and technology of improvement of wear resistance and reconditioning of machine parts», as well as specialists in technical fields, called Engineers, and Masters [1–3].

At the end of 1998 Materials Science Chair was added to the Faculty. In the same year the Ministry of Education and Science of Ukraine took a decision on changing a number of names of specialities, in particular in 0923 «Welding» and 0901 «Applied Materials Science» training fields. Here speciality 8.092302 «Technological and metallurgical processes

of welding» was moved to one of the specializations of speciality 8.092301. Thus, from 1998 up to 2010 PSTU Welding Faculty conducted training and awarded diplomas of Bachelors, Specialists (Engineers) and Masters in the following specialities:

- 8.092301 «Technology and equipment of welding» (TEW);
- 8.092302 «Welding systems»;
- 8.092303 «Technology and equipment for reconditioning and improvement of wear resistance of machines and structures» (TERIWRMS);
- 8.090101 «Applied materials science» (AMS).

Starting from 2011 PSTU Welding Faculty will perform training and award diplomas to Bachelors, Specialists and Masters in the following specialities:

- 8.05.04.01 «Welding technology and equipment»;
- 8.05.04.03 «Reconditioning and improvement of wear resistance of parts and structures»;
- 8.0504301 «Applied materials science».

Up to 2007 the stage of training Bachelors in the above-mentioned specialities was completed by fulfillment of graduation (qualification) work with its subsequent defense before a State Certification Commission under the condition of successful passing of examination session of VIII semester. Bachelor's graduation work was the summing-up work of the four years of training at the University, and had the objective of systematizing, consolidation and widening of theoretical knowledge through independent development of topics in one of the branches of welding fabrication, applied materials science, envisaged by the individual task; development of design-graphic skills of students and skills of independently solving technical, organizational, design and other tasks.

Composition and scope of graduation work are determined by Graduation Chair. As a rule, the structure of graduation work consisted of explanatory note of not more than 60 pages and graphic part of 4–5 sheets of A1 format.

Starting from 2007 the stage of Bachelor training in the above specialities is completed by passing a state examination before the members of the State Certification Commission.

Bachelors, having basic higher education, can get complete higher education and Specialist qualification in three specialities having passed the second training stage (Figure) during two semesters, which is completed by defending the diploma project before the State Examination Commission.

Realization of the program of training Masters in welding specialities started in 1995 by special curricula based on engineering education [1]. In keeping with the Act of the Cabinet of Ministers of Ukraine of January 20, 1998, #65 «Regulations on education-qualification levels», starting from 1999 the Faculty began training Masters based on the qualifications of Bachelor and Specialist. The main tasks solved in Master training are as follows:

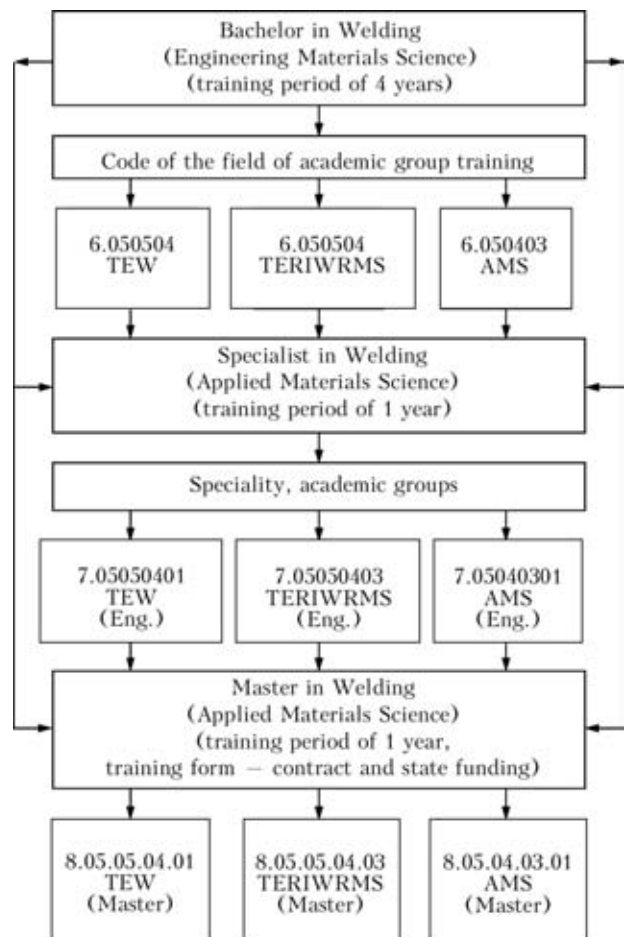
- more profound and specialized study of problems of the respective scientific field;
- narrow specialization in the respective branch of knowledge;
- state training for scientific-pedagogical activity in a higher educational establishment, etc.

On the whole, training of Masters at the Faculty is performed by the following schematic (see the Figure):

- after obtaining the qualification of Bachelor, for one school year (two semesters) on budget funding basis;
- after obtaining the qualification of Specialist, for one school year (two semesters) predominantly on contract basis by individual curricula. Contract cost is approximately equal to Specialist training cost.

In both the cases the applicants to Masters course should have a positive recommendation of the Graduation Chairs and Scientific Councils of PSTU Institute of Metallurgy and Welding (established in February 2010) and the University. In addition, the University established entrance quotas for Masters course, equal to 20% of the total number of graduates with higher education.

Masters training is completed by fulfillment and defense of qualification work before the State Examination Commission.



Block diagram of specialist training in PSTU Welding Faculty

Quality of specialist training under the conditions of multilevel higher education system, in our opinion, is directly related to solving a number of problems [1]:

- improvement of the level of applicant training;
- including secondary technical school leavers into PSTU student membership and reverse rotation of university students into PSTU secondary technical schools;
- ensuring the correspondence of the process of specialist training to European and international standards;
- improvement of scientific-pedagogical level of professors and lecturers;
- improvement of educational process by application of modern technical teaching means, including computers;
- improvement of mastering of foreign languages and economic education of graduates, etc.

During the last eight years the practice of enrolling secondary school graduates into the second and third years has been justified. As a rule this student category is characterized by quite conscientious attitude to studies and high level of practical training. In 2000 the curricula for all the specialities of the Faculty for the first and second semesters and curricula of PSTU secondary technical schools were finally coordinated in order to reduce the scope of a number of subjects, in which additional exams were required, and facilitating the first stage of training at the University.

Junior students, unable to continue their university studies for some reasons, are given an opportunity to complete their education in one of PSTU secondary technical schools. This was made possible by inclusion of three secondary technical schools into the University structure in 1998: mechanico-metallurgical, mechanical engineering, industrial and technical lyceum.

Further development of higher education in Ukraine is unthinkable without taking into account the world and European experience of training specialists, as well as requirements of international standards as regards education and certification of welding specialists [1]. In this connection, participation of our Faculty in the activities of International Association «Welding» is believed to be advantageous. Being an IAW member for about 15 years, the Faculty has a real possibility of establishing and maintaining contacts with scientists and science-production organizations in CIS and distant foreign countries.

The main requirement and most important condition of market economy development is improvement of product quality in all the industries. Welding fabrication products most often come into the category of critical structures. In this connection, the factor of correspondence of these products to the European and world standards is believed to be highly important.

Professional level of professors and lecturers of Welding Faculty Graduation Chairs is quite high: 96 % of the lecturers have the degrees of Candidate and Doctor of Science. 8 Doctors of Science, 9 Professors are working in the Faculty Chairs. At present 12 persons are taking the post-graduate course and 3 persons — the Doctor's course. During the last 5 year period more than 30 lecturers and scientific staff have improved their qualifications through a system of ongoing courses at the University in the following directions: art of teaching, psychology and pedagogy, computer training, etc.

Because of financial difficulties it is still impossible (the situation has not changed since 1996) [1] to improve the lecturers, qualifications in the leading higher educational establishments of Ukraine, CIS and foreign countries', or organize practical studies of lecturers in the leading enterprises. For the same reason the facilities of Graduation Chairs are upgraded not as intensively, as it is required by the modern conditions.

Module-rating system of student knowledge assessment which is used for stage-by-stage assessment of knowledge and level of subject mastering, was tried out within the Faculty and the University as a whole in 1980s, and at present is widely used in the Faculty Chairs. Boulogne system of student knowledge assessment was introduced into the teaching process for all the academic years at the Faculty and is quite effective.

In conclusion it should be noted that the Faculty has for a long time maintained the business and creative contacts with its graduates, working in different industrial organizations, business units, enterprises and teaching establishments, that allows revealing the need for specialists of certain qualification.

1. Belousov, Yu.V., Shaferovsky, V.A. (1996) Improvement of staff training in conditions of multilevel system of higher education. *Avtomatich. Svarka*, **8**, 6–8.
2. Razmyshlyayev, A.D., Shaferovsky, V.A., Belousov, Yu.V. (2001) Education of specialists at the Welding Faculty of the Priazovsky State Technical University. *The Paton Welding J.* **8**, 5–7.
3. Razmyshlyayev, A.D., Shaferovsky, V.A. (2006) Personnel training at the PSTU Welding Department. *Ibid.*, **8**, 2–4.

TO THE 65th ANNIVERSARY OF THE WELDING EQUIPMENT AND TECHNOLOGY CHAIR OF THE PRIAZOVSKY STATE TECHNICAL UNIVERSITY

V.A. ROYANOV

Priazovsky State Technical University, Mariupol, Ukraine

The work of the Welding Equipment and Technology Chair of the Priazovsky State Technical University during 65 year is analysed. Challenges of the Chair in training of specialists in welding and cutting of metals are considered.

Keywords: *welding production, higher education, specialisation, scientific developments*

The Chair of Welding Production Equipment and Technology was founded in 1946 at the Zhdanov Metallurgical Institute (since 1994 – Priazovsky State Technical University). The key task of the Chair was to train specialists in welding and cutting of metals. At that time, the Ilyich Iron and Steel Works completed preparation for commissioning of its pipe welding shop 1 founded by the initiative and with the direct participation of Prof. Evgeny O. Paton.

Engineer A.Ya. Shadrin was appointed in 1946 to be the first acting head of the Chair. At that same year A. Shadrin was replaced by Associate Professor P.S. Elistratov, Candidate of Technical Sciences. The first diplomas in a new speciality were defended in 1947. The first five graduates of the Chair (D.P. Antonets, A.A. Filchakov, K.I. Korotkov, Yu.N. Grishchenko and D.A. Rogovin) became great authorities and organisers of welding production, and two of them (D.P. Antonets and D.A. Rogovin) defended their candidate theses.

In August 1952, K.V. Bagryansky was elected to be the head of the Chair. With his arrival the Chair widened and strengthened its contacts with the E.O. Paton Electric Welding Institute, N.E. Bauman Moscow State Technical University, Kiev Polytechnic Institute and many enterprises of the city and country. The welding building was constructed with the assistance of Boris E. Paton. That allowed the level of training of specialists to be improved and the Chair to become one of the leading chairs of a welding profile. Such talented educational specialists and scientists as Associate Professors, Candidates of Technical Sciences Z.A. Dobrotina, D.S. Kassov, G.S. Kuzmin, and teachers P.F. Lavrik, A.A. Filchakov, V.A. Muratov and V.T. Sopin, were working together with K.V. Bagryansky. Since 1968 the Chair has started training welding engineers in new speciality «Metalurgy and Processes of Welding Production».

In the 1960s the Chair swiftly developed its scientific activity. In these years the process of sub-

merged arc welding of nickel by using ceramic flux was successfully applied at the «Bolshevik» factory in Kiev (the work was supervised by Dr. G.S. Kuzmin). The method for submerged arc welding and surfacing of copper alloys by using ceramic flux, which was applied to advantage at metallurgical works of Ukraine, had been developed under the leadership of Associate Professor D.S. Kassov. Associate Professors V.Ya. Zusin and A.D. Korneev developed the method for submerged arc welding of aluminium under a layer of flux which was used for welding of elements of current-conducting bus-bars at the Bratsk Hydroelectric Power Station. The process of submerged arc surfacing by using ceramic flux was applied to repair forming rolls and machine parts at the Metallurgical Works in Rustavi (Georgia), Ilyich Iron and Steel Works and «Azovstal» in Mariupol, Enakievo Iron and Steel Works and Ust-Kamenogorsk Ore Mining and Processing Enterprise (Kazakhstan). Associate Professor A.A. Filchakov managed investigations on development and application of new grades of electrodes at «Azovmash», and Associate Professor K.A. Olejnichenko headed development of the procedure for quantitative estimation of harmful emissions in welding. Also, they offered recommendations for improvement of working conditions of welders.

30 candidate of technical sciences theses and one doctoral thesis were prepared and defended at the Chair during a period of 1955–1980. In those years the following books were published: manual «Theory



Team of the Welding Equipment and Technology Chair of the Priazovsky State Technical University



Visit to the Welding Equipment and Technology Chair by people's deputy B.A. Olijnyk (from left to right): senior teacher V.P. Semenov, Chair Head V.A. Royanov, Rector of the Priazovsky State Technical University V.S. Voloshin, B.A. Olijnyk, Pro-Rector A.P. Chejlyakh

of Welding Processes» by K.V. Bagryansky, Z.A. Dobrotin and K.K. Khrenov, which was three times re-issued, textbook «Calculation and Design of Welded Structures» by A.N. Serenko, M.N. Krumbolt and K.V. Bagryansky, monographs «Welding of Nickel and Its Alloys» by K.V. Bagryansky and G.S. Kuzmin, and «Ceramic Fluxes for Welding and Surfacing» by K.V. Bagryansky.

In 1971 the Branch R&D Surfacing Laboratory was arranged at the Chair. The purpose of the Laboratory was to develop new surfacing technologies and consumables for reconditioning and repair of parts of metallurgical equipment. The Laboratory was headed by Associate Professor, Candidate of Technical Sciences V.N. Matvienko.

From 1973 till 1979 the Chair was headed by Candidate of Technical Sciences A.N. Serenko. Research on static and dynamic strength of welded joints and structures was carried out, and efforts on investigations of single-pass welding of 40 mm thick and thicker steels with programming of the welding process were launched during that period. The investigation results were summarised in candidate of technical sciences theses by V.A. Shaferovsky and A. Skshipchik (Poland), and found practical application at «Azovmash» and «Zaliv» Ship Yard.

In 1980 the Chair was headed by L.K. Leshchinsky. New ceramic fluxes and flux-cored wires for electric



Students of the Chair at the Surfacing Laboratory

arc surfacing of forming rolls and parts of the metallurgical equipment were developed in collaboration with the Branch Surfacing Laboratory.

Investigations were conducted to study surfacing and welding processes using strip electrodes by the submerged arc method. The investigation results were applied at machine building and metallurgical enterprises, and were summarised in the candidate of technical sciences theses by Yu.V. Belousov, V.I. Shchetinina, V.N. Matvienko, V.P. Lavrik and A.V. Zarechensky. The Chair was active in upgrading of equipment for automation of the surfacing processes and control of the deposited metal quality. Results of these efforts were covered in the doctoral thesis by S.V. Gulakov.

Research in the field of plasma hardening of parts, including after surfacing, received intensive development. The research results are presented in monograph «Surface Plasma Hardening» by L.K. Leshchinsky, S.S. Samotugin, I.I. Pircha and V.I. Komar.

Since 1985 the Chair has been headed by Doctor of Technical Sciences, Professor V.A. Royanov, honorary member of the Donetsk State Engineering Academy. Material resources of the Chair were expanded and strengthened, and disciplines on robotisation of welding production were included into the education process with his participation. Computation facilities and new information technologies are used in classes to prepare term papers and diploma projects. Flux-cored wires for electric arc metallising, which are widely utilised at Kiev Association «Kievtraktorredtal», at vehicle repair enterprises of Poltava, Tashkent and other cities, were developed. The investigation results were generalised in the candidate of technical sciences thesis by E.V. Vojtsekhovsky and doctoral thesis by V.A. Royanov. The intensive work is performed on application of elements of the Bologna Education Process. The credit-modular education system is introduced. The method learning school-books for self-education of students were developed and published. And curricula are continuously improved.

S.V. Gulakov, V.A. Royanov, L.K. Leshchinsky, A.D. Razmyshlyayev, S.S. Samotugin and A.N. Serenko defended their doctoral theses at the Chair during a period of 1998–2001. A.N. Serenko was given the rank of Professor. The doctorate courses were instituted, where two persons working for the doctor's degree are completing now their theses. The Special Board on defence of candidate and doctor of technical sciences theses in speciality «Welding and Related Processes and Technologies» is working at the Chair.

Manuals «Welding. Introduction into Profession» (A.N. Serenko, V.A. Royanov), «Formation of Defects in Welding and Related Processes», «Defects and Quality in Welding and Related Processes» (V.A. Royanov, V.Ya. Zusin and S.S. Samotugin), «Welding and Surfacing of Aluminium and Its Alloys» (V.Ya. Zusin and V.A. Serenko), «Repair of Machines by Welding and Related Technologies» (V.A. Royanov)

nov, G.G. Psaras and V.K. Rubajlo), and monograph «Magnetic Control of Weld Formation in Arc Welding» by A.D. Razmyshlyaev, stamped by the Ministry of Education and Science, were prepared and published during the last three years.

During the 65 years period the team of the Chair educated about 6000 engineers, including for the countries of Europe, Asia, Africa and Latin America, and 42 candidates and 8 doctors of technical sciences defended their theses. The Chair published over 30 manuals and monographs, and 760 scientific papers. Over 280 developments are covered by the author's certificates and foreign patents.

Graduates of the Chair A.D. Chepurnoj, T.G. Kravtsov, V.Ya. Zusin, V.I. Shchetinina and V.N. Kalianov successfully defended their doctoral theses. Many graduates became recognised specialists in the field of welding production and headed industrial enterprises of Ukraine, Russia and other countries: A.V. Savchuk, Doctor of Economic Sciences and Chairman of the Board of «Azovmash»; Doctor of Technical Sciences A.D. Chepurnoj, L.P. Khadzhinov, Director General of «Zaporozhtransformator», K.Kh. Kazmiridi, Director General of «Pozhzhashchita», etc.

At present, three professors — doctors of technical sciences, ten associate professors — candidates of technical sciences, one senior teacher and one assistant are working at the Chair. The Chair has been accredited as corresponding to level IV by the Commission of the Ministry of Education and Science of Ukraine. It trains specialists in professions «Technology and Equipment for Welding» and «Welding Units».

Specialists of the Chair take part in activities of International Association «Welding». Along with traditional cooperation with chairs of the higher education institutes of Moscow, St.-Petersburg, Chelyabinsk, Yekaterinburg, Tbilisi, Minsk, Mogilyov and other cities of the former Soviet Union countries, the Chair has established contacts with higher education institutes and organisations of «far-foreign» countries, such as the Institute of Welding in Gliwice (Poland), University of Miskolc (Hungary), Harbin Institute of Technology (China), etc.

The Chair meets its 65th anniversary with active and creative work on improvement of training of the staff for national economy of the country and development of research in the field of welding and related processes and technologies.

INFLUENCE OF HARDFACING TECHNOLOGY AND HEAT TREATMENT ON STRUCTURE AND PROPERTIES OF METAL DEPOSITED ON CARBON STEEL BY LN-02Kh25N22AG4M2 STRIP ELECTRODE

V.P. IVANOV and V.Yu. IVASHCHENKO

Priazovsky State Technical University, Mariupol, Ukraine

Possibility for improvement of structural state of fusion zone metal in hardfacing of carbon steel by LN-02Kh25N22AG4M2 strip electrode was investigated. The recommendations on selection of heat treatment modes were provided for improvement of structure and properties of this zone.

Keywords: arc hardfacing, strip electrode, carbon steel, bimetal, corrosion-resistant layer, fusion zone, microstructure, thermocyclic treatment, mechanical properties

Bimetal structures are widely used in manufacture of equipment for chemical machine building. One of the traditional methods of obtaining of bimetal billets is automatic arc hardfacing of corrosion-resistant layer on low-carbon steel, performed by single strip electrode of 0.5–0.8 mm thick at the width of 60 mm with fraction of the base metal not more than 15–20 %.

Presence of the residual stresses and structural inhomogeneity in fusion zone are specific peculiarities of the hardfaced bimetal. These factors promote appearance of new or development of existing microcracks that can result in loss of working capacity

of the part under hard operation conditions of equipment in chemical industry.

Selection of reasonable modes of hardfacing and heat treatment of the deposited metal can help to achieve specific positive effect on reduction of the residual stresses and homogenizing of the chemical composition.

The aim of present study is to investigate influence of modes of hardfacing and heat treatment on structure and mechanical properties of the bimetal layer.

Electric arc hardfacing was carried out on templates from steel 20 of 400 × 600 × 15 mm size by LN-02Kh25N22AG4M2 strip electrode of 0.5 × 60 mm section with 48-OF-10 flux without preheating at current of hardfacing $I_{hf} = 750\text{--}800$ A and arc voltage

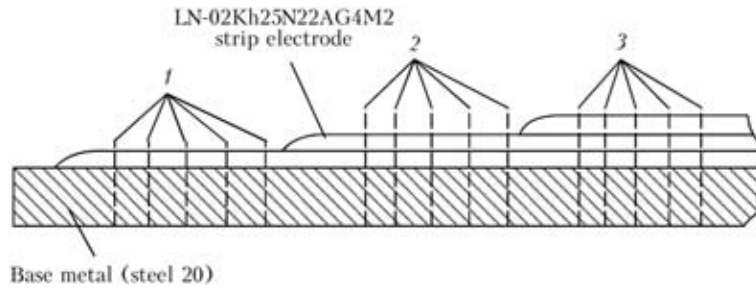


Figure 1. Scheme of hardfacing of one-, two- and three-layered specimens 1-3

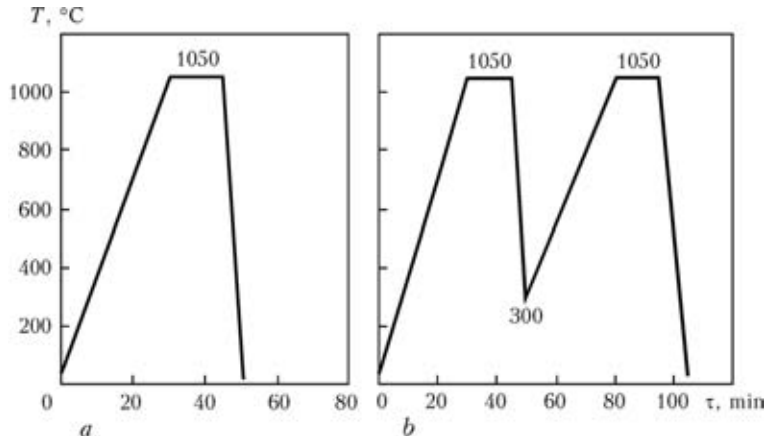


Figure 2. Modes of heat treatment of deposited specimens: a – high-temperature normalization; b – HTTCT; τ – time of HT

$U_a = 28-30$ V. Deposited layer contained the areas of different heights, from which test specimens were cut out (Figure 1). At that, effect of the subsequent layers on mechanical properties and structure of the base metal and HAZ can be evaluated. Influence of the heat treatment (HT) on distribution of the structural constituents across section of the deposited metal

(modes of HT are given in Figure 2, cooling in air) was also investigated.

Application of HT mode on variant, provided in Figure 2, a, does not allow grain refining in the base metal since heating to 920 °C and cooling in air (1050 °C for stainless chromium-nickel steels) are provided for standard normalization of steel 20. Spreading in the microhardness values (Figure 3, a) can be well explained for high-alloyed steels tending to segregation at solidification under the non-equilibrium conditions. Similar microhardness measurements were carried out after high-temperature thermocyclic treatment (HTTCT) (Figure 3, b). Positive effect of HTTCT indicated in many studies [1, 2] since such a treatment promotes grain size refinement, formation of more developed substructure, intensification of diffusion processes and increase of chemical homogeneity of the metal. This results in increase of impact toughness and improvement of complex of mechanical properties in whole.

Dendrite segregation in different layers of deposit occurs in structure of the deposited layer. Thus, austenite structure with obviously etched grain boundaries and carbides (Figure 4, a) is formed in the first layer, and dendrite segregation (Figure 4, b) is noticed in the second layer of the double-layered specimens. Similar segregation takes place in the second and third layers of three-layered specimen.

Coarse grains and mixed ferrite-pearlite (F-P) structure with separate Widmanstaetten zones are formed in the HAZ, that indicates significant overheating relative to A_{c3} point and tendency to brittle cracking. Simple F-P banding with elongated lines of

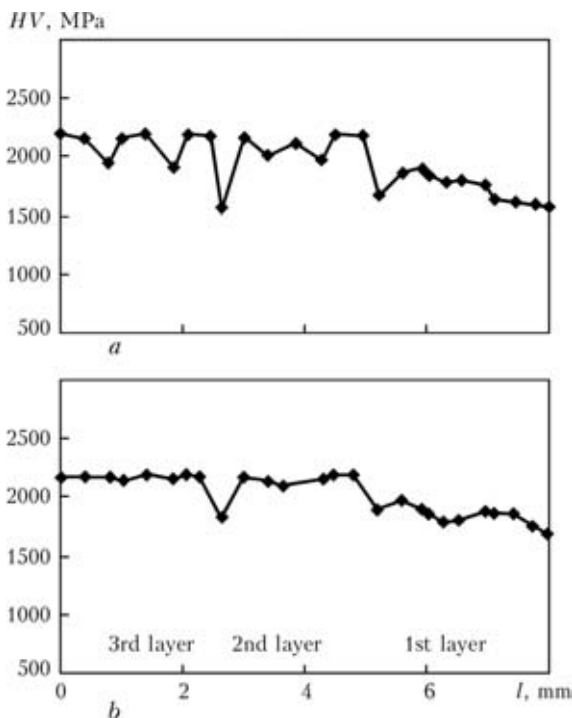


Figure 3. Change of microhardness across the section of deposited layer after hardfacing without HT (a) and after HTTCT (b): l – distance to the surface

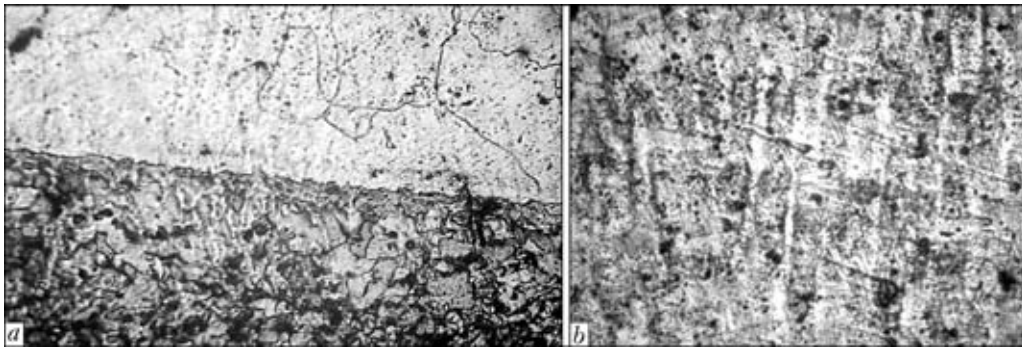


Figure 4. Microstructures ($\times 600$) of corrosion-resistant layer of double-layered deposited specimen: *a* – fusion zone with base metal; *b* – dendrite segregation in the 2nd deposited layer

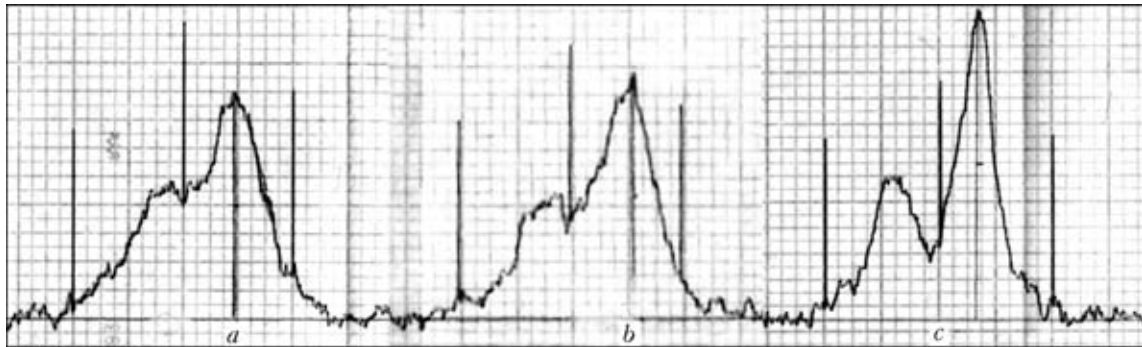


Figure 5. Diffraction patterns of the specimens with 1st (*a*), 2nd (*b*) and 3rd (*c*) deposited layers

Table 1. Mechanical test results of base metal

Base metal	σ_t , MPa	$\sigma_{0.2}$, MPa	δ , %	KCU, J/cm ²
As delivered	400	225	26	65
After hardfacing	345	185	19	40
After high-temperature normalization	350	210	20	52
After HTTCT	380	255	24	84

sulfides character for hot-rolled metal occurs out of the HAZ.

Positive effect of HTTCT was observed in testing of mechanical properties of the base metal (Table 1), namely values of tensile strength ρ and yield strength $\sigma_{0.2}$ as well as elongation δ after HTTCT were close to initial ones, but impact toughness index was 30 % higher after HTTCT (38.4 % reduction after hardfacing).

X-ray structure analysis of the specimens was carried out. It was based on registration of the distortions in crystal lattice of the metal using X-ray irradiation. The level of elastic stresses of the second order rising in the metal was determined by calculations based on these values. At that, standard calculation technique from study [3] was used.

Investigations of elastic microstresses in the deposit layer showed that the largest distortions take place after hardfacing of three-layered specimens (Figure 5 and Table 2), high-temperature normalization promotes decrease of these stresses to 71–76 MPa and HTTCT – to 54–56 MPa.

Table 2. Calculated data on elastic microstresses

Version of technology	Amount of deposited layers	Elastic microstresses, MPa
In the hardfaced state without HT	1	86.0
	2	107.5
	3	112.0
After high-temperature normalization	1	71.5
	2	76.0
	3	75.0
After HTTCT	1	57.0
	2	54.5
	3	59.0

CONCLUSIONS

1. Structural inhomogeneity in the fusion zone and high level of residual stresses, which are proportional to amount of deposited layers, take place in electric arc hardfacing of carbon steel by LN-02Kh25N22AG4M2 strip electrode.

2. Heat treatment of hardfaced billets is recommended for correcting of the structure, improvement of mechanical properties and elimination of tendency to brittle fracture. Double-cycle HTTCT is preferred for bimetal billets.

1. Fedyukin, V.K. (1977) *Thermocyclic treatment of steels and cast irons*. Leningrad: Mashinostroenie.
2. Baranov, A.A. (1974) *Phase transformations and thermocycling of metals*. Kiev: Naukova Dumka.
3. Boky, G.B., Poraj-Koshits, M.A. (1964) *X-ray structure analysis*. Moscow: AN SSSR.

MODIFICATION OF MEDIUM-CHROMIUM DEPOSITED METAL

K.K. STEPNOV, V.N. MATVIENKO and A.I. OLDAKOVSKY
Priazovsky State Technical University, Mariupol, Ukraine

Investigation results of influence of rare-earth metals on structure and properties of medium-chromium deposits were presented. It is shown that effect of the rare-earth metal additives appears in increase of technological strength, impact toughness and resistance to thermal fatigue failure of metal used for hardfacing of rollers of hot rolling.

Keywords: arc hardfacing, ceramic flux, rare-earth metals, deposited metal, technological strength, impact toughness, specific fracture work

Life time of the hardfaced parts, which suffer from dynamic and thermo-cyclic loading in a process of operation, significantly depends on resistance to nucleation and propagation of the technological and service cracks. This in full refers to deposited metal of Kh5MF and Kh12MF type applied for repair of forming rolls and rollers of machines for continuous casting of billets. Structure of such a metal, mechanical properties as well as functional characteristics in many respects depend on content of carbon in it. An increase of the latter in deposited metal of Kh5MF steel type raises hardness and resistance to wear due to metal-to-metal friction (Figure 1). At the same time, a possibility of hot crack formation increases since critical rate of deformation A_{cr} reduces in a process of weld solidification. If high-tempered martensite is formed in the metal structure at carbon content up to 0.25 wt.% and impact toughness makes not less than 0.30 MJ/m², than structure of Kh5MF type deposit, in which carbon content is more than 0.25 wt.%, is characterized by presence of acicular martensite, reduced grain-boundary strength and increased embrittlement. Presence of twinned (laminar) martensite

[1] is observed together with lath (packet) martensite in structure of Kh5MF deposited metal with 0.33–0.35 wt.% C. Failure of the deposit occurs on micro-mechanism of intercrystalline chip at dynamic loading. This explains its low (less than 0.15 MJ/m²) impact toughness. Along with it, resistance to fatigue crack propagation is reduced that, approximately, is evaluated by value of specific fracture work A_f (Figure 2, a).

Introduction of the rare-earth metals (REM) in the deposited metal allows increasing technological strength and crack resistance. This effect is obtained due to binding of sulfur in the refractory fine compounds, eliminating of lamination during its distribution, reducing of microchemical inhomogeneity and refining of austenite grain [2, 3]. At that, weld metal contamination by non-metallic inclusions are also reduced. Number of inclusions rises insignificantly in the metal deposited using ceramic flux of ZhSN type, containing cerium fluoride, however, intensive increase of their dispersion (Table) is observed and shape is changed to globular one.

The critical rate of deformation A_{cr} rises with increase of cerium content in the flux (and in deposit) due to refining and modification at hardfacing by Sv-08A as well as PP-Np-30KhGSA wires (Figure 3). As

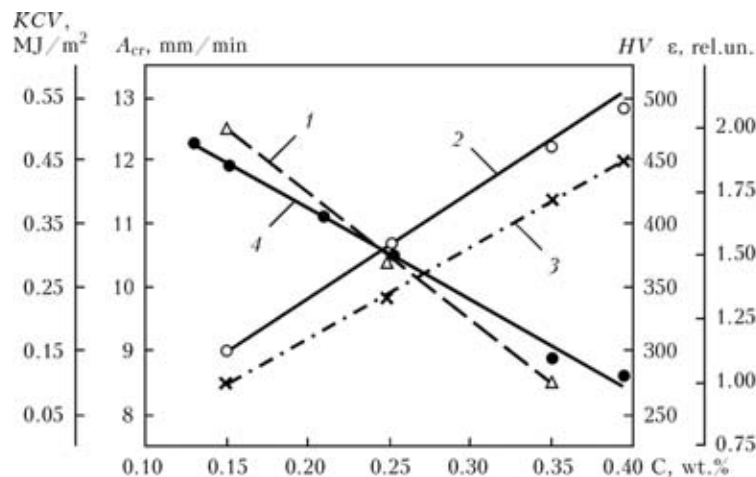


Figure 1. Influence of carbon content on critical deformation rate A_{cr} (1), hardness HV (2), wear resistance ϵ (3) and impact toughness KCV (4) of deposited metal of Kh5MF type

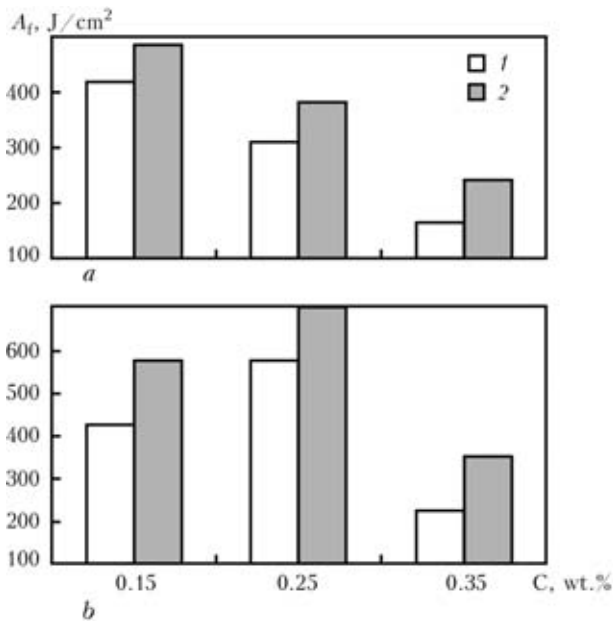


Figure 2. Influence of carbon and cerium content on specific fracture work A_f of deposited metal of Kh5MF (a) and Kh12MF (b) type without (1) and with (2) cerium

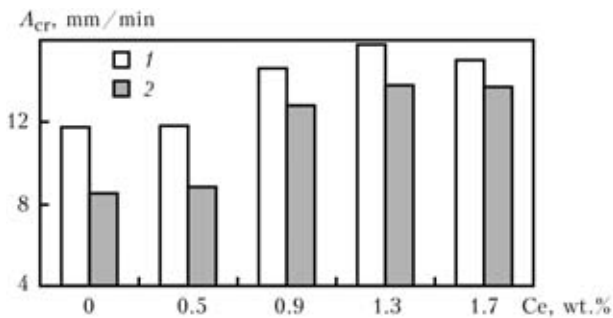


Figure 3. Dependence of critical deformation rate on cerium content in ceramic flux of ZHSN type in hardfacing with Sv-08A (1) and PP-Np-30KhGSA (2) type

can be seen from the Figure, A_{cr} rises only up to obtaining of optimum cerium fraction in the flux and in the deposited metal, respectively. Impact toughness of 20Kh6GMFS metal increases from 0.40 to 0.54 MJ/m² at optimum cerium content (0.008–0.009 wt.%). The level of metal contamination by non-metallic inclusions (see the Table) rises at further (above optimum one) increase of its content. Value of the critical rate of deformation A_{cr} reduces at that.

The specific fracture work of Kh12MF deposited metal is influenced by carbon content in contrast to

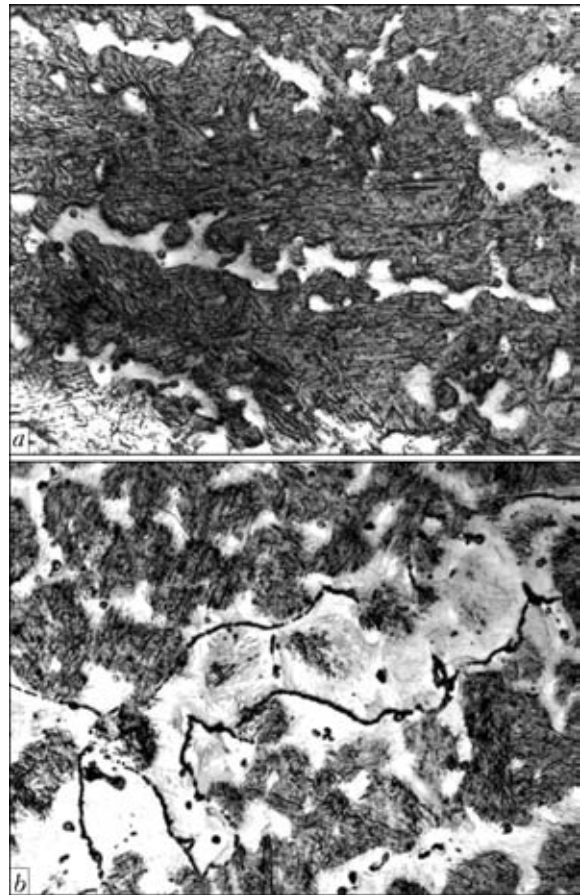


Figure 4. Microstructures (x500) of deposited metal 35Kh8GSMF (a) and 34Kh8GSMF with REM (b)

Kh5MF steel deposit. This dependence becomes maximum at carbon content of 0.25 wt.% (see Figure 2, b). Structure of such a metal contains martensite and ferrite-carbide mixture, that increases the resistance to fatigue failure owing to crack arrest near the interface of martensite with more ductile ferrite. The A_{cr} values rapidly reduce at further increase of carbon content due to low crack resistance of high-carbon martensite. Add of cerium in the composition of deposited Kh12MF steel increases its failure resistance in all range of carbon content.

It is a tendency to improve the properties of surface (wear-resistant) layer for increasing a life time of the hardfaced part.

However, working capacity of the part in many respects depends on composition of a sublayer, its

Amount of non-metallic inclusions per 1 mm² in Ce-contained 20Kh6GMFS deposited metal

Ce, wt. %	NMI volume fraction, %	Size of NMI, μm					
		1.0–1.5	1.5–2.0	2.0–2.5	2.5–3.0	3.0–5.0	<5.0
0	0.217	682	113	110	3	7	49
0.005	0.288	816	138	49	5	7	2
0.008	0.279	887	209	77	18	12	3
0.011	0.274	830	125	46	9	7	0
0.015	0.339	1116	302	105	24	16	2

plasticity [4], reliability of fusion with the base metal as well as formation of hot and cold cracks in it. The hot cracks appearing in the process of sublayer hardfacing can provoke formation of failure of chip type during rollers' operation.

The wires containing REM are used for hardfacing of the sublayer of electrode materials with increased resistance to hot crack formation, however, their choice is limited by using of Sv-15GSTYuTsA and Sv-20GSTYuA ones.

Composite low-alloyed metal of 0.18–0.26 C, up to 1.5 Cr, 0.75–1.05 Mn, 0.55–0.75 Si, ≤ 0.025 S, ≤ 0.025 P and 0.020–0.058 wt.% of REM was investigated for evaluation of the possibility of its application as a sublayer obtained by hardfacing with flux-cored wire and flux. High technological strength and crack resistance of metal with 0.18–0.20 % C and 0.040–0.045 wt.% of REM allows recommending PP-Np-26Kh1G1S flux-cored wire for hardfacing of the sublayer during forming rolls repair.

Along with it, application of PP-26Kh1G1S flux-cored wire with 0.25–0.26 wt.% C and 0.047–0.052 % of REM for hardfacing with ceramic flux ZhSN-5 allows obtaining of wear-resistant layer with the structure more favorable in comparison with obtained with PP-Np-30KhGSA wire.

In both cases, the metal has martensite-ferrite structure with well-defined dendrite pattern (Fi-

gure 4). At the same time, crystals of the tempered martensite become more dispersed (Figure 4, *b*) due to REM addition, besides, the fraction of martensite component increases, that determines high hardness *HV* 450 and sufficient plasticity of deposited metal.

Such a metal differs by higher technological strength and resistance to thermal fatigue fracture: deposit of 35Kh8GSMF type has relative strength index 1.0 at average 230–380 number of thermal cycles up to crack appearance, and deposited 34Kh8GSMF metal with REM has, respectively, index 1.3–1.4 at 370–490 cycles at average.

Thus, addition of REM in the composition of Kh5MF and Kh12MF deposits applied for repair of forming rolls and rollers of machines for continuous billet casting increases its technological strength, impact toughness, resistance to thermal fatigue fracture and specific fracture work.

1. Samotugin, S.S., Leshchinsky, L.K. (2003) *Plasma strengthening of tool materials*. Donetsk: Novy Mir.
2. Efimenko, N.G. (1990) About mechanism of REM influence on the process of solidification and formation of primary structure in welding of steel. *Svaroch. Proizvodstvo*, 7, 12–14.
3. Efimenko, N.G. (2002) Modifying, refining and alloying with yttrium in welding of steels. *The Paton Welding J.*, 6, 8–12.
4. Senchenko, I.K., Ryabtsev, I.A., Chervinko, O.P. et al. (2010) Computational method for evaluation of thermal stability of deposited metal. *Svaroch. Proizvodstvo*, 7, 3–8.

EFFECT OF MANGANESE ON STRUCTURE AND WEAR RESISTANCE OF DEPOSITED METAL OF THE LOW-CARBON STEEL TYPE

V.L. MALINOV

Priazovsky State Technical University, Mariupol, Ukraine

Investigation results are presented on structure and wear resistance of metal deposited by using flux-cored strips and having chemical composition of the low-carbon steel type with differing manganese content. The possibility of improving wear resistance of the deposited metal due to subsequent heat and thermochemical treatments is studied. It is shown that achievement of the optimal amount of meta-stable austenite in structure leads to improvement of wear resistance of the deposited metal.

Keywords: arc cladding, flux-cored strips, deposited metal, structure, martensite, austenite, bainite, strengthening, tempering, case-hardening

Peculiarities of commercial application of consumables providing formation of meta-stable austenite in the deposited metal and characterised by dynamic deformation martensitic transformation (DDMT) are described in study [1]. Also, it is noted in that study that inadequate attention is given now to development of such consumables. Known austenitic cladding consumables of the 110G13L steel type, containing an increased amount of manganese and carbon, as well

as chrome-manganese consumables of the PP-Np-25Kh10G10T type are insufficiently practicable, as metal deposited with them is hard to process by machining [2]. In a number of cases expensive alloying elements are used in such consumables. Therefore, the problem of development of sparsely alloyed cladding consumables is still topical. This problem can be addressed by providing the multi-phase structure in the deposited metal, where austenite is present along with other components (martensite, carbides, carbonitrides, etc.), rather than the austenitic one. For this it is important to have the meta-stable structure that is self-transformable under loading and characterised

Table 1. Chemical composition and properties of deposited metal

Content of alloying elements, wt.%				Hardness HRC	Presence of cracks
C	Mn	Si	Ti		
0.15	5.1	0.71	0.09	36	No
0.16	8.2	0.63	0.11	42	No
0.14	10.0	0.67	0.11	47	Yes
0.15	12.2	0.61	0.08	45	Yes
0.16	14.1	0.68	0.12	34	No

by occurrence of various structural and phase transformations leading not only to strengthening, but also to relaxation of microstresses. In particular, it is the meta-stable austenite experiencing DDMT that can serve as such a structure [3, 4]. The above transformations can be accompanied by the dynamic processes of twinning and ageing, changes in the dislocation density, dispersion of structure, etc.

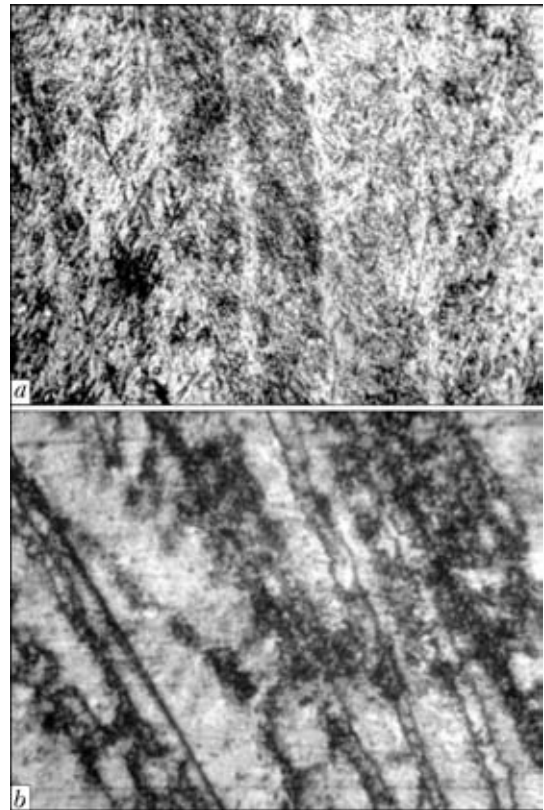
Cladding consumables providing the low-carbon Fe–Mn–C base deposited metal of the martensitic, martensitic-austenitic and austenitic-martensitic grades, as well as improvement of properties of the deposited metal as a result of heat and thermochemical treatments hold promise for manufacture of parts subjected to mechanical wear (various guides, shafts, rollers, sleeves, crane wheels, etc.).

Single-seam flux-cored strips 10 × 3 mm in size, with a fill factor of 48–50 %, were made from the charge containing a different amount of manganese metal and iron powder, as well as a small amount of ferrotitanium to refine grains in the deposited metal structure. A strip of cold-rolled steel 08kp (rimming) was used as a steel sheath. Cladding was performed in three layers on a 30 mm thick plate of steel VSt3sp (killed) by the submerged-arc method using flux AN-26 under the following conditions: current 450–500 A, voltage 30–32 V, cladding speed 25 m/h, no preheating. Subsequent beads were deposited after cooling to a temperature not higher than 250 °C.

Tempering of specimens cut out from the deposited metal was carried out at temperatures of 450, 550, 650 and 750 °C with holding for 1 h and subsequent cooling in air. The specimens were also subjected to case-hardening in solid carburiser at a temperature of 950 °C for 10 h. After that, part of the specimens was subjected to tempering at 650 °C. Chemical composition of the metal deposited with the experimental flux-cored strips is given in Table 1 (S, P ≤ 0.03 %).

Durometric and metallographic examinations were carried out. Phase composition was studied by the X-ray method using diffractometer DRON-4.

Microstructure of the deposited metal containing 5 and 8 % Mn (without heat treatment) was martensitic (Figure 1, *a*). No ferrite was detected in the deposited metal structure, this being in agreement with the data of study [5], which reports that diffu-

**Figure 1.** Microstructure (×500) of deposited metal with 5 (*a*) and 14 % Mn (*b*)

sionless martensitic $\gamma \rightarrow \alpha$ transformation in Fe–Mn steels containing more than 5 % Mn occurs at the usual rates of air cooling. The α -martensite region extended to 8 % Mn, and increase of the manganese content led to lowering of temperature ranges of the $\gamma \rightarrow \alpha$ transformations. The highest hardness of the deposited metal was fixed at 10 and 12 % Mn, this being caused by higher hardening of α -martensite, compared to 5 % Mn. As the manganese content was increased to 14 %, in addition to α -martensite, ϵ -martensite (about 20 %) and austenite (about 50 %) (Figure 1, *b*), having a much lower hardness, appeared in the deposited metal structure, thus causing decrease in hardness of the deposited metal.

No cracks were fixed in the deposited metal at a manganese content of 5, 8 and 14 %. Formation of cracks in the deposited metal containing 10–12 % Mn can be explained by the highest degree of hardening of α -martensite at a very low level of ductile properties. This is caused by intensive localisation of bond between the iron crystalline lattice atoms due to redistribution of external electrons from the iron to manganese atoms [6]. The absence of cracks at a manganese content increased to 14 % is explained by decrease in the degree of hardening of the deposited metal and increase of its ductility because of an increased amount of austenite formed in structure. The deposited metal containing 10–12 % Mn was not used in further investigations because of its low crack resistance.

The flux-cored strips being developed are intended for repair and strengthening of parts subjected to wear

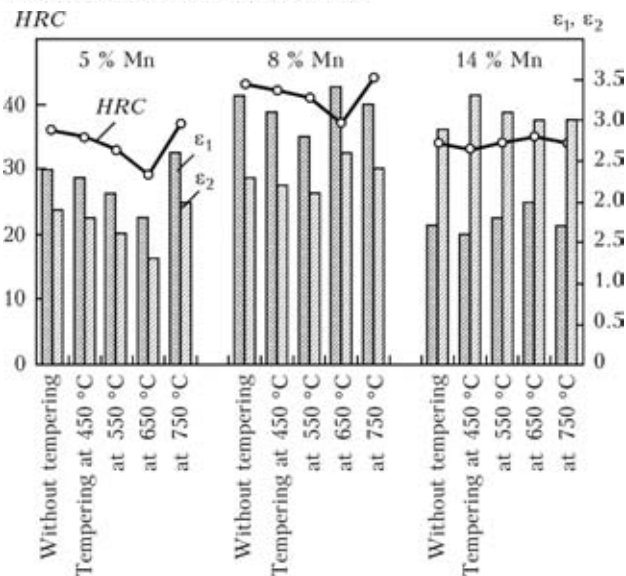


Figure 2. Hardness and relative wear resistance of deposited metal in dry friction, ϵ_1 , and without heat treatment and after tempering in grit flow tests, ϵ_2

in metal on metal friction. They are meant to be used instead of the widely applied cladding consumables providing the deposited metal of the low-carbon steel type, e.g. Np-30KhGSA and PP-Np-18Kh1G1M, and in a number of cases of the chrome-manganese austenitic steel type, e.g. PP-Np-14Kh12G12ST.

Wear resistance of parts is usually estimated by the results of the tests simulating interaction under the sliding and rolling friction conditions.

The tests under the sliding friction conditions were conducted by the block-roller scheme in dry friction (wear resistance ϵ_1). The speed of rotation of the 70 mm diameter roller of steel 55 with hardness HRC 56 was 200 rpm. Pressing of a flat specimen was provided by using the 8 kg load.

Comparative wear resistance tests of the deposited metal of different structural grades under the rolling friction conditions by the roller-roller scheme (pressure 320 MPa, speed of rotation of the rollers 0.98 m/s, slippage 0.09 m/s) and under the dynamic effect of a grit flow at different attack angles were carried out at a preliminary stage of the investigations. Manufacture of specimens for the second type of the tests was much less labour and material consuming. In this case, the surface of the flat specimen was affected by grits transported with a compressed air flow at a pressure of 5 atm in the system. The diameter of a nozzle at exit of the jet from a mixer was 16 mm. The time of testing of the specimens was determined by consumption of 20 kg of the grits.

The tests under the rolling friction conditions and under the effect of the grit flow resulted in fatigue fracture of the surface volumes of metal under the repeated force impact. Variations in the grit attack angle allowed the fracture conditions to be varied. Close values were obtained in the course of the investigations in tests by the roller-roller scheme and under

the effect of the grit flow at an attack angle of 60°. The latter scheme of wear was used for further investigations (ϵ_2). Results of the tests by the roller-roller and grit flow schemes were selectively rechecked on individual specimens of the deposited metal. The values of wear resistance were close in all the cases of the tests by the above schemes.

The metal deposited with a widely applied flux-cored strip PP-Np-18Kh1G1M, subjected to tempering at 600 °C to hardness of HB 280, was used as a reference for evaluation of a relative wear resistance.

The investigation results on wear resistance of the deposited metal containing 5, 8 and 14 % Mn without heat treatment and after tempering at different temperatures are shown in Figure 2.

Correlation of wear resistance of the deposited metal with its hardness was observed in dry friction. And on the contrary, when tested in the grit flow, the deposited metal with 14 % Mn exhibited the highest wear resistance together with the lowest hardness, this being caused, according to the X-ray analysis data, by transformation of retained austenite into martensite during wear. This transformation was not pronounced in dry friction, probably, because of heating of the surface above the martensitic transformation temperature [4].

As the tempering temperature was increased from 450 °C to A_{c1} , wear resistance and hardness of the deposited metal containing 5 and 8 % Mn decreased due to weakening of martensite. The highest wear resistance of such a deposited metal at different types of wear was achieved in an intercritical temperature range (ICTR of $A_{c1} < t < A_{c3}$). This temperature corresponded to 750 °C for the deposited metal with 5 % Mn, and 650 °C — for the deposited metal with 8 % Mn. Redistribution of carbon and manganese between the α - and ϵ -phases and their enrichment with the latter took place in ICTR. As a result, in addition to martensite and a small amount of carbides, the deposited metal also contained austenite, i.e. 9 and 18 % at 5 and 8 % Mn, respectively. This austenite was meta-stable, and under loading it completely transformed into martensite. Figure 3, *a* and *b*, shows the data for the deposited metal with 8 % Mn. In addition, after heating and holding in ICTR, part of the austenite in cooling to room temperature transformed back to the martensite having a higher hardness due to its increased content of carbon and manganese. Along with the meta-stable austenite, that provided increase in wear resistance.

Heating of the deposited metal containing 14 % Mn in a temperature range of 450–750 °C had an unambiguous affect on wear resistance. In a case where stabilisation of austenite occurred with regard to DDMT (tempering at 450 °C), the wear resistance decreased in dry friction and increased in tests in the grit flow. And on the contrary, in destabilisation of

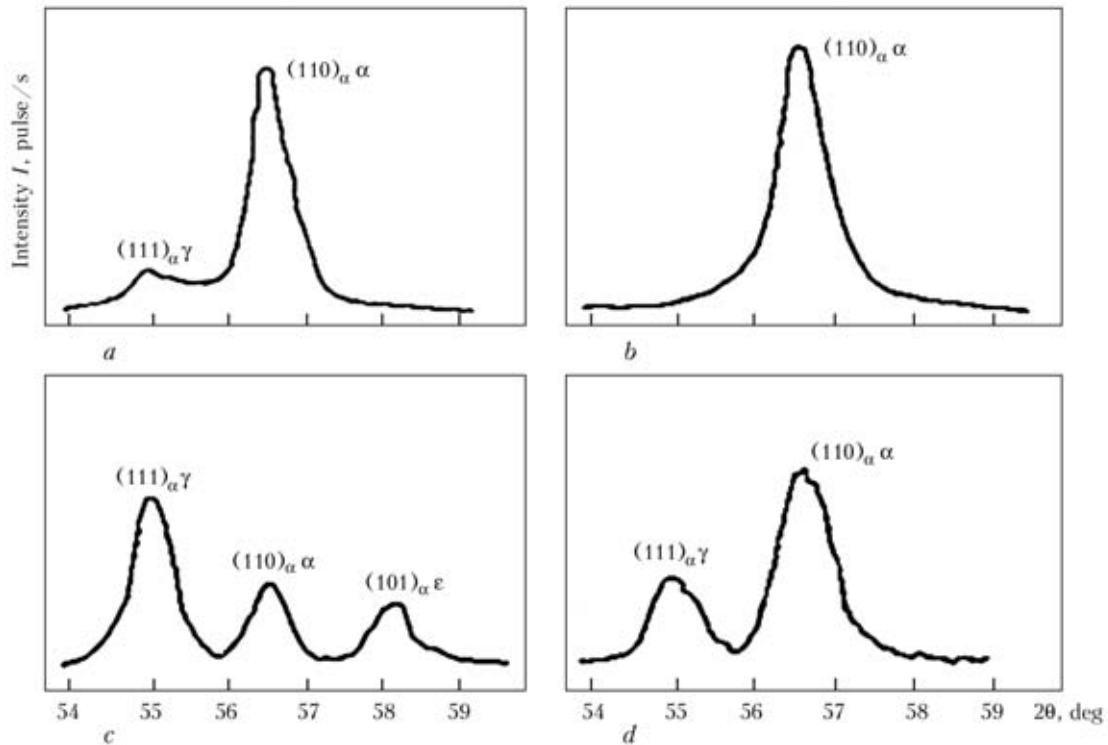


Figure 3. Diffraction patterns of deposited metal containing 8 (*a, b*) and 14 % Mn (*c, d*) after tempering at 650 °C before wear in grit flow (*a, c*) and after wear (*b, d*)

austenite because of precipitation of carbides (tempering at 550 °C and especially at 650 °C), wear resistance increased in dry friction and decreased in the grit flow tests. A change in phase composition of the deposited metal is confirmed by the diffraction patterns shown in Figure 3, *c* and *d*. Austenite prevailed in structure before wear, and martensite – after wear, the ϵ -phase being absent. After tempering at 750 °C, the structure and wear resistance were close to those in the as-clad condition.

It is a known fact that increase in the carbon content of steels leads to improvement of their wear resistance. However, the high-carbon deposited metal is difficult to machine, and is susceptible to cracking. An efficient technological approach is cladding with low-carbon steels followed by their case-hardening [7]. The data on the effect of case-hardening and tem-

pering at 650 °C on structure and properties of the deposited metal are given in Table 2.

The highest wear resistance after case-hardening under the dry friction conditions was exhibited by the deposited metal containing 5 % Mn. In this case, the structure contained 35–40 % of meta-stable austenite, along with martensite and carbides. With increase in the manganese content to 8 and 14 %, the wear resistance of the deposited metal in dry friction decreased due to an increased content of austenite in its structure.

Because of weakening of martensite and decomposition of retained austenite, tempering of the deposited metal containing 5 % Mn at 650 °C led to decrease of its wear resistance under the dry friction conditions. And on the contrary, wear resistance of the deposited metal containing 8 and 14 % Mn increased after tem-

Table 2. Properties of deposited metal after case-hardening and subsequent tempering

Mn content, %	Treatment	Phase content*	Hardness <i>HRC</i>	Wear resistance	
				ϵ_1	ϵ_2
5	Case-hardening	35–40 % A + (M + C)	48	7.2	3.7
	Same + tempering at 650 °C	20–25 % A + (M _t + M + C)	36	5.5	2.9
8	Case-hardening	75–80 % A + (M + C)	39	6.4	5.8
	Same + tempering at 650 °C	50–55 % A + (M _t + M + C)	41	6.9	5.3
14	Case-hardening	95–97 % (A + C)	26	3.7	4.1
	Same + tempering at 650 °C	85–90 % A + (M + C)	35	4.8	4.6

* A – austenite; C – carbides; M – martensite; M_t – tempered martensite.

pering at 650 °C due to activation of DDMT as a result of precipitation of carbides from austenite.

In grit flow tests, the highest wear resistance was fixed after case-hardening of the deposited metal with 8 % Mn and containing 75–80 % of retained austenite in its structure.

As established, tempering may have a different effect on wear resistance of the deposited metal when tested in the grit flow, depending on its manganese content. At the 5 and 8 % Mn content, it decreased after tempering at 650 °C, whereas at the 14 % Mn content it increased. This can be explained as follows. Tempering at 650 °C is accompanied by weakening of martensite and excessive activation of DDMT at the 5 and 8 % Mn content, when stability of austenite is low, this leading to decrease in wear resistance. At a manganese content of 14 %, when stability of austenite is increased, activation of DDMT, on the contrary, increases wear resistance.

In all the cases, the method proposed for improvement of wear resistance by subjecting the low-carbon deposited metal alloyed with manganese to case-hardening provides for formation of retained meta-stable austenite in its structure, in addition to martensite and carbides. This is its characteristic feature, as traditional methods are aimed at providing the martensite-carbide structure after case-hardening and subsequent heat treatment, whereas retained austenite is considered to be an undesirable structural component that decreases hardness and wear resistance. At the same time, it is important to take into account that the highest wear resistance can be achieved at the optimal stability of austenite with regard to DDMT for a specific type of loading or testing.

High stability of overcooled austenite in the deposited metal containing no more than 5 % Mn to formation of the ferrite-cementite mixture allows using no special hardening environments, as self-hardening takes place during the process of air cooling. Important advantages in this case are the absence of cracks, increase in wear resistance, simplification of

the technology, as well as the cost-effective and environment-friendly technological process.

CONCLUSIONS

1. It is shown that development of sparsely alloyed cladding low-carbon manganese-containing consumables, which provide formation of the martensitic or martensitic-austenitic structure in the deposited metal, holds high promise.

2. High tempering conducted to relieve stresses in the deposited metal with the martensitic structure should provide formation of a certain amount of meta-stable austenite, which transforms into martensite during wear. For this, the temperature of heating and holding of the clad parts should ensure fitting the intercritical temperature range.

In a case of the primarily austenitic structure of the deposited metal, tempering should regulate stability of austenite with regard to deformation transformation of martensite allowing for the loading conditions.

3. It is suggested that deposited metal of the low-carbon steel type containing no more than 5 % Mn should be subjected to case-hardening to improve its wear resistance.

1. Malinov, V.L. (2006) Sparsely alloyed consumables providing in the deposited metal deformation hardening in operation. *The Paton Welding J.*, **8**, 25–28.
2. Tarasenko, V.V., Khomenko, G.V., Titarenko, V.I. et al. (2006) Experience of joint works of OJSC «Zaporozhstal» and PP «Remmash» in development and application of new surfacing materials. In: *Proc. of 2nd Sci.-Pract. Conf. on Improvement and Reequipment of Enterprises. Efficient Technologies of Repair and Recovery of Parts.* (Dnepropetrovsk, 2006), 39–43.
3. Bogachev, I.N., Mints, R.I. (1972) *Cavitation fractures and cavitation-resistant alloys.* Moscow: Metallurgiya.
4. Malinov, L.S., Malinov, V.L. (2007) *Sparsely doped alloys with martensitic transformations and strengthening technologies.* Kharkov: KhFTI.
5. Bogachev, I.N., Egoiaev, V.F. (1973) *Structure and properties of iron-manganese alloys.* Moscow: Metallurgiya.
6. Litvinov, V.S. (1979) *Structure and stability of phases with high contact resistance.* Syn. of Thesis for Dr. of Techn. Sci. Degree. Sverdlovsk: S.M. Kirov UPI.
7. Malinov, L.S., Malinov, V.L. *Method of strengthening.* Pat. 63462 Ukraine. Int. Cl. C21 D1/2. Publ. 15.01.2004.

STRUCTURE AND PROPERTIES OF DEPOSITED WEAR-RESISTANT Fe–Cr–Mn STEEL WITH A CONTROLLABLE CONTENT OF METASTABLE AUSTENITE

Ya.A. CHEJLYAKH and V.V. CHIGAREV

Priazovsky State Technical University, Mariupol, Ukraine

The paper gives the results of investigation of the structure and phase transformations of metal deposited with flux-cored wire PP-Np-20Kh12G10SF. Possibility of controlling the content, degree of metastability of austenite and wear resistance of deposited metal of Fe–Cr–Mn system is shown.

Keywords: arc hardfacing, flux-cored wire, wear resistance, metastable austenite, martensite

Development of highly efficient methods of reconditioning and strengthening of worn working surfaces of rapidly wearing parts of diverse equipment remains to be a highly urgent task. One of its solutions is development of hardfacing materials, providing deformational metastability of austenite of the deposited alloyed steel, capable of considerable deformation strengthening during wear [1–3]. A considerable contribution into formation of properties of such deposited metal is made by realization of deformation $\gamma \rightarrow \alpha'$ and $\gamma_{res} \rightarrow \alpha'$ martensite transformations at testing (DMTT) or in service [2–8]. However, these advantages are so far insufficiently used in flux-cored hardfacing consumables and metastable wear-resistant steels deposited using them, and published data on studying the capabilities of controlling the degree of metastability of deposited metal are quite limited [6, 7]. Therefore, development of new electrode materials, ensuring deposition of such metastable sparsely-alloyed steels with a controllable amount and metastability of austenite, is a quite urgent task, which is of a certain scientific and applied interest.

The purpose of this work is studying the structure, phase transformations, possibilities for controlling the quantity and metastability of austenite and properties of Fe–Cr–Mn wear-resistant steel deposited with developed flux-cored wire PP-Np-20Kh12G10SF [8].

Deposition with developed 4 mm flux-cored wire was performed with AN-348 flux on steel St3 and steel 45 in the following modes: $I_{hf} = 320\text{--}480$ A, $U_a = 28\text{--}32$ V, $v_{hf} = 22\text{--}32$ m/h. Various design-technological schematics of hardfacing were used: in one, two and three layers, as well as four-five layers similar to the way it is done for actual parts. Samples for investigations were prepared from the deposited metal. Fraction of base metal in the weld metal was determined by the ratio of penetration area to total area

of deposited metal. Digital images were entered into the computer, where they were processed by the procedure from [9]. Fraction of base metal was varied by adjustment of hardfacing parameters (I_{hf} , U_a , v_{hf}) that allowed controlling the composition of the deposited metal, particularly chromium and manganese content [1].

Analysis of chemical composition was conducted in vacuum quantometers «Spectrovac 1000» and «SpectroMAXx» by the spectral method, phase analysis of deposited metal was performed in X-ray diffractometer DRON-3 in Fe- K_α -radiation, in the range of angles $2\theta = 54\text{--}58^\circ$, macroscopic analysis – on transverse and longitudinal macrosections of deposited metal with deep etching in an acid mixture (100 ml HCl, 10 ml HNO₃ and 100 ml H₂O). Microstructures were studied in metallographic microscopes MMR-2 and «Neophot-21» ($\times 50\text{--}500$), microhardness of structural components was measured in PMT-3 microhardness meter by indentation of a tetrahedral diamond pyramid under 1.96 N load, and deposited metal hardness – in TK (Rockwell) instrument with 1500 N (HRC) and 600 N (HRA) load. Dynamic testing was conducted in an impact pendulum-type testing machine IO5003 on samples of $10 \times 10 \times 55$ mm size with U-shaped notch. Wear testing at dry metal-to-metal friction was performed in MI-1M machine on samples of $10 \times 10 \times 27$ mm size by the schematic of the block (tested sample)–roller (rider) rotating at the speed of 500 min^{-1} (linear speed in the friction zone of 1.31 m/s, friction path of 1965 m). Time of wearing between two weighing operations was equal to 5 min that ensured heating of the contact surface (similar to heating of equipment parts under the actual wearing conditions), total wearing time was 25 min. Weighing was conducted with the accuracy of up to 0.0001 g. Relative wear resistance was determined from the following formula

$$\varepsilon = \frac{\Delta m_r}{\Delta m_s}$$

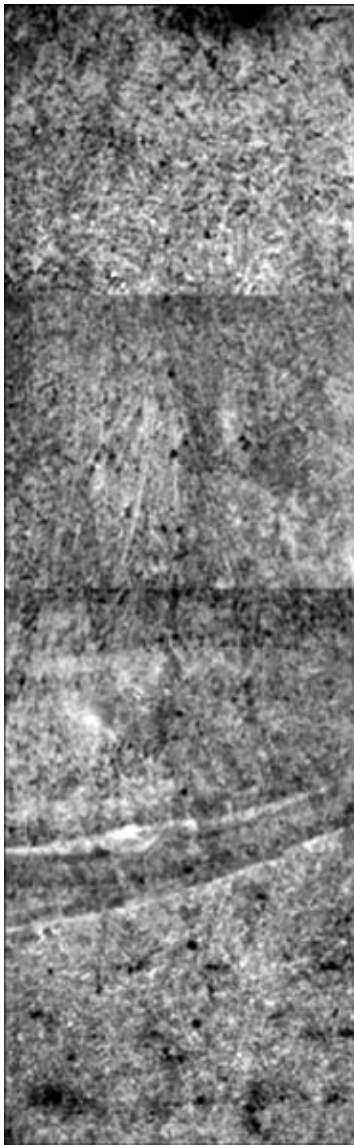


Figure 1. Change of microstructure ($\times 50$) of Fe-Cr-Mn steel in single-layer deposited state

where Δm_r , Δm_s is the weight loss of reference sample and deposited metal sample during the same wearing period, respectively.

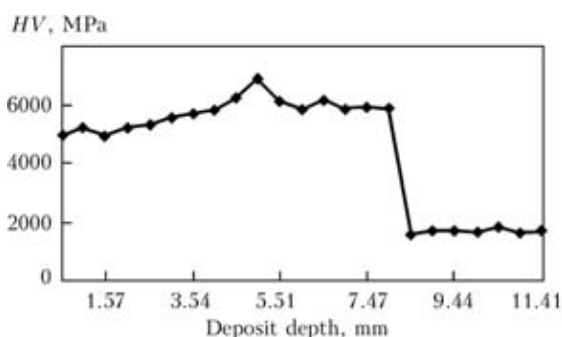


Figure 2. Distribution of microhardness by depth of single-layer deposited Fe-Cr-Mn metal

Steel 45 of hardness HB 180–190 was used as the reference sample. Testing for impact-abrasive wear was conducted in a unit shown in [10] in the environment of cast iron shot (0.5–1.5 mm particle size) with the speed of sample rotation of 2800 min^{-1} . Testing for abrasive wear was conducted by Brinell–Howard schematic. Relative impact-abrasive $\varepsilon_{\text{im,a}}$ and abrasive ε_a wear resistance was also determined by the above formula.

At flux-cored wire hardfacing the required formation of the deposited layer without any visible defects and good separability of the slag crust were ensured. Height of the deposited layer at one-layer hardfacing was 6–8, at two-layer — 11–15 and at three-layer 16–18 mm, respectively. Composition of the deposited metal, depending on the number of layers and welding-technological parameters, corresponds to the composition of steel of 20Kh(7–12)G(5–9)SF type. In the case of one- and two-layer hardfacing chromium content in the deposited metal was in the range of 6.41–7.98 %, that of manganese — 4.86–5.60 %.

Microstructure* of one-layer deposited metal consists of martensite and 15–35 % residual austenite A_{res} (see Figure 1). Structure is non-uniform across deposited metal thickness. Martensite has a pack (lath) structure, which is indicative of the fact that this is low-carbon martensite. Upper zone of small dimensions (0.6–0.8 mm) in one-layer deposit has fine-crystalline structure (see Figure 1). This is followed by a rather extended (2–5 mm) zone with clear-cut elongated predominantly towards the hardfaced surface crystals of about 0.02 mm thickness and about 0.3 mm length. The crystals are elongated in the direction opposite to that of heat removal in-depth of the base metal. Located under it is a uniform transition zone of 0.14 to 0.30 mm thickness that borders on the fusion zone, which is adjacent to the HAZ and further on is the ferritic-pearlitic structure of base metal.

Microhardness variation in-depth of deposited Fe-Cr-Mn steel is given in Figure 2. Higher values of microhardness correspond predominantly to martensite phase, and lower values — to austenite phase. Microhardness is equal to HV 5000–5600 MPa by deposit depth of 0.59–3 mm that corresponds to austenitic-martensitic structure with prevalence of the austenite component, whereas higher values of HV 5800–7000 MPa (at the depth of 3.5–8.5 mm) — to martensitic-austenitic structure with prevalence of martensite. This is due to some possible gradient of chromium and manganese concentration by the depth of the deposited layer, affecting the position of martensite points (M_s and M_f), which predetermines the phase relationship between martensite and austenite. Then a transition zone from deposited metal to base metal is observed, characterized by an abrupt lowering of microhardness from HV 5900 MPa to HV 1600–1900 MPa and of hardness from HRC 46–48 to HRC 28, respectively.

* O.I. Trofimets participated in investigations.

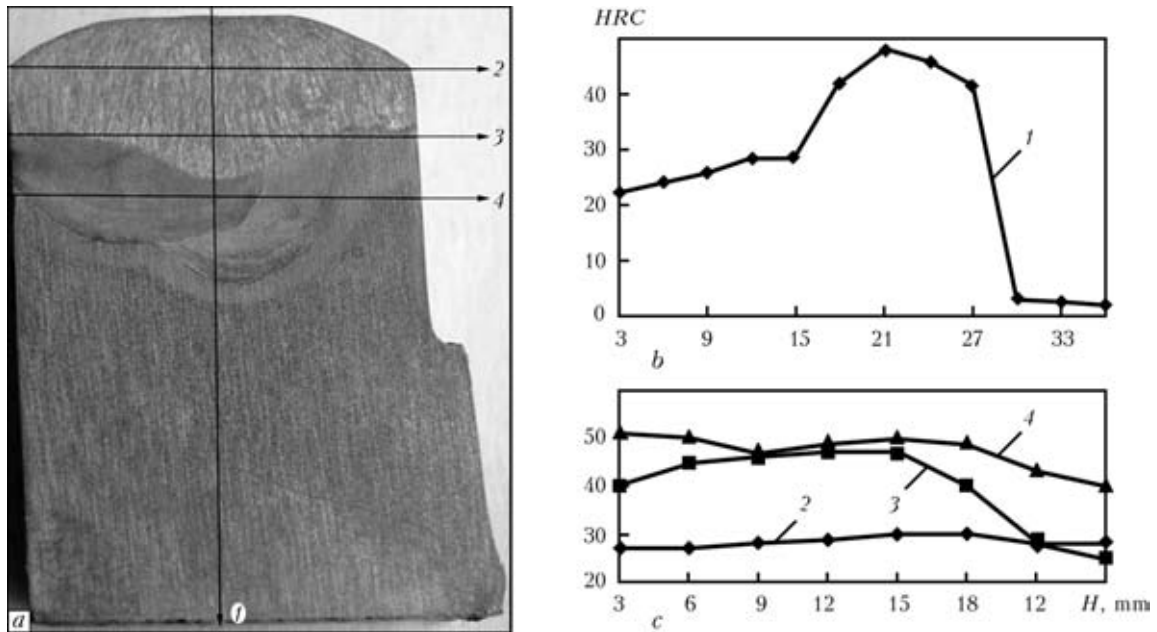


Figure 3. Macrostructure (a) and variation of hardness of transverse macrosection of multilayer deposited metal of 20Kh12G9SF type in vertical (b) and horizontal (c) directions (1–4)

Macrostructure of multilayer deposited metal* is given in Figure 3, where individual layers of deposited Fe–Cr–Mn metal are characterized by different degrees of etchability. The first (lower) layers have higher etchability compared to upper layers. This is attributable to different degree of their alloying: lower layers are less alloyed, as mixing and greater dilution of the weld pool by unalloyed steel of the base occurred in them. Macrostructure of the first (lower) layers features fine grains that may be due to the processes of metal recrystallization at heating, due to the heat of the deposited next layer. HAZ metal is of a lighter colour that is also attributable to recrystallization of the base metal under the fusion zone. The upper layer is characterized by a dendritic structure.

The panorama of the change of deposited Fe–Cr–Mn metal microstructure at multilayer hardfacing is given in Figure 4. Upper layer microstructure consists predominantly of austenite with carbide particle inclusions of $(\text{Cr, Fe})_{23}\text{C}_6$, VC composition. Located under it are deposited metal layers with austenitic-martensitic and further on with martensitic-austenitic structure, also reinforced by carbide inclusions. In the upper deposited layers austenitic dendrites elongated normal to the surface are observed, which were growing in the direction opposite to that of heat removal. Austenite grains contain sliding lines and twins, as well as indications of ϵ -martensite structure, that is indicative of its deformation metastability, i.e. ability of self-strengthening at the expense of dynamic twinning and $\gamma \rightarrow \alpha'$ DMTT. Deposited metal composition is strongly influenced by the degree of penetration and fraction of base metal in the deposit metal. At

multilayer hardfacing the composition of each layer is different, depending on the fraction of base metal involved in formation of the next deposited layer.

Change of the fraction of base metal (St3) in the deposited metal influenced the composition of the deposited layers by the content of chromium (8–12 %) and manganese (5.6–9.0 %), while carbon, silicon and vanadium content remained practically constant. Differences in alloying element content within the above limits influenced the position of martensite points (M_s , M_f) and phase composition, namely quenching martensite and metastable austenite content.

The predominantly austenitic structure of the deposit upper layer is indicative of the highest content of chromium and manganese in it, lowering martensite points M_s and M_f (apparently, below room temperature). Medium deposited layers have austenitic-martensitic structure, which is due, probably, to somewhat lower content of chromium and manganese compared to upper layers. Formation of martensitic-austenitic structure in the first deposited layers is indicative of an even lower content of alloying elements due to greater mixing with the base metal. As a result, martensite point M_s is above room temperature that leads to formation of predominantly quenching martensite at cooling with a small quantity of A_{res} . Thus, hardfacing parameters responsible for different penetration, fraction of base metal participation in weld pool formation, as well as number of deposit layers allow effectively controlling its chemical and phase composition. In its turn, the degree of deformation metastability of austenite and kinetics of $\gamma \rightarrow \alpha'$ DMTT [11] essentially depend on the ratio of martensite and austenite that determines formation of mechanical characteristics, and at optimum parameters an increased level of deposited steel wear resistance is achieved.

* N.E. Karavaeva participated in investigations.

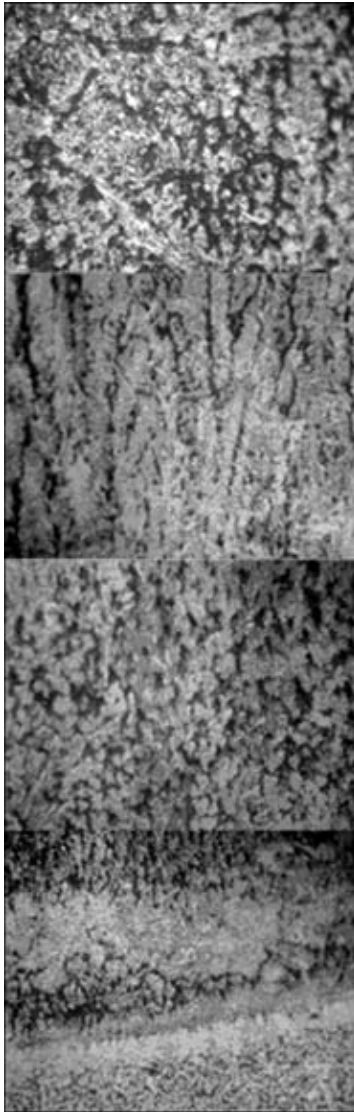


Figure 4. Change of microstructure ($\times 170$) of a transverse section of multilayer deposited Fe-Cr-Mn steel

Variation of hardness of transverse sections of deposited Fe-Cr-Mn steel in multilayer hardfacing is indirect confirmation of the nature of variation of phase composition and microstructure. Measurements were performed in keeping with the schematic, given in Figure 3, *a*, and change of hardness values in the vertical 1 and horizontal 2–4 directions is shown in Figure 3, *b*, *c*. Upper layer of the deposited metal is characterized by low hardness from *HRC* 22 up to *HRC* 28 that corresponds to the austenitic structure. Hardness increases by the layer depth. The highest hardness is found in the medium and lower layers of the deposited metal (*HRC* 42–47) (see Figure 3, *b*), having martensitic-austenitic structure. An abrupt lowering of hardness from approximately *HRC* 47 to *HRC* 5 takes place in the fusion zone, while martensitic-austenitic structure transforms into the initial ferritic-pearlitic structure.

Hardness variation corresponding to the considered layers is also observed in the horizontal direction (see Figure 3, *c*). Upper layer is characterized by the

Mechanical properties of deposited steel

Type of deposited metal alloying	Hardness <i>HRC</i>	Impact toughness, KCU, MJ/m ²	ε	$\varepsilon_{im.a}$	ε_a
20Kh8G6ASF	34	0.35	1.22	3.44	1.4
20Kh12G9SF	33	0.42	1.05	3.52	1.5
08Kh20N10G7ST	19	1.10	1.10	2.10	0.9

lowest hardness of *HRC* 28–30 with its uniform distribution, and medium and upper layers of the deposited metal have a higher hardness. Hardness of the medium and lower layers corresponds to *HRC* 46–48 and *HRC* 48–50. Hardness lowering to the left and right of the center along a horizontal shows an actual transition into the upper layer.

Comparative testing of wear resistance of developed Fe-Cr-Mn and Fe-Cr-Ni deposited metal of austenitic class, as well as that deposited with imported wire of Sv-08Kh20N10G7ST type (applied for hardfacing the rolls of Pilger rolling mill at «Ilyich Metallurgical Works») at different wearing conditions was conducted. Mechanical properties of hardfaced steels (without heat treatment) are given in the Table. It follows from the Table that impact toughness of Fe-Cr-Ni deposited metal is 2 times higher than that of Fe-Cr-Mn that is due to purely austenitic stable structure with a low hardness (*HRC* 19), lower content of carbon and positive influence of nickel on the ductility and toughness properties [12].

Under the conditions of dry metal-to-metal friction (with heating of friction surface) wear resistance ε of deposited Fe-Cr-Mn metal is by 10–15 % higher than that of Cr-Ni metal, and under the conditions of abrasive and impact-abrasive wear $\varepsilon_{im.a}$ is 1.5–1.8 times higher. This is attributable to metastability of austenite in the structure of 20Kh8G6ASF steel and considerable self-strengthening of the surface layer during wearing due to running of $\gamma \rightarrow \alpha'$ DMTT. If before wearing deposited 20Kh8G6ASF metal contained 15 % of quenching martensite and 85 % of metastable austenite, after abrasive-impact wearing martensite content in the surface layer increased up to 41 %. Deposited 20Kh12G9SF metal contained 100 % of metastable austenite, and after wearing at dry friction 27.5 % of deformation martensite was detected in the surface layer of samples, alongside austenite. Obtained data are indicative of the fact that a higher level of service durability of the developed nickel-free deposited metal can be achieved, compared to Cr-Ni one, deposited with 08Kh20N10G7ST wire (deficit and much more expensive – approximately 1300–1500 USD/t).

Composition of deposited 20Kh12G9SF metal should be regarded as optimum in terms of complete implementation of the capabilities of $\gamma \rightarrow \alpha'$ DMTT for increase of wear resistance. Methods of heat treat-

ment, chemico-thermal treatment, plasma or electron beam impact can be used to additionally create new heterophase-structural modifications to control the properties of the developed deposited metal.

CONCLUSIONS

1. Composition and structure of the deposited metal change by a certain law across the deposit thickness, depending on the number of deposited layers, degree of penetration and fraction of base metal in the deposit.

2. Modes of electric arc surfacing allows effective control of phase composition (austenite and martensite ratio), degree of metastability of the austenite component of deposited Fe–Cr–Mn metal, and, as a result, its mechanical properties.

3. Comparative testing showed an increased wear resistance of the deposited metastable Fe–Cr–Mn metal, compared to the known Cr–Ni composition of metal deposited using expensive and deficit 08Kh20N10G7ST wire.

1. Livshits, L.S., Grinberg, N.A., Kurkumelli, E.G. (1969) *Principles of alloying of deposited metal*. Moscow: Mashinostroenie.
2. Razikov, M.I., Tolstov, I.A., Kulishenko, B.A. (1966) Experience in application of deposited metal of 30Kh10G10T

type for hardfacing of rapidly wearing parts. *Svarochn. Proizvodstvo*, **9**, 30–31.

3. Kulishenko, B.A., Shumiyakov, V.A., Maslich, S.Yu. (1985) Application of martensite transformation in deformation for increase in wear resistance of deposited metal. In: *Hardfacing: experience and efficiency of application*. Kiev.
4. Filippov, M.A., Litvinov, V.S., Nemirovsky, Yu.P. (1988) *Steels with metastable austenite*. Moscow: Metallurgiya.
5. Kovalchuk, A.I., Oldakovsky, A.I., Malinov, L.S. et al. (1984) Increase in serviceability of cylinders of pilgrim mills by hardfacing using new flux-cored wire 35ZhN. *Svarochn. Proizvodstvo*, **7**, 12–13.
6. Malinov, L.S., Chejlyakh, A.P., Kharlanova, E.Ya. et al. (1995) Development and investigation of new flux-cored strip for hardfacing of bridge crane wheels. *Ibid.*, **10**, 22–25.
7. Malinov, V.L., Chigarev, V.V. (1997) Influence of structure on wear resistance of deposited metal in different types of impact-abrasive wear. *Vestnik PGTU*, Issue 3, 141–144.
8. Cheiliakh, Y., Chigarev, V., Sheychenko, G. (2009) The creation of a new economical (nickel free) powder-like wire for surfacing made of metastable metal, self-strengthened during wearing. In: *Proc. of 1st Mediterranean Conf. on Heat Treatment and Surface Engineering in the Manufacturing of Metallic Engineering Components* (Sharm El-Sheikh, 1–3 Dec., 2009).
9. Akulov, A.I., Alyoshin, N.P., Chernyshov, G.G. (2004) *Welding. Cutting. Control: Refer. Book. Vol. 2*. Moscow: Mashinostroenie.
10. Chejlyakh, A.P., Olejnik, I.M. *Unit for testing on impact-abrasive wearing*. USSR author's cert. 1820300. Int. Cl. G01N 3/56. Publ. 07.06.93.
11. Chejlyakh, A.P. (2003) *Sparcellly alloyed metastable alloys and strengthening technologies*. Kharkov: KhFTI.
12. Meskin, V.S. (1964) *Principles of alloying of steel*. Moscow: Metallurgiya.

INTERNATIONAL SCIENTIFIC-METHODOLOGICAL CONFERENCE

September 26, 2011

A.M. Petrichenko Chair of
Metal Technology and Materials Science
KhARI, Kharkov

Organizers: Kharkov National Automobile and Road University (KhARI), CJSC SPA «Aerokosmoekologiya Ukrainy», Moscow Automobile-Road Institute (MADI), A.A. Baikov Institute of Metallurgy and Materials Science, Belgorod V.G. Shukhov STU, SE «Zavod in. V.A. Malysheva».

Conference subjects:

- urgent problems of determination of material hardness by kinetic indentation
- modern materials science – state-of-the-art, problems, prospects
- structural material technologies: foundry, welding fabrication, metal machining, metal forming

Contacts: mvi@khadi; kharkov.ua



ADMISSIBLE PRESSURE FOR FILLER OF SEALED SLEEVES USED TO REPAIR MAIN PIPELINES

V.I. MAKHNENKO, E.A. VELIKOIVANENKO, A.S. MILENIN, O.I. OLEJNIK, G.F. ROZYNKA and N.I. PIVTORAK
E.O. Paton Electric Welding Institute, NASU, Kiev, Ukraine

Main variants of strengthening of thinning of pipeline walls by installing a sealed sleeve are considered. It is shown that the variant of the repair technology involving a sleeve structure with a liquid agent filling the gap between the pipe walls and sleeve requires a detailed substantiation, allowing for properties of the filler during polymerisation, as well as corresponding estimation of the load-carrying capacity of the welds.

Keywords: repair of active pipelines, sealed sleeves, slot welds, volumetric changes during polymerisation

In the last years, repair of extended corrosion defects on walls of active main pipelines, i.e. under the internal pressure of gas or oil, has been performed in Ukraine by using sealed sleeves of different designs, the main purpose of which is to partially unload the defective region of the pipeline wall, this being sufficient in a number of cases for changing characterisation of a defect from «inadmissible» to «admissible» [1].

For the linear part of a pipeline loaded mostly by the internal pressure, the efficiency of unloading of the defective pipe wall using a sleeve depends on many structural and technological factors providing a contact fit between the sleeve and pipe wall.

Figure 1 presents the known mechanical methods providing a good fit of the pipe walls and sleeve, which show a high labour intensiveness and complexity of the control means used to check their efficiency. This problem can be solved much simpler by using the appropriate filler for the gap between the pipe walls and sleeve. Sleeves of this type are more attractive, as they allow reliable and simple unloading of the defective pipe wall due to the controllable pressure in a liquid filler of the gap between the walls.

The scheme shown in Figure 2 demonstrates the principle of operation of a structure, which has certain

advantages and peculiarities. The latter include the presence of circumferential welds 6, which adjoin the gap containing the filler with pressure P_f , its maximal value being specified by the authors of patent [3] in a range of up to repair pressure P_{rep} in a pipe.

A crack-like slot forms in the adjoining zone at the presence of steel ring 2 (see Figure 2), which provides the required gap between the walls, i.e. circumferential welds 6 should be classed with the so-called slot joints, which are designed on the basis of fracture mechanics approaches for crack-containing bodies [4]. The limiting state for this type of the welded joints is usually specified based on a condition that the adjoining sharp cavity, i.e. crack, should be in the field of the stressed state, in which the conditions of its spontaneous growth are met. Worthy of attention among such sufficiently grounded conditions is a two-parameter criterion of tough-brittle fracture [4], which relates parameter of a purely brittle fracture at the crack apex, $K_r = K_I/K_{Ic}$ (where K_I is the stress intensity factor at the normal fracture crack apex, and K_{Ic} is the critical value of this indicator for a given material) to parameter of purely tough fracture for a given crack, $L_r = \sigma_{ref}/\sigma_y$ (where σ_{ref} is the reference stress that conditionally takes place at the apex of the given crack at the indicated value of loading and condition of ideal yield of the material with yield stress

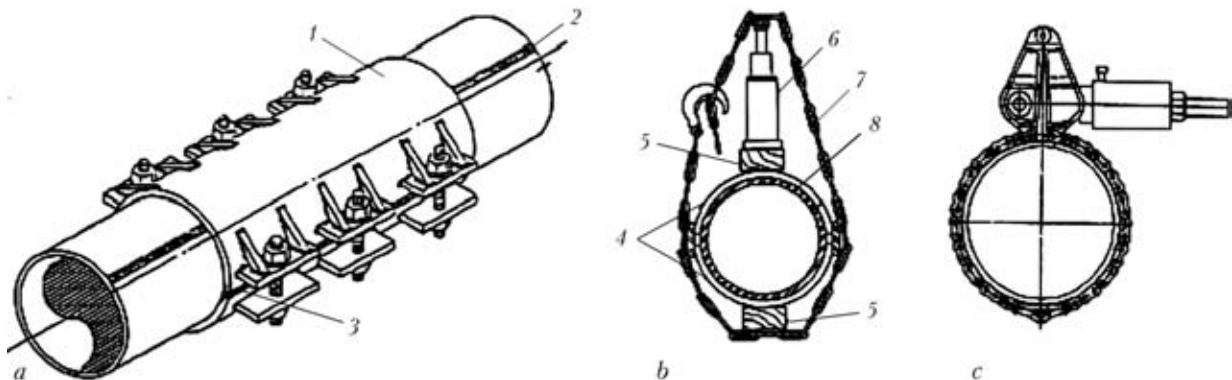


Figure 1. Schematics of mechanical methods providing fit of the sleeve to pipe wall [2]: *a* – bolted method; *b* – standard method; *c* – with chain pinch; 1 – repair sleeve; 2 – longitudinal weld; 3 – weld with full penetration and fusion with the substrate (two symmetric joints are used more frequently); 4 – sleeve halves with side supports; 5 – wood skid; 6 – hydraulic press; 7 – high-strength chain; 8 – pipeline being repaired

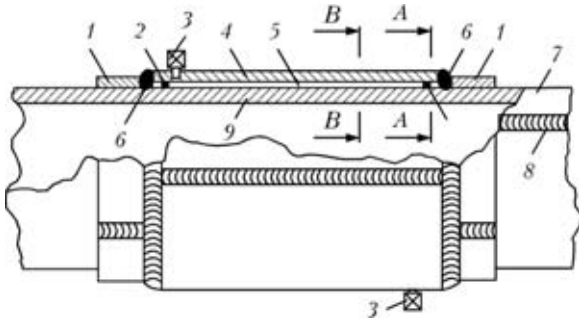


Figure 2. Schematic of the repair method using the sealed sleeve with filler [3]: 1 – technological rings; 2 – additional thin-walled ring; 3 – union; 4 – sleeve; 5 – filler; 6 – circumferential welds; 7 – pipeline; 8 – longitudinal weld; 9 – defective region

σ_y). According to [4], this criterion can be represented as follows:

$$K_r = f(L_r) \text{ at } L_r < L_r^{\max} \approx \frac{\sigma_y + \sigma_t}{2\sigma_y}; \quad (1)$$

$$K_r = 0 \text{ at } L_r > L_r^{\max},$$

where $f(L_r)$ is the experimental function for the given material (Figure 3).

According to [4], curve $f(L_r)$ (see Figure 3) for structural steels at $L_r < L_r^{\max}$ can be adequately described by relationship

$$f(L_r) = (1 - 0.14L_r^2)[0.3 + 0.7 \exp(-0.65L_r^6)]. \quad (2)$$

According to [4], values K_1 and σ_{ref} for the slot-type welded joints (see Figure 2) can be conveniently computed by preliminarily computing bending moment M and intersecting force Q acting in the zone of the welded joint per its unit length (along the circumference) and by using the following relationships [4]:

$$K_1 = \frac{0.5369}{\sqrt{h}} \left(Q \cos \varphi + \frac{8M}{h} \right), \quad (3)$$

$$\sigma_{ref} = \sqrt{\left(\frac{4M}{h^2} + \frac{Q \cos \varphi}{h} \right)^2 + 3 \left(\frac{Q \sin \varphi}{h} \right)^2}, \quad (4)$$

where h is the minimal size from the sharp cavity apex in the weld to a free surface (Figure 4). There are two such sizes h_1 and h_2 . It is likely that size h_1 is more conservative:

$$h_1 = \delta_s \cos \varphi; \cos \varphi = (1 + \beta^2)^{-0.5}; \beta = \frac{\delta_s + \Delta - \delta_{t,r}}{a}. \quad (5)$$

Safety factor $n \geq 1$ is determined from the computed values of K_r and L_r by points nK_r and nL_r on dependence (2).

As follows from the above-said, the limiting state of tough-brittle fracture (spontaneous growth of the crack, i.e. sharp cavity, adjoining the circumferential weld) is determined by bending moment M and intersecting force Q , which depend on the internal pressure in the pipe, P_p , and in the filler, P_f , as well as by the geometric sizes of a section (see Figure 4), i.e.

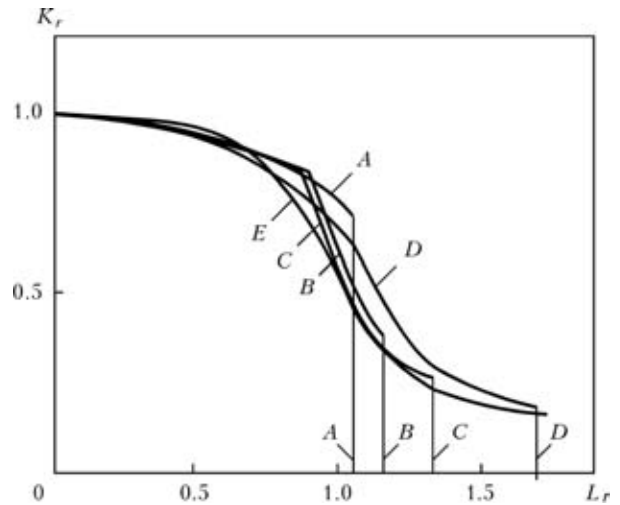


Figure 3. Diagram of limiting state $K_r = f(L_r)$ for different types of structural steels: A – high-strength steel EN408; B – pressure vessel steel A533B; C – manganese-containing low-carbon steel; D – austenitic steel; E – calculated curve plotted from dependence (2)

pipeline diameter D , thicknesses of the pipeline and sleeve, δ_p and δ_s , respectively, and those of technological rings $\delta_{t,r}$, sizes c , a , and b of the welded joint, inter-wall gap Δ , and corresponding characteristics K_{1c} , σ_y and σ_t of the welded joint material in sections of minimal sizes h_1 and h_2 .

To generate the appropriate quantitative results, by using computer system «Weldpredictions» the E.O. Paton Electric Welding Institute developed a software to compute the stressed state for corresponding geometrical sizes and loads P_p and P_f by the finite element method. Moment M and intersecting force Q at the apex of the sharp cavity were computed from normal stresses σ_{zz} in section $z = z^*$ (see Figure 4) corresponding to the apex of the sharp cavity growing in direction h_1 or h_2 .

Moment M can be represented in the form of difference $M = M_1 - M_2$, where

$$M_1 = \int_{-\frac{\delta_s}{2}}^{\frac{\delta_s}{2}} \sigma_{zz} \xi d\xi; \quad M_2 = \int_{-\frac{\delta_s + \Delta}{2}}^{\frac{\delta_p + \Delta}{2}} \sigma_{zz} \xi d\xi, \quad (6)$$

for a variant of crack propagating in direction h_1 , and respectively

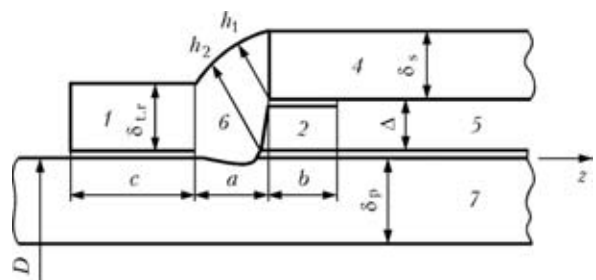


Figure 4. Schematic of section of circumferential weld 6 with designations of elements as given in Figure 2



$$M_1 = \int_{-\frac{\delta_s + \Delta}{2}}^{\frac{\delta_s + \Delta}{2}} \sigma_{zz} \xi d\xi; \quad M_2 = \int_{-\frac{\delta_p}{2}}^{\frac{\delta_p}{2}} \sigma_{zz} \xi d\xi \quad (7)$$

for a variant of crack propagating in direction h_2 .

Corresponding computation results for a pipeline of steel X70 at $D = 1420$ mm, $\delta_p = 20$ mm and working pressure $P_p = 7.5$ MPa are given below for a sleeve 1400 mm long with thickness $\delta_s = 14$ mm ($a = 20$ mm under repair pressure $P_{rep} = 7.5$ MPa, and $a = 14$ mm under $P_{rep} = 0.7P_p = 5.25$ MPa).

Sizes of technological rings $\delta_{t,r}$ and c were assumed to be as follows: $\delta_{t,r} = \delta_s$, and $c = 140$ mm. Gap Δ was regulated by using additional rings 2 (see Figure 4) having width $b = 30$ mm.

Table 1. Computed values of bending moments M and intersecting forces Q at $P_{rep} = P_p$, $a = 20$ mm and $\sigma_y = 440$ MPa

P_p , MPa	P_f , MPa	n	K_I , MPa·mm ^{1/2}	σ_{ref} , MPa	M , MPa·mm ²	Q , MPa·mm
$\Delta = 3$ mm, $h_1 = 13.845$ mm						
7.5	2.0	58.35	7.6	1.9	91.6	0
7.5	2.5	8.35	53.4	13.4	640.5	0
7.5	3.0	4.49	99.2	24.8	1189.6	0
7.5	3.5	3.08	145.0	36.3	1738.8	0
7.5	4.0	2.34	190.8	47.7	2288.0	0
7.5	4.5	1.88	236.6	59.2	2837.2	0
7.5	5.0	1.58	282.3	70.7	3386.4	0
7.5	5.5	1.36	328.1	82.1	3935.5	0
7.5	6.0	1.19	373.9	93.6	4484.7	0
7.5	6.5	1.05	422.7	105.0	5033.9	20.9
7.5	7.0	0.94	473.4	116.5	5583.1	54.6
7.5	7.5	0.85	523.4	127.8	6125.6	88.2
0	7.5	0.62	719.0	162.0	7763.2	497.3
$\Delta = 12$ mm, $h_1 = 12$ mm						
7.5	0.5	8.89	50.1	13.5	484.8	0
7.5	1.0	3.72	119.7	32.2	1159.1	0
7.5	1.5	2.78	160.0	43.0	1549.6	0
7.5	2.0	2.22	200.8	54.0	1944.1	0
7.5	2.5	1.84	241.6	64.9	2339.6	0
7.5	3.0	1.58	282.4	75.9	2735.2	0
7.5	3.5	1.38	323.4	86.9	3130.8	0.9
7.5	4.0	1.20	369.8	97.9	3526.4	36.4
7.5	4.5	1.07	416.1	108.9	3922.0	71.8
7.5	5.0	0.96	462.5	119.8	4317.6	107.3
7.5	5.5	0.88	508.8	130.8	4713.2	142.7
7.5	6.0	0.80	555.2	141.8	5108.8	178.1
7.5	6.5	0.74	601.5	152.8	5504.4	213.6
7.5	7.0	0.69	646.8	163.5	5890.6	248.8
7.5	7.5	0.65	690.4	173.8	6260.2	283.6
0	7.5	0.71	632.1	148.3	5342.4	518.9

Note. Here and in Tables 2–4: $D = 1400$ mm, $\delta_p = 20$ mm, $\delta_s = 14$ mm, $b = 30$ mm and $c = 140$ mm.

Tables 1–4 give the computation results on bending moments M and intersecting forces Q for different variants of input data and fracture in direction h_1 (see Figure 4). K_I , σ_{ref} and safety factor n at $K_{Ic} = 1500$ MPa·mm^{1/2} [4] and $\sigma_y = 360$ and 440 MPa were computed on the basis of the M and Q values. It can be seen from these data that a change in yield stress from 440 to 360 MPa (for steels X70 and X60, respectively) at $P_{rep} = P_p = 7.5$ MPa and $P_{rep} = 0.7P_p$ has no significant effect on the admissible pressure in the filler $[P_f]$ at safety factor $n \approx 2$.

The substantial effect is exerted by gap Δ . As it is increased from 3 to 12 mm, $[P_f]$ decreases from 4.3 to 2.3 MPa at $P_{rep} = P_p$ (Tables 1 and 2) and from 3.5 to 1.7 at MPa $P_{rep} = 5.25$ MPa (Tables 3 and 4).

Increase in pressure P_f above the said admissible value of $[P_f]$ is undesirable, as this causes a pronounced decrease in safety factor n .

A variant of fracture in direction h_2 (see Figure 4) was also considered. The corresponding results confirm the above assumption of a more conservative variant of fracture in direction h_1 .

Therefore, it follows from the obtained computation results (see Tables 1–4) that, at the indicated sizes of the sealed sleeve [2] and conditions of filling of the inter-wall gap, it can be recommended that the pressure should be set based on a condition of maintaining integrity of the circumferential welds at a level of $[P_f] = 4.3$ –4.5 MPa at $P_{rep} = 5.25$ –7.50 MPa and $\Delta = 3$ mm. Increase of the Δ value to 12 mm causes a dramatic decrease of the admissible pressure in the filler to 1.7–2.3 MPa. As value D of the gap in many cases is within 3 mm and generated pressure P_f is not higher than 4 MPa, the structure of the repair sleeve under consideration for main pipelines with $D = 1420 \times 20$ mm, made from steels X60 and X70, can ensure high unloading of the defective zone in the pipeline wall, naturally, providing that the set value of pressure of the liquid filler does not substantially changes after its polymerization. However, this important issue requires special consideration.

Worthy of attention at the given stage is providing the admissible value of pressure P_f for specific sizes of the pipeline and sleeve considered, as recommendations of the authors of study [2] on the upper limit at a level of P_{rep} are insufficiently substantiated. Consider what happens to pressure in the filler during solidification of the latter. It is well known that transformation from the liquid state to the solid one is accompanied by a change in the relative free volume, the weight of the matter remaining unchanged. On a condition of incompressibility of the liquid phase and at a coefficient of volumetric compression of the filler equal to

$$K_f = (1 - 2\nu_f)/E_f$$

(where E_f is the normal elasticity modulus of steel and solid filler, and ν_f is the Poisson ratio of the solid



Table 2. Computed values of bending moments M and intersecting forces Q at $P_{rep} = P_p$, $a = 20$ mm and $\sigma_y = 360$ MPa

P_p , MPa	P_f , MPa	n	K_f , MPa·mm ^{1/2}	σ_{ref} , MPa	M , MPa·mm ²	Q , MPa·mm
$\Delta = 3$ mm, $h_1 = 13.845$ mm						
7.5	2.0	56.62	7.8	2.0	94.0	0
7.5	2.5	8.28	53.6	13.4	642.9	0
7.5	3.0	4.47	99.4	24.9	1292.0	0
7.5	3.5	3.06	145.2	36.3	1741.2	0
7.5	4.0	2.32	191.0	47.8	1290.4	0
7.5	4.5	1.87	236.7	59.3	2839.6	0
7.5	5.0	1.57	282.7	70.7	3390.2	0
7.5	5.5	1.35	328.6	82.2	3940.8	0
7.5	6.0	1.19	374.5	93.7	4491.4	0
7.5	6.5	1.05	423.4	105.2	5042.1	20.8
7.5	7.0	0.94	472.3	116.2	5570.8	54.0
7.5	7.5	0.85	521.1	127.3	6099.8	87.1
0	7.5	0.64	690.7	155.3	7440.9	487.3
$\Delta = 12$ mm, $h_1 = 12$ mm						
7.5	0.5	8.81	50.3	13.5	486.9	0
7.5	1.0	3.69	119.9	32.2	1161.3	0
7.5	1.5	2.76	160.2	43.1	1551.7	0
7.5	2.0	2.20	201.0	54.0	1946.3	0
7.5	2.5	1.83	241.8	65.0	2341.8	0
7.5	2.5	1.57	282.7	76.0	2737.3	0
7.5	3.0	1.37	323.7	87.0	3132.9	1.0
7.5	3.5	1.20	370.0	97.9	3528.5	36.5
7.5	4.0	1.06	416.4	108.9	3924.1	71.9
7.5	4.5	0.96	462.7	119.9	4319.7	107.4
7.5	5.0	0.87	509.2	130.9	4716.7	142.7
7.5	5.5	0.80	555.7	141.9	5113.9	178.1
7.5	6.0	0.74	599.5	152.3	5486.6	212.9
7.5	6.5	0.69	643.5	162.7	5860.5	247.6
7.5	7.0	0.65	685.6	172.6	6217.5	281.3
0	7.5	0.76	585.5	136.3	4911.8	505.4

Table 3. Computed values of bending moments M and intersecting forces Q at $P_{rep} = 0.7P_p$, $a = 20$ mm and $\sigma_y = 440$ MPa

P_p , MPa	P_f , MPa	n	K_f , MPa·mm ^{1/2}	σ_{ref} , MPa	M , MPa·mm ²	Q , MPa·mm
$\Delta = 3$ mm, $h_1 = 13.7$ mm						
5.25	1.50	1899	23.5	5.9	276.9	0
5.25	1.75	935	47.7	12.0	562.0	0
5.25	2.00	6.20	71.8	18.1	847.2	0
5.25	2.25	4.64	96.0	24.2	1132.3	0
5.25	2.50	3.71	120.2	30.3	1417.5	0
5.25	2.75	3.09	144.4	36.3	1702.6	0
5.25	3.00	2.64	168.6	42.4	1987.8	0
5.25	3.25	2.31	192.8	48.5	2272.9	0
5.25	3.50	2.05	216.9	54.6	2558.1	0
5.25	3.75	1.85	241.1	60.7	2843.2	0
5.25	4.00	1.68	265.3	66.8	3128.4	0
5.25	4.25	1.53	290.4	72.9	3413.5	6.6
5.25	4.50	1.41	317.1	78.9	3698.7	23.6
5.25	4.75	1.30	343.7	85.0	3983.8	40.7
5.25	5.00	1.20	370.4	91.1	4269.0	57.8
5.25	5.25	1.12	397.1	97.2	4554.1	74.8
5.50	5.25	1.14	390.7	96.1	4502.2	61.3
5.75	5.25	1.17	382.7	94.6	4431.9	47.2
6.00	5.25	1.19	374.6	93.1	4360.6	33.0
6.25	5.25	1.22	366.5	91.6	4289.3	18.8
6.50	5.25	1.24	358.4	90.0	4217.9	4.6
6.75	5.25	1.27	351.6	88.5	4146.6	0
7.00	5.25	1.29	345.6	87.0	4075.3	0
7.25	5.25	1.31	339.5	85.5	4003.9	0
7.50	5.25	1.34	333.5	83.9	3932.6	0
0	5.25	0.82	541.9	123.4	5778.9	357.1
$\Delta = 12$ mm, $h_1 = 10.63$ mm						
5.25	0.25	7.60	58.5	16.7	471.9	0
5.25	0.50	4.37	101.7	29.1	820.7	0
5.25	0.75	3.52	126.2	36.1	1018.4	0
5.25	1.00	2.95	150.8	43.1	1217.1	0
5.25	1.25	2.53	175.5	50.1	1416.1	0
5.25	1.50	2.22	200.2	57.2	1615.1	0
5.25	1.75	1.98	224.8	64.2	1814.2	0
5.25	2.00	1.78	249.5	71.3	2013.3	0
5.25	2.25	1.62	274.2	78.3	2212.3	0
5.25	2.50	1.48	300.0	85.4	2411.4	6.7
5.25	2.75	1.36	327.5	92.4	2610.4	23.8
5.25	3.00	1.25	354.9	99.5	2809.5	40.9
5.25	3.25	1.16	382.4	106.5	3008.6	58.1
5.25	3.50	1.09	409.9	113.6	3207.6	75.2
5.25	3.75	1.02	437.4	120.6	3406.7	92.3
5.25	4.00	0.96	464.9	127.7	3605.8	109.4
5.25	4.25	0.90	492.4	134.7	3804.8	126.6
5.25	4.50	0.86	519.9	141.7	4003.9	143.7
5.25	4.75	0.81	547.4	148.8	4202.9	160.8
5.25	5.00	0.77	574.9	155.8	4402.0	177.9
5.25	5.25	0.74	602.4	162.9	4601.1	195.0
5.50	5.25	0.74	604.3	163.8	4626.9	187.4
5.75	5.25	0.73	605.6	164.6	4648.3	179.2
6.00	5.25	0.73	606.9	165.3	4669.5	170.9
6.25	5.25	0.73	608.2	166.1	4690.7	162.7
6.50	5.25	0.73	609.4	166.8	4711.9	154.5
6.75	5.25	0.73	610.7	167.6	4733.1	146.2
7.00	5.25	0.73	612.0	168.3	4754.3	138.0
7.25	5.25	0.73	613.2	169.1	4775.5	129.8
7.50	5.25	0.72	614.5	169.8	4796.7	121.5
0	5.25	0.81	553.6	141.3	3991.2	357.7

filler), the relationship derived for the solid phase between the relative change of the volume in transformation from the liquid state to the solid one per unit weight will have the following form:

$$\frac{\Delta V}{V} = 3K_f(\sigma_{sol} - \sigma_{liq}) + \frac{\gamma_{sol} - \gamma_{liq}}{V}, \quad (8)$$

where σ_{sol} and σ_{liq} are the pressures with an opposite sign in the solid and liquid phases, i.e. $\sigma_{liq} = -P_f$; and γ_{sol} and γ_{liq} are the volumes of the solid and liquid phases per unit weight.

The $(\gamma_{sol} - \gamma_{liq})/V$ value is a constant of a given environment (e.g. for epoxy it is approximately equal to -0.06 [5, etc.]).

If solidification occurs without violation of integrity of the filler and with conservation of bonds to the pipe and sleeve, then $\Delta V/V = 0$, and

$$\sigma_{sol} = \sigma_{liq} - \frac{1}{3K_f} \frac{\gamma_{sol} - \gamma_{liq}}{V}. \quad (9)$$

As compression pressure σ_{liq} is a negative value, solidification at $(\gamma_{sol} - \gamma_{liq})/V < 0$ is accompanied by decrease of compression in the filler. The lower the K_f value in the solid filler, the more intensive is this decrease.

For example, for polyurethane that is widely used in Ukraine, the value of K_f is at a level of 0.002 MPa⁻¹, i.e. at $(\gamma_{sol} - \gamma_{liq})/V$ it is lower than -0.03 . The condition of conservation of $\sigma_{sol} < 0$ requires that the



Table 4. Computed values of bending moments M and intersecting forces Q at $P_{rep} = 0.7P_p$, $a = 20$ mm and $\sigma_y = 360$ MPa

P_p , MPa	P_{re} , MPa	μ	K_f , MPa·mm ^{1/2}	σ_{res}^f , MPa	M , MPa·mm ²	Q , MPa·mm
$\Delta = 3$ mm, $h_f = 13.7$ mm						
5.25	1.50	1890	23.5	5.9	276.9	0.0
5.25	1.75	9.31	47.7	12.0	562.0	0.0
5.25	2.00	6.18	71.8	18.1	847.2	0.0
5.25	2.25	4.62	96.0	24.2	1132.3	0.0
5.25	2.50	3.69	120.2	30.3	1417.5	0.0
5.25	2.75	3.07	144.4	36.3	1702.6	0.0
5.25	3.00	2.63	168.6	42.4	1987.8	0.0
5.25	3.25	2.30	192.8	48.5	2272.9	0.0
5.25	3.50	2.05	216.9	54.6	2558.1	0.0
5.25	3.75	1.84	241.1	60.7	2843.2	0.0
5.25	4.00	1.67	265.3	66.8	3128.4	0.0
5.25	4.25	1.53	290.4	72.9	3413.5	6.6
5.25	4.50	1.40	317.1	78.9	3698.7	23.6
5.25	4.75	1.29	343.7	85.0	3983.8	40.7
5.25	5.00	1.20	370.4	91.1	4269.0	57.8
5.25	5.25	1.12	397.1	97.2	4554.1	74.8
5.50	5.25	1.14	390.7	96.1	4502.2	61.3
5.75	5.25	1.16	382.7	94.6	4431.9	47.2
6.00	5.25	1.19	374.6	93.1	4360.6	33.0
6.25	5.25	1.21	366.5	91.6	4289.3	18.8
6.50	5.25	1.24	358.4	90.1	4218.8	4.5
6.75	5.25	1.26	351.8	88.5	4148.1	0.0
7.00	5.25	1.28	345.7	87.0	4076.8	0.0
7.25	5.25	1.31	339.8	85.5	4006.4	0.0
7.50	5.25	1.33	333.8	84.0	3935.8	0.0
0	5.25	0.83	536.8	122.2	5723.5	354.6
$\Delta = 12$ mm, $h_f = 10.63$ mm						
5.25	0.25	7.56	58.5	16.7	471.9	0.0
5.25	0.50	4.35	101.7	29.1	820.7	0.0
5.25	0.75	3.50	126.2	36.1	1018.4	0.0
5.25	1.00	2.95	150.8	43.1	1217.1	0.0
5.25	1.25	2.52	175.5	50.1	1416.1	0.0
5.25	1.50	2.21	200.2	57.2	1615.1	0.0
5.25	1.75	1.97	224.8	64.2	1814.2	0.0
5.25	2.00	1.77	249.5	71.3	2013.3	0.0
5.25	2.25	1.61	274.2	78.3	2212.3	0.0
5.25	2.50	1.47	300.0	85.4	2411.4	6.7
5.25	2.75	1.35	327.5	92.4	2610.4	23.8
5.25	3.00	1.25	354.9	99.5	2809.5	40.9
5.25	3.25	1.16	382.4	106.5	3008.6	58.1
5.25	3.50	1.08	409.9	113.6	3207.6	75.2
5.25	3.75	1.01	437.4	120.6	3406.7	92.3
5.25	4.00	0.95	464.9	127.7	3605.8	109.4
5.25	4.25	0.90	492.4	134.7	3804.8	126.6
5.25	4.50	0.85	519.9	141.7	4003.9	143.7
5.25	4.75	0.81	547.4	148.8	4202.9	160.8
5.25	5.00	0.77	574.9	155.8	4402.0	177.9
5.25	5.25	0.74	602.4	162.9	4601.1	195.0
5.50	5.25	0.73	604.3	163.8	4626.9	187.4
5.75	5.25	0.73	605.6	164.6	4648.3	179.2
6.00	5.25	0.73	606.9	165.3	4669.5	170.9
6.25	5.25	0.73	608.2	166.1	4690.7	162.7
6.50	5.25	0.73	609.4	166.8	4711.9	154.5
6.75	5.25	0.72	610.7	167.6	4733.1	146.2
7.00	5.25	0.72	612.1	168.3	4755.1	137.9
7.25	5.25	0.72	613.4	169.1	4777.0	129.6
7.50	5.25	0.72	614.7	169.9	4798.2	121.4
0	5.25	0.83	536.0	136.5	3855.6	359.1

initial pressure in the filler, $P_f = -\sigma_{sol}$, be higher than $0.03/3 \cdot 0.002 = 5$ MPa, which, as follows from the above-said, is a limit of structural capabilities of the circumferential welds of the welded joints in the sleeves under consideration [3].

Moreover, it should be taken into account that providing the σ_{sol} value in the solidified filler at a zero level, the value of volumetric compression coefficient

$K_f = (1 - 2\nu_f)/E_f$ being low, may lead to an insufficient unloading of the defective wall, i.e. it may affect the efficiency of operation of the sleeve, which will require an additional 2–3 MPa increase in P_f .

Therefore, the structure of the sleeve and its welds should withstand the inter-wall pressure at a level of that of the working gas in a pipe, which is quite realistic if the defect in the pipe wall under the sleeve for this or that reason becomes a through defect.

The extent of unloading of the defective region of a pipeline due to installing the sealed sleeve with the filler can be estimated by using the following approximating dependence:

$$\Delta P = -\sigma_{res}^f + \frac{P - P_{rep}}{1 + \frac{\delta_p}{\delta_s} + A_f}, \quad A_f = K_f \frac{E\delta_p\delta_f}{(D/2)^2}, \quad (10)$$

where ΔP is part of working pressure P relieved due to the sealed sleeve with the filler in the gap between the walls of a pipe and sleeve, σ_{res}^f is the residual mean normal pressure in the solid filler, $K_f = (1 - 2\nu_f)/E_f$ is the coefficient of volumetric compression of the solid filler, and δ_f is the thickness of the filler.

In case of a purely mechanical contact of the pipe and sleeve, in (10) $\delta_f = 0$, $A_f = 0$ and, accordingly,

$$\sigma_{res}^f = 0. \text{ At the same time, in (10) } \Delta P = \frac{P - P_{rep}}{\delta_s + \delta_p} \delta_s$$

depends on $P - P_{rep}$, and it can be insufficient for efficient unloading of the defective region of the wall. Here it is the filler that provides wider possibilities. However, in this case the geometric sizes of the sleeve and welded joints should guarantee achievement of the corresponding value of σ_{res}^f in the solidified filler.

CONCLUSIONS

1. Structures of the sealed sleeves with fillers, as recommended in modern literature for repair of thinning defects in walls of main pipelines without interruption of their operation, are insufficiently substantiated in a number of cases, as welded joints cannot withstand the internal pressure of the liquid filler at a level of the working pressure of gas in a pipe.

2. When developing such structures, it is necessary to pay special attention to a change in properties of the filler taking place during its solidification from the stand point of providing the required pressure for efficient unloading of the defective region of the pipeline wall.

- (2000) *Fitness-for-service: Recommended practice 579*. American Petroleum Institute.
- (2006) *Updated pipeline repair manual*. Revision by Edison Welding Institute.
- But, V.S., Marchuk, Ya.S., Podolyan, O.P. et al. *Method for repair of defective section of active pipeline*. Pat. 77931 Ukraine. Int. Cl. F 16 L 55/16, B 23 K 31/02. Publ. 15.01.2007.
- Makhnenko, V.I. (2006) *Residual safe life of welded joints and assemblies in current structures*. Kiev: Naukova Dumka.
- Zarelli, V., Skordos, A.A., Partridge, I.K. (2000) Investigation of cure induced shrinkage in unreinforced epoxy resin. *Plastics, Rubber and Composites Processing and Application*, **31**, 377–384.



FEATURES OF FORMATION OF DISSIMILAR METAL JOINTS IN HOT ROLL WELDING IN VACUUM

I.M. NEKLYUDOV, B.V. BORTZ and V.I. TKACHENKO

National Science Center «Kharkov Institute of Physics and Technology», NASU, Kharkov, Ukraine

Features of formation of the boundary of solid-phase joint of dissimilar materials are presented, and its influence on tensile strength is shown, depending on ductility of materials being joined. Experimental results are compared with the theoretical model, which allows for plastic deformation of materials at their joining temperature, as well as shear forces arising in material rolling and having a determinant role in the process of solid-phase joining of materials. The paper gives experimental results of X-ray microprobe analysis, metallography, as well as investigations of the boundary of solid-phase joint of samples, including tensile, micro- and nanohardness tests. Obtained data led to the conclusion about the possibility of forming strength characteristics of dissimilar metal joint boundary.

Keywords: vacuum roll welding, solid phase, joint boundary, formation features, strength, ductility

Solid-phase welding of dissimilar materials by hot rolling in vacuum opened up new promising directions in application of this joining process in industry [1–5]. Known methods of joining dissimilar materials are based on plastic deformation of material and, as a rule, in the uniaxial direction. Theory of solid-phase joining was developed for the case of these technologies [3]. Features of distribution of atoms in metals at pulsed impact were studied in [6]. Processes of plastic deformation have been experimentally studied in [7–9]. Problem of mass transfer was studied in [7, 10, 11], and the phenomenon of phase formation under the conditions of increased rates of dissimilar material deformation in pressure welding — in [7, 12].

Method of hot rolling in vacuum [13–17] essentially changes the theoretical concept of the phenomenon of solid-phase joining of large massive plates from dissimilar materials across their thickness and along their length. Solid-phase welding of dissimilar materials by rolling method is achieved through plastic deformation of materials. Material of a higher ductility deforms to a greater extent and slides over the material of a lower ductility. At sliding and action of forces pressing the plates together, friction forces are induced, cleaning of subsurface layers proceeds, and at further deformation solid-phase joining of materials takes place [18–21].

Dry sliding friction between the ductile solid materials is an example of macroscopic property, controlled by localized plastic deformation on the meso-level, whereas the structure on the atomic level and composition of contacting surfaces are the determinant factors for solid-phase joining of materials. Interrelation of the contacting solids and disordering on the atomic level were theoretically traced in the interface zone [22].

The purpose of this work is investigation of the processes occurring in solid-phase welding of dissimi-

lar materials by the method of hot rolling in vacuum, determination of the regularities of variation of tensile strength of the solid-phase joint boundary σ_t , comprehensive investigation by the methods of X-ray microanalysis and metallography of the sample joining boundary and its tensile, micro- and nanohardness testing to study the processes affecting the strength of the joint boundaries.

Solid-phase joining of dissimilar metals was performed at high temperature in a vacuum rolling mill DUO-170 (Figure 1). The machine consists of a vacuum system, ensuring a vacuum of $p = 1 \cdot 10^{-2} - 1 \cdot 10^{-3}$ Pa, furnace for sample heating up to temperature $T \approx 900 - 1200$ °C and roll chamber providing rolling speed $v_0 = 0.03 - 0.30$ ms⁻¹ and cogging force $P = (2 - 32) \cdot 10^2$ MPa.

Metallographic investigations were conducted in an optical microscope «Olympus GX-51». X-ray microanalysis spectra were obtained in scanning electron microscope ZEISS-EVO-50 fitted with energy-dispersive analyzer INCA-450. Changes of micro- and nanohardness were studied on the surface in the direction normal to the material joint boundary in micro-LECO LM-700 and nanohardness meter Nana Indenter G200, MTS Systems, USA. Tensile testing was performed using Instron 5581 machine, fitted with a vacuum chamber with a furnace for heating up to 1100 °C.

Experiments on solid-phase joining of stainless and carbon steel of steel 20 type were conducted in a vacuum rolling mill. Solid-phase joining of dissimilar materials was performed by the method of hot rolling of a pack of plates at the temperature of 1100 °C and in the vacuum at $p = 1 \cdot 10^{-2}$ Pa. Then samples for rupture testing were cut out of the plate of obtained bimetal composite, which were tested in Instron 5581 machine. In Figure 2 it is clearly seen that tensile strength σ_t of the joint zone is higher than that of the weaker material, namely that of steel 20. In this case, rupture of the obtained composite ran through steel 20, tensile strength σ_t was equal to 430 MPa. Boundary of the solid-phase joint is much stronger than steel 20.

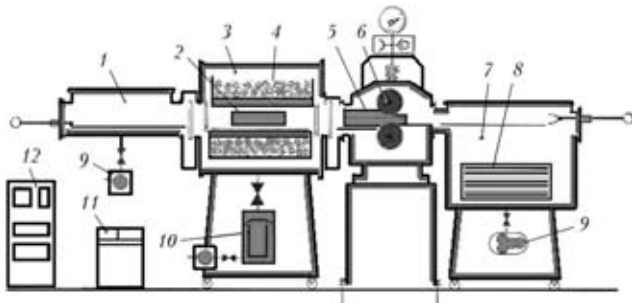


Figure 1. Diagram of vacuum rolling mill for joining dissimilar materials in the solid phase [14]: 1 – loading chamber; 2 – pack of plates being welded in the furnace; 3 – vacuum furnace; 4 – ceramic insulator; 5 – welded pack of plates in the roll chamber; 6 – rolls; 7 – chamber for unloading and collection of finished products; 8 – finished products in rolled stock collector; 9, 11 – control consoles for technological process of rolling; 10 – vacuum system consisting of diffusion and roughing pumps; 12 – automated system of monitoring and control of technological process of rolling

To understand the processes running in joining of dissimilar materials in the solid phase, a pack consisting of dissimilar 12Kh18N10T–Cu–Nb–Ti materials was selected. Cu–Nb materials in the range of 0.58–0.73 at.% by the equilibrium diagram are intersoluble at the temperature of 800–1000 °C. Copper is the less strong material in this composition. Therefore, it is of interest to clarify the influence of adjacent materials on the strength of copper interlayer. With this purpose, rupture testing of samples was performed (Figure 3), depending on copper interlayer thickness and testing temperature. Testing was conducted in a vacuum chamber fitted with heater up to 1100 °C. A variable parameter in this experiment is thickness of the copper interlayer (0.075, 0.35 and 1.5 mm).

Conducted testing showed that rupture always runs through the least strong material, in this case – through copper. At testing of material with different thickness of copper interlayer the tensile strength of the joint rises with reduction of copper interlayer thickness. Figure 4 shows the dependence of tensile strength σ_t of stainless steels and copper interlayer of different thickness on temperature.

From the results of experiments on determination of the composite tensile strength it follows that its

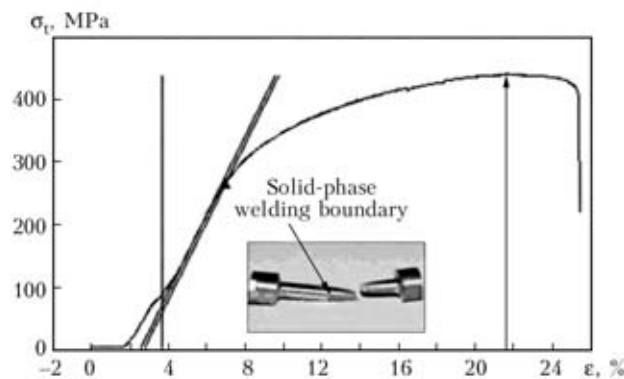


Figure 2. Diagram of tensile testing of 12Kh18N10T–steel 20 composite at the temperature of 20 °C (photo shows a sample broken in steel 20)

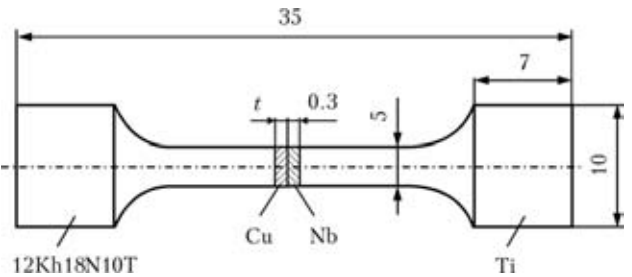


Figure 3. Diagram of a sample for rupture testing of materials welded in the solid phase

strength depends on the thickness of copper interlayer; the thinner it is, the higher the composite material tensile strength. So, at copper interlayer thickness of 1.5 mm σ_t of the composite approaches the value of σ_t of copper (200 MPa) at $T = 20$ °C. Under the same conditions, but at a thinner interlayer of copper (0.35 mm) the composite tensile strength rises, and at copper interlayer thickness of 0.075 mm σ_t value of the composite increases, becoming closer to tensile strength of the composite material and is equal to 550 MPa. The same effect is observed at the temperature of right up to 1000 °C.

This effect can be explained using the spectra of distribution of these materials on the boundaries of solid-phase joint of metals (Figure 5).

Let us consider the boundaries of 12Kh18N10T–Cu and Cu–Nb joint in a laminated composite. In keeping with the above mechanism of solid-phase joining of materials and based on the spectra given in Figure 5, we can see that the stainless steel atoms consisting of iron, chromium, nickel and niobium, mechanically mix with copper and are transferred into the copper interlayer located between the two metals. Atoms of 12Kh18N10T and niobium move due to dry sliding friction of rubbing surfaces into the copper interlayer from two sides towards each other to a depth of several tens of micrometers. Such a mechanism of mechanical mixing and displacement of atoms of one material into another was calculated by the method of molecular dynamics in [23]. Thus, the copper interlayer is strengthened by iron, chromium and nickel,

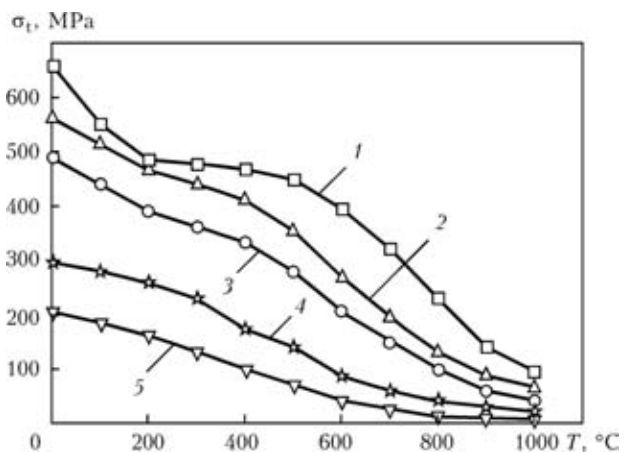


Figure 4. Temperature dependence of tensile strength σ_t : 1 – 12Kh18N10T steel; 2–4 – stainless steel–copper interlayer of 0.75, 0.35 and 1.5 mm thickness, respectively; 5 – copper

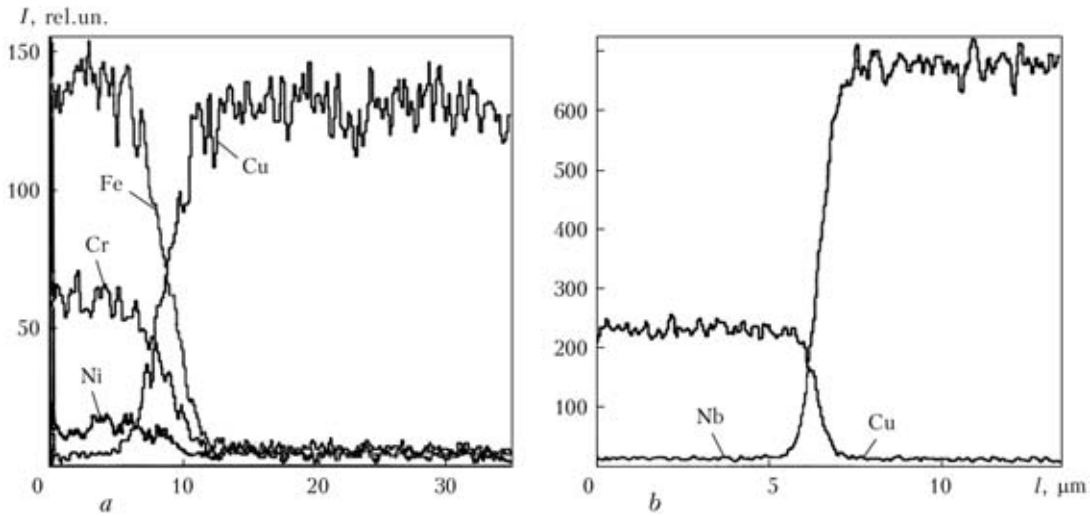


Figure 5. Spectra of X-ray microanalysis near the boundaries of solid-phase joint of metals: a – 12Kh18N10T-Cu; b – Cu-Nb

on the one side, and niobium atoms, on the other side. Figure 4 shows the dependence of tensile strength on temperature of solid-phase joining of 12Kh18N10T-Cu-Nb-Ti composition produced by the method of hot rolling in vacuum: it is the higher the thinner the copper interlayer and the more it is filled by atoms of metals adjacent from both sides. In the considered case the highest strength in the experiment is achieved at copper interlayer thickness of 0.075 mm, close to that of stainless steel, and it decreases at increase of copper interlayer thickness.

To confirm the change of strength of joint boundaries, investigations of the nature of material properties, their micro- and nanohardness were performed. Nanohardness was measured as close as possible to the boundary of solid-phase joint. So, the nanoindenter allows approaching the joint boundary to a distance of about 0.15 μm, while microhardness meter LM-700 with minimum load of 10 N for copper allows obtaining valid results at not less than 6 μm distance from the joint zone.

Joint structure determined during metallographic examination of solid-phase joint of 12Kh18N10T-Cu-Nb-Ti materials, is shown in Figure 6, from which it is seen that the joint boundaries form clear junctions, without formation of intermetallic zones on the boundaries. This is particularly important at measurement of nano- and microhardness of samples.

In Figure 7, which shows the change of micro- and nanohardness on the boundary of the joint of two metals, it is clearly seen that materials change their strength properties to the right and left of the joint boundary (coordinate 0). The less strong material (copper) becomes stronger near the joint boundary, both from the side of stainless steel, and from the niobium side. On the other hand, strength decreases on the boundary of the joint of stainless steel and niobium with copper.

Work [24] gives the calculation model, which allows prediction, based on material formation, of tensile strength of dissimilar metal joint boundary. Un-

like the model described in [3], the developed one allows for the forces of the metal displacement relative to each other, created by rolls along the boundary of metal joining.

In keeping with the proposed model tensile strength on the boundary of dissimilar metal joint can be found from the following expression:

$$\sigma_t^{M_1 + M_2} \equiv \frac{\sigma_t^{M_1 + M_2}}{\sigma_t^{M_1}} = \frac{1}{2} \frac{kT}{E_A} \frac{P_{pl}}{P_*} \frac{\sigma_{Sp}^{M_2}}{\sigma_{S0}^{M_1}} \frac{\sigma_{S0}^{M_2} + \sigma_{Sp}^{M_1}}{\sigma_{S0}^{M_2} - \sigma_{Sp}^{M_1}} \times \ln \left(\frac{\sigma_{S0}^{M_2}}{\sigma_{Sp}^{M_1}} \right) \equiv \frac{Q_{M_1 + M_2} (\sigma_{S0}^{M_2} / \sigma_{Sp}^{M_1})}{Q_{M_1 + M_1} (\sigma_{S0}^{M_1} / \sigma_{Sp}^{M_1})} \quad (1)$$

where $\sigma_t^{M_1 + M_2}$ is the tensile strength of the boundary of joint of metals M_1 and M_2 .

It should be noted that the values of $Q_{M_1 + M_1} \times (\sigma_{S0}^{M_1} / \sigma_{Sp}^{M_1})$ parameter for similar metals are always greater than a unity.

In expression (1) value E_A should be referred to a more ductile metal M_1 ($\sigma_t^{M_2} > \sigma_t^{M_1}$).

It follows from formula (1) that limit values of the range of tensile strength on the boundary of the joint of two dissimilar materials can be determined assuming that $M_1 \rightarrow M_2$ or $M_2 \rightarrow M_1$. Then, for the value for the lower limit of the range we have $\sigma_t^{M_1 + M_2} |_{M_2 \rightarrow M_1} = \sigma_t^{M_1}$. At $M_1 \rightarrow M_2$ it is not difficult

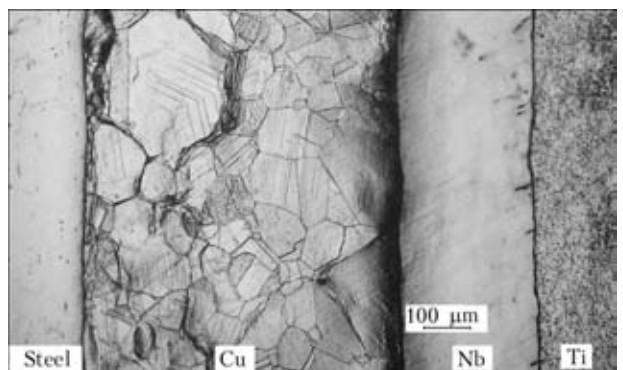


Figure 6. Microstructure obtained at metallographic investigation of solid-phase 12Kh18N10T-Cu-Nb-Ti joint

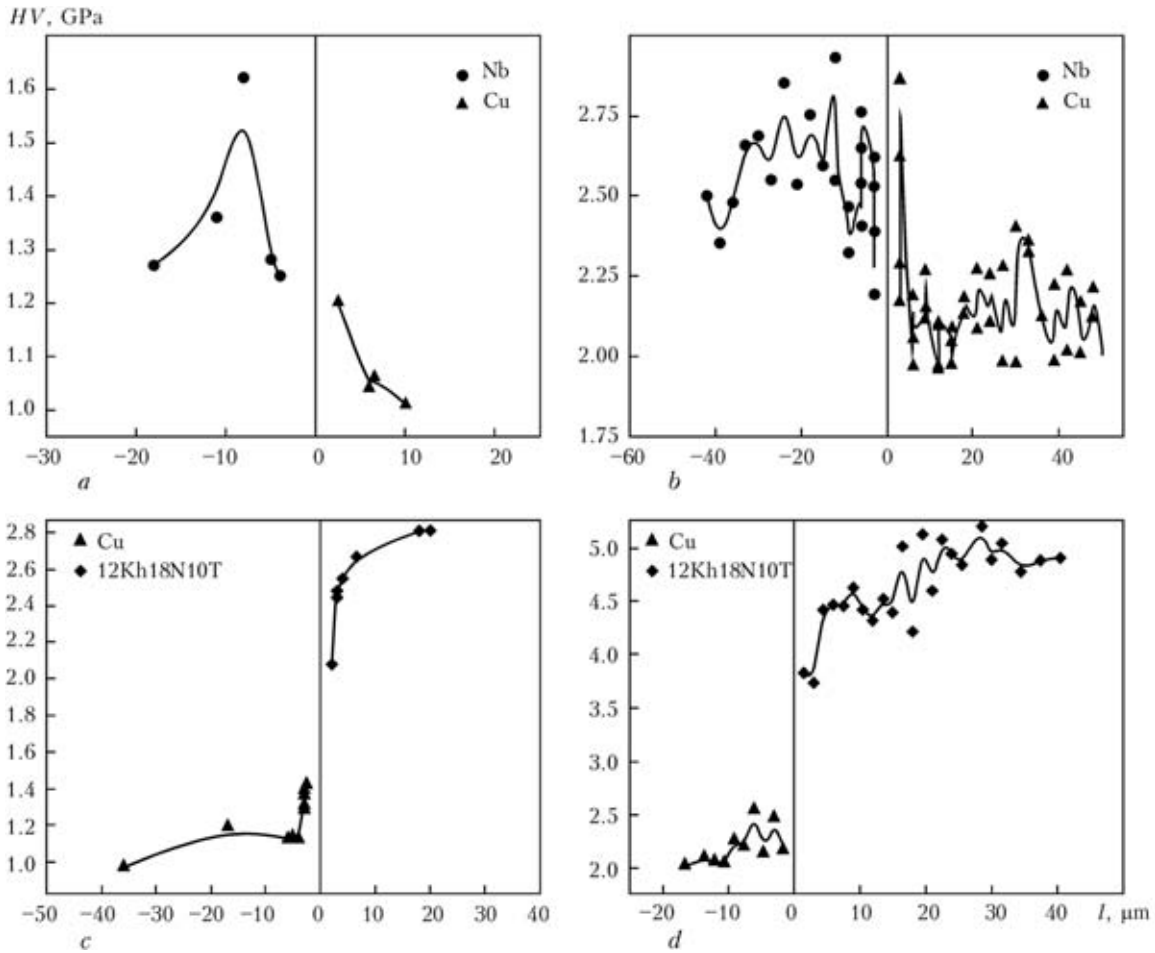


Figure 7. Change of micro- (*a, c*) and nanohardness (*b, d*) at maximum load on the boundary of Nb-Cu (*a, b*) and Cu-12Kh18N10T (*c, d*) joint

to determine the upper limit of this range $\sigma_t^{M_1 + M_2} |_{M_2 \rightarrow M_1} = \sigma_t^{M_2}$.

Thus, the value of tensile strength on the boundary of solid-phase joint of two dissimilar metals should satisfy the following inequality:

$$\sigma_b^{M_1} \leq \sigma_t^{M_1 + M_2} \leq \sigma_t^{M_2}. \quad (2)$$

Let us evaluate the tensile strength on the boundary of the joint of two dissimilar metals from expression (1). For this purpose in (1) we will introduce the coefficient of widening of the ductility range $g = \sigma_{S0}^{M_2} / \sigma_{S0}^{M_1}$. It should be noted that $\sigma_{S0}^{M_1}$ and $\sigma_{S0}^{M_2}$ are

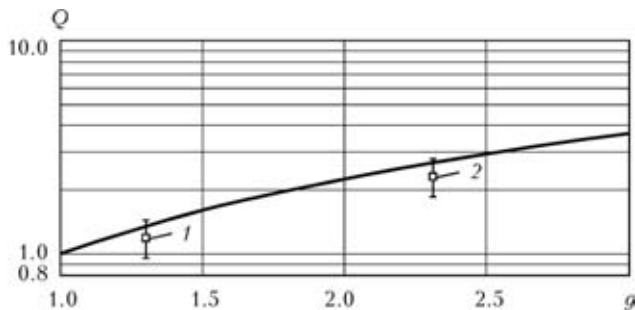


Figure 8. Dependence of relative tensile strength Q of metal joint on the coefficient of widening of ductility range g : 1, 2 – experimental Q values for joint 12Kh18N10T-steel 20 and 12Kh18N10T-Cu

determined by tensile strength of metals M_1 and M_2 , respectively.

In Figure 8, which gives dependence of $Q = \ln \frac{\sigma_t^{M_1 + M_2}}{\sigma_t^{M_1}}$ on parameter g , experimentally measured

points 1 and 2 have coordinates $Q = 1.2 \pm 0.24$, $g_1 = 1.2$; $Q_2 = 2.738 \pm 0.55$, $g_2 = 2.311$, and are described well by the theoretical model given in [24]. Error of measurements of relative tensile strength $Q_{1, 2}$ was determined by the error of measurement of hard alloy microhardness. It follows from this model that with increase of the coefficient of widening of the ductility range of two dissimilar metals joined in the solid phase, strength characteristics of the composite boundary are increased compared to tensile strength of the softer metal. Such an increase proceeds until the composite strength range is determined by the harder metal. In this case the relative tensile strength of the composite boundary is determined by the tensile strength of the harder metal.

In vacuum hot rolling surface activation occurs at the expense of shear plastic deformation [18], caused by dry sliding friction of the surfaces to be welded in the solid phase. This mechanism of surface cleaning the most effectively destroys the oxide films and en-



sure mixing of surface atoms at sliding of one material over the other (Figure 9).

It is experimentally established that dry sliding between ductile metals results in wear and intensive plastic deformation at rolling.

Shear plastic deformation of two dissimilar materials leads to rotation of the crystalline lattice [25] at simultaneous sliding of one material over another one. Juvenile surfaces of the materials being joined cleaned from oxides are thus produced. Mechanical mixing and mutual transfer of the atoms of the two metals occur at friction of one material over the other one that is clearly visible in Figure 5. Excitation centers form on the cleaned surfaces being welded, which are related to dislocation nucleation and transfer of atoms entrapped on the boundary of materials being joined into the metal bulk.

Figure 9 does not need any additional description, as all the acting forces and points of their application are shown in the drawing, and do not require any special explanation. Calculation of the forces shown in Figure 9, which act on the sample at rolling, is given in [18].

Considering the assumption made in [22] that dislocations initiate on the contact surface and propagate in-depth of the material, entraining the atoms of metals rubbing against each other, captured on the surface (this is a manifestation of deformation by dislocation sliding), it may be assumed that simultaneous plastic deformation of materials is required to achieve their solid-phase joining. Here, in addition to dislocation sliding, also accommodating rotations of the crystalline lattice are required that is achieved at hot rolling in vacuum, which combines both material deformation and shear displacement of material.

Each dislocation is an effective path, along which runs the flow of dissimilar material atoms directed away from the joint boundary. Mutual transport of atoms proceed along these channels. Here, the probability of simultaneous excitation of atoms of two opposing surfaces is quite high. Further deformation of material leads to movement towards each other of atoms of metals having a higher energy, promoting migration through the formed channels of the defective structure to a rather large distance. During experiments (see Figure 7) metal atoms were detected, which migrated into another material to the depth of up to 15–20 μm . Atoms of dissimilar materials approach each other to the distance of the action of interatomic forces that leads to energy release in the form of collective processes of electronic interaction. These phenomena are reduced to collectivization of valence electrons by positive ions, leading to formation of a strong metallic bond between the system of atoms forming the crystalline lattice, connected by electrons and ions of the two materials. This bond results in establishment of a redistributed composition of atoms of dissimilar materials being joined, in a

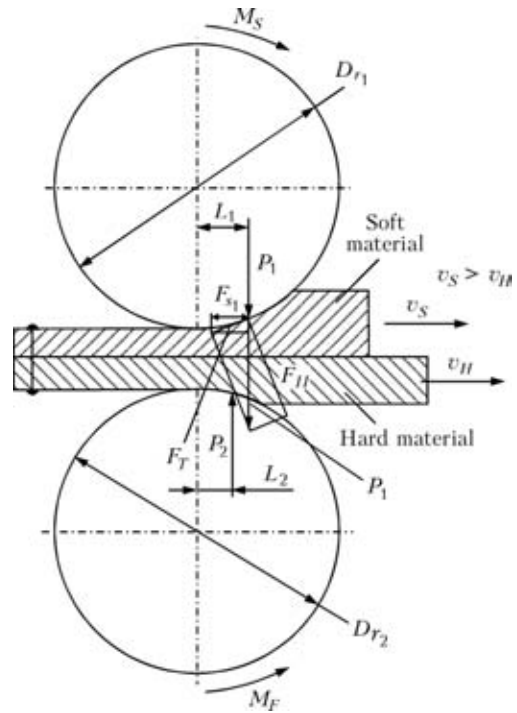


Figure 9. Schematic image of forces applied to material plates in the pack at rolling: F_{S1} – acting on plates in the pack, depending on material strength properties; M_S , M_F – moments arising at deformation of the soft and hard materials in the pack in welding; v_S , v_H – relative speeds of material displacement; P_1 , P_2 – acting in the point of application of forces at plate deformation; L_1 , L_2 – arm of forces P_1 , P_2 ; F_T , F_H – tangential forces arising at rotation and deformation of plates by rolls; D_{r1} , D_{r2} – roll diameters

narrow range (1–20 μm), ensuring solid-phase joining of dissimilar materials. Thus, the formed joint boundary of the two dissimilar metals becomes stronger during intensive plastic deformation with simultaneous sliding of the surfaces being welded through application of hot rolling in vacuum. During welding the joint boundary is formed from materials involved in the direct contact of materials being welded. Strength properties of the joint boundary proper are determined by the properties (strength and ductility) of materials welded in the solid phase. The intermediate layer is formed at the expense of many microstructural factors and deformation mechanisms, observed in the experiments (see Figures 4 and 5). Here a multitude of characteristic features are found, which include intensive plastic deformation, associated friction losses and adiabatic heating, mechanical mixing, nanocrystallization, transfer of the softer material towards the harder one, and vice versa. Plastic deformation is loosely related to interphase adhesion, namely «gripping» on the interface (as a starting factor) causes lattice deformation, that inevitably leads to plastic flow of the material. Adhesion forces are highly sensitive to the nature of the bonds between the parts and to interface crystallography. Thus, it is anticipated that plastic deformation values (and, therefore, friction) will also depend on these factors, and there is experimental proof of it (see Figures 7 and 8). Such a nature and deformations observed in the experiments



on solid-phase welding, are unique for this rolling system, providing sliding-friction between materials in their solid-phase joining. It turns out that the acting dynamic forces, caused by rolling of a multilayer pack, induce similar reactions in all the systems of friction surfaces to be welded, while the strength of boundaries in a multilayer joint depends on ductility of materials welded in the solid phase.

CONCLUSIONS

1. Solid-phase joint is produced due to intensive plastic deformation with materials sliding over each other with coming together of these materials up to lattice parameters, mechanical mixing of atomic layers of the material, participating in sliding-friction and excitation of atomic layers of opposing surfaces, having a higher energy and moving along the formed channels of the defective structure to a rather large distance.

2. Transfer of atoms of dissimilar metals from one plate into another during solid-phase welding by the method of hot rolling in vacuum was experimentally confirmed.

3. During welding the joint boundary forms from materials involved in the direct contact of materials being welded. Strength properties of the joint boundary are determined by the properties (strength and ductility) of metals welded in the solid phase.

4. Strength limit of dissimilar metal boundary is much higher than the tensile strength of the weaker metal.

5. Joint boundary of two dissimilar materials, produced in hot rolling in vacuum, is a new material, produced by intensive plastic deformation and mechanical mixing of metal atoms, involved in shear and mixing of the subsurface atomic layers of dissimilar materials being welded.

- Gelman, A.S. (1970) *Principles of pressure welding*. Moscow: Mashinostroenie.
- Ajnbindler, S.B., Glude, R.K., Loginova, A.Ya. et al. (1964) Principles of pressure welding. *Avtomatich. Svarka*, **5**, 21–27.
- Karakozov, E.S. (1976) *Solid-phase joining of metals*. Moscow: Metallurgiya.
- Sakhatsky, G.P. (1979) *Technology of solid-phase welding of metals*. Kiev: Naukova Dumka.
- Tylecote, R.F. (1994) Investigation on pressure welding. *Brit. Welding J.*, **5**, 117–134.
- Arsenyuk, V.V., Gertsriken, D.S., Mazanko, V.F. et al. (2001) Peculiarities of atom distribution in metals under pulse action. *Metallofizika i Nov. Tekhnologii*, **23(9)**, 1203–1212.
- Markashova, L.I., Grigorenko, G.M., Arsenyuk, V.V. (2001) Processes of plastic deformation, mass transfer, phase formation under the conditions of higher deformation rates. *Ibid.*, 1259–1277.
- Markashova, L.I., Arsenyuk, V.V., Berdnikova, E.N. et al. (2001) Peculiarities of vapor formation under the conditions of pressure welding of dissimilar materials at high deformation rates. *Ibid.*, **10**, 1403–1417.
- Markashova, L.I., Arsenyuk, V.V., Grigorenko, G.M. (2002) Peculiarities of plastic deformation of dissimilar materials in pressure joining. *The Paton Welding J.*, **5**, 9–13.
- Markashova, L.I., Arsenyuk, V.V., Grigorenko, G.M. et al. (2002) Mass transfer processes in pressure joining of dissimilar metals. *Ibid.*, **7**, 38–43.
- Markashova, L.I., Arsenyuk, V.V., Grigorenko, G.M. et al. (2004) Peculiarities of mass transfer processes in pressure welding of dissimilar materials. *Svarochn. Proizvodstvo*, **4**, 28–35.
- Markashova, L.I., Arsenyuk, V.V., Grigorenko, G.M. (2004) Relation of plastic deformation in welding of dissimilar materials. *Ibid.*, **8**, 26–32.
- Amonenko, V.M., Tron, A.S., Mukhin, V.V. et al. (1960) Vacuum rolling mill. *Stal*, **10**, 920–922.
- Amonenko, V.M., Tron, A.S., Mukhin, V.V. (1966) Producing of bimetal by vacuum rolling and their properties. *Tsvet. Metally*, **12**, 78–81.
- Skorobogatsky, I.N., Syropyatov, V.G., Tron, A.S. et al. (1976) Upgraded mill 300 for vacuum hot rolling of bimetal. *Elektron. Tekhnika*. Series Metals, Issue 2, 122–126.
- Amonenko, V.M., Tron, A.S., Mukhin, V.V. (1968) Properties of nickel–copper and nickel–copper–nickel bimetal produced by vacuum rolling. *Tsvet. Metally*, **9**, 107–110.
- Ivanov, V.E., Amonenko, V.M., Tron, A.S. (1978) High-temperature vacuum rolling of metals, alloys and multilayer materials. *Ukr. Fizich. Zhurnal*, **23(11)**, 1782–1789.
- Borts, B.V., Vanzha, A.F., Lopata, A.T. et al. (2005) Investigation of welding processes of multilayer structures from crystallites of different chemical composition with vacuum hot rolling. *Voprosy Atomm. Nauki i Tekhniki*. Series Physics of radiation damages and radiation materials science, **5(88)**, 156–158.
- Manesh, D., Karimi Taheri, H.A. (2005) An investigation of deformation behavior and bonding strength of bimetal strip during rolling. *Mechanics of Materials*, **37**, 531–542.
- Zhao, D.S., Yan, J.C., Wang, Y. et al. (2009) Relative slipping of interface of titanium alloy to stainless steel during vacuum hot rollbonding. *Materials Sci. and Eng. A*, **499**, 282–286.
- Borts, B.V. (2009) Producing of composites by vacuum hot rolling. *Voprosy Atomm. Nauki i Tekhniki*. Series Physics of radiation damages and radiation materials science, **2(60)**, 128–134.
- Gostomelsky, V.S., Rojtburd, A.L. (1986) Dislocation mass transfer near the interface of dissimilar materials at their plastic deformation. *Doklady AN SSSR*, **288(2)**, 366–369.
- Evangelakis, G.A., Pontikis, V. (2008) Molecular dynamics study of Pb-substituted Cu(100) surface layers. *J. Alloys and Compounds*, **7**, 221.
- Borts, B.V. (2010) Investigation of relation between tensile strength of solid-phase joining boundary of dissimilar metals and their ductility. *Voprosy Atomm. Nauki i Tekhniki*. Series Physics of radiation damage and radiation materials science, **96(5)**, 108–118.
- Rybin, V.V. (1986) *High plastic deformation and fracture of metals*. Moscow: Metallurgiya.



WEAR- AND HEAT RESISTANCE OF DEPOSITED METAL OF GRAPHITIZED STEEL TYPE

I.A. RYABTSEV, I.A. KONDRATIEV, V.V. OSIN and G.N. GORDAN

E.O. Paton Electric Welding Institute, NASU, Kiev, Ukraine

Wear resistance of deposited metal of the graphitized steel type in metal-on-metal friction without lubrication at room and elevated temperatures was investigated, and its heat resistance was evaluated. It was established that the as-deposited metal alloyed with 1.4–1.6 wt.% C and 1.5–2.0 wt.% Si contains the optimal amount of graphite inclusions is characterised by high wear resistance, and has a decreased friction coefficient in metal-on-metal sliding friction at room temperature.

Keywords: arc surfacing, surfacing materials, flux-cored wires, graphitized steels, wear- and heat resistance

Steels and cast irons are referred to graphitized iron-carbon alloys, the structure of which has free inclusions of the different-shape graphite [1]. Application of these materials is one of the ways of improving the tribotechnical characteristics of parts of friction pairs and some types of die tools, in particular drawing dies. In this case the inclusions of graphite play a role of lubricant.

It was shown earlier [2] that the deposited metal of a graphitized steel type can be produced at content of carbon of above 1.6 wt.% and silicon of above 2.0 wt.%. For graphitizing the deposited with content of not less than 1.5 wt.% C and 1.1 wt.% Si it is recommended to use the heat treatment instead of high-temperature annealing: directly after surfacing the part is placed into furnace at 400 °C temperature, and after holding for 2 h it is slowly cooled. Modifying the deposited metal by aluminium and calcium allows activating the process of graphitization.

The present work is aimed at the investigation of wear resistance of the deposited metal of a graphitized steel type in metal-on-metal friction without lubrication at room and elevated temperature, and also evaluation of its heat resistance. The multilayer surfacing of specimens was performed under the layer of AN-26 flux using three experimental flux-cored wires. Chemical composition of deposited metal and its hardness after surfacing and annealing are given in Table 1.

The investigations of wear- and heat resistance were carried out in a modular-type installation, developed at the E.O. Paton Electric Welding Institute [3].

Investigations of wear resistance of deposited metal in metal-on-metal friction at room temperature were carried out in a test installation friction module, which was equipped additionally by a system of specimens positioning with respect to a rotary shaft-counterbody. Tests were performed by the method of wiping-out craters using the shaft–plane scheme without an additional feeding of lubricant into the friction zone.

The shaft-counterbody of 40 mm diameter and 12 mm height was manufactured of steel 45 of HRC 42 hardness. The test specimens of 3 × 15 × 25 mm size were cut out from the deposited metal so, that the test plane of the specimen could enter the upper layers of the deposited metal (Figure 1). As a reference the specimens of deposited metal (steel of 20KhGS type), produced by using the flux-cored wire PP-AN194, were used.

During tests the specimen was pressed with a definite force against the counterbody by the plane having 3 × 25 mm size in design. The following test condition was selected: rate of sliding of 1 m/s; loading of 30 N; frequency of rotation of shaft-counterbody of 30 rpm; friction path – 113 m. This condition provides the stabilization of tribotechnical characteristics of all the test specimens. The application of positioning system made it possible to test each deposited specimen not less than three times on the new region of friction surface of the specimen and friction path of the counterbody.

During testing the deposited specimen the friction force, wear of deposited specimen in the volume of wiped-out crater and counterbody were determined from the difference of its mass before and after the test. The coefficient of friction was calculated as a quotient from division of friction force value by load at an error of not more than 5 %.

Table 1. Chemical composition (wt.%) and hardness of metal deposited by experimental flux-cored wires

Grade of flux-cored wire	Elements, wt.%					HRC	
	C	Si	Mn	Al	Ca	After surfacing	After annealing
PP-Np-Op-1	1.5	1.15	0.60	–	–	43	26
PP-Np-Op-2	1.8	1.46	0.58	–	–	49	20
PP-Np-Op-3	1.5	1.45	0.49	0.09	0.02	43	38

Note. Metal, deposited by wire PP-Np-Op-3, was subjected to annealing at 400 °C for 2 h, the rest metal – to annealing at 680 °C for 6 h.

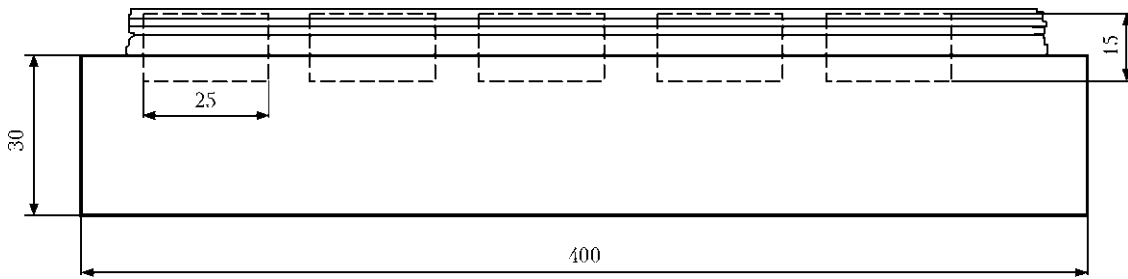


Figure 1. Scheme of cutting out of specimens for tribotechnical investigations of deposited metal

Wear m of counterbody was determined from loss of its mass as a result of testing at an error of not more than 0.0005 g. The error of determination of wear of specimen and counterbody did not exceed 1 %.

Results of carried out tests are presented in Table 2. The best wear resistance was in specimens of metal, deposited by experimental flux-cored wires PP-Np-Op-1 and PP-Np-Op-2, which possessed the optimum combination of hardness and free inclusions of graphite [2]. Heat treatment contributed to increase in content of free inclusions of graphite in the deposited metal structure [2], but simultaneously it decreased its hardness and, respectively, also wear resistance of deposited metal of both tested types.

Metal, deposited by the flux-cored wire PP-Np-Op-3 with modifying additions of aluminium and calcium, was also characterized by a sufficiently high wear resistance. Annealing at 400 °C for 2 h led to the reduction in hardness and wear resistance of deposited metal of this type.

The graphitized steels as compared with low-alloy steel 20KhGS have the lower coefficient of friction and with a higher content of graphite inclusions, formed as a result of annealing, the value of friction coefficient is lower. Addition of calcium and aluminum allows decreasing the temperature of a graphitizing annealing and coefficient of friction of metal deposited by the flux-cored wire PP-Np-Op-3, the value of which after annealing at 400 °C is at the same level with the friction coefficient value of ordinary graphitized steels after annealing at the higher temperatures.

The tests of wear resistance of deposited metal of graphitized steel type in metal-on-metal friction at high temperature were performed by shaft-plane

scheme without additional feeding of lubricant into the friction zone. For comparison, the specimens deposited by the flux-cored wire PP-Np-25Kh5FMGS were tested as a reference.

Specimens of 40 × 10 × 17 mm size were manufactured from deposited templates, in this case the area of friction plane was 10 × 40 mm, and the thickness of deposited layer was 8–10 mm.

The wearing ring was heated by oxy-natural gas flame. Owing to a strictly definite consumption of natural gas and oxygen the temperature of a wearing ring was maintained constant (950–980 °C) and controlled periodically using an optical pyrometer.

Wear tests in metal on metal friction at elevated temperature were carried out for 1 h at 175 N load; rate of rotation of the ring-counterbody was 30 rpm. As a counterbody the 120 mm diameter ring of hardened steel 45 was used. Temperature of surface of test specimen in the wear zone was equal approximately to 600 °C. During tests the specimen realized the reciprocal movement in vertical plane at 20 mm amplitude of oscillations and 62 min⁻¹ frequency of oscillations. Test results (mean value of three specimens) are given in Table 3.

The tests showed that the wear resistance of metal, deposited by the flux-cored wire PP-Np-Op-1, not subjected to heat treatment, is higher than that of metal, passed the annealing, that can be explained by a significant reduction in hardness as a result of annealing. It should be noted that the presence of a large amount of free graphite in the structure of deposited metal of this type hinders the transfer and sticking of metal on the counterbody. Decrease in heat treatment temperature reduces the wear of deposited specimens

Table 2. Wear resistance of deposited metal of graphitized steel type at room temperature

Grade of flux-cored wire	Heat treatment	Wear of specimen, mm ³ /km	Wear of counterbody, g/km	Coefficient of friction
PP-Np-Op-1	Directly after surfacing	0.00203	0.00205	0.62
	Same after tempering at 680 °C for 6 h	0.06020	0.00210	0.57
PP-Np-Op-2	Directly after surfacing	0.00204	0.00207	0.60
	Same after tempering at 680 °C for 6 h	0.07230	0.00101	0.51
PP-Np-Op-3	Directly after surfacing	0.00302	0.00310	0.59
	Same after tempering at 400 °C for 2 h	0.00801	0.00204	0.52
PP-AN194 (reference)	Directly after surfacing	0.08900	0.00450	0.65



Table 3. Wear resistance of deposited metal of graphitized steel type at elevated temperature

Grade of flux-cored wire	Heat treatment	Wear $m \cdot 10^4$, kg/km	
		Specimen	Counterbody
PP-Np-Op-1	Directly after surfacing	16.579	+17.452
	Same after annealing at 680 °C for 6 h	29.602	59.488
	Same after annealing at 400 °C for 2 h	23.352	36.879
PP-Np-Op-2	Directly after surfacing	12.723	89.562
	Same after annealing at 680 °C for 6 h	25.945	132.765
	Same after annealing at 400 °C for 2 h	15.132	93.453
PP-Np-Op-3	Directly after surfacing	7.984	168.656
	Same after annealing at 400 °C for 2 h	7.277	147.761
PP-Np-25KhFMGS (reference)	Directly after surfacing	4.287	142.102

Note. + denotes the increase in mass of counterbody as a result of metal sticking.

Table 4. Test results on heat resistance of deposited metal of graphitized steel type

Grade of flux-cored wire	Heat treatment	Number of heating-cooling cycles	
		Before appearance of the first cracks	Before appearance of net of fire cracks
PP-Np-Op-1	Directly after surfacing	5	240
	Same after annealing at 680 °C for 6 h	3	190
	Same after annealing at 400 °C for 2 h	5	210
PP-Np-Op-2	Directly after surfacing	8	180
	Same after annealing at 680 °C for 6 h	4	140
	Same after annealing at 400 °C for 2 h	7	160
PP-Np-Op-3	Directly after surfacing	4	110
	Same after annealing at 400 °C for 2 h	5	80

and counterbodies, however this characteristic still remains higher than that in specimens directly after surfacing.

The metal, deposited by the flux-cored wire PP-Np-Op-2, possessed somewhat better characteristics of wear resistance. Metal, modified by aluminium and calcium, is characterized after surfacing or low-temperature annealing by a higher wear resistance, which

is at the level of that of the known chrome-molybdenum die steel 25Kh5FMGS.

Heat resistance is one of the most important characteristics of materials designed for the restoration and strengthening of tools for hot deformation of metals. The test procedure should envisage the optimum sizes and shape of the deposited specimen, temperature and rate of its heating and cooling close to service

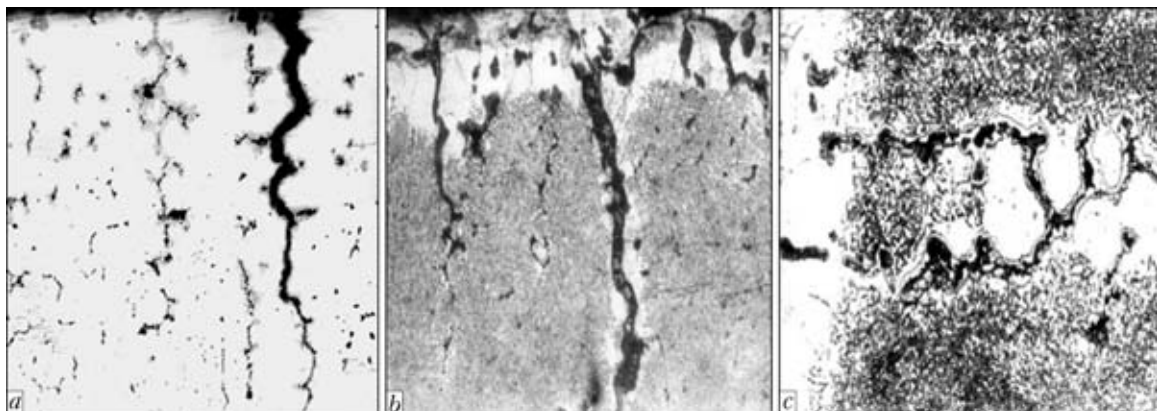


Figure 2. Microstructures of deposited metal produced by using the flux-cored wire PP-Np-Op-3: *a* – section without etching (surface layer), $\times 250$; *b* – the same with etching in nitric acid, $\times 200$; *c* – central zone of specimen section with etching in nitric acid, $\times 500$

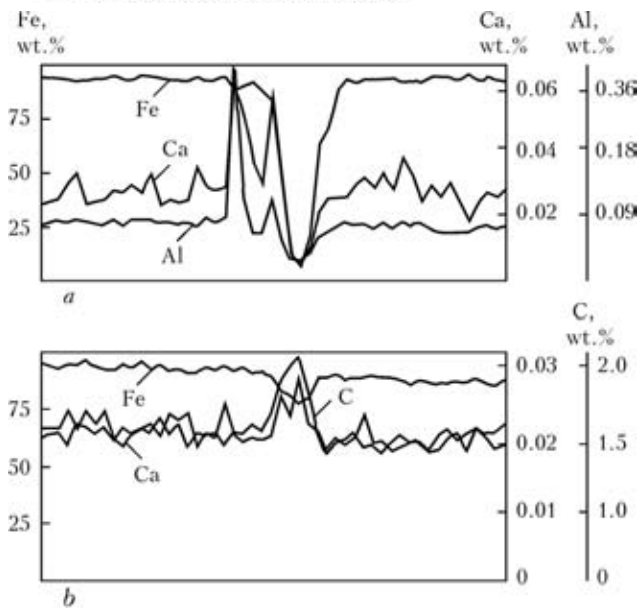


Figure 3. Distribution of main alloying elements Ca, Al (a) and Ca, C (b) in deposited metal produced by using flux-cored wire PP-Np-Op-3

values, environment condition, etc. The specimen should have first of all the sufficient mass to provide the gradient of temperatures, simulating the full-scale conditions, during the process of its heating.

Heat resistance tests of deposited specimens were performed using the following procedure: $30 \times 40 \times 40$ mm size of specimen, heating of deposited surface of specimen by a gas cutter up to 800°C (15 mm heating spot, 40×40 mm specimen surface being heated), cooling of heated surface by a water jet down to 60°C . Cycles of heating-cooling were repeated until appearance of a net of fire cracks, visible with a naked eye. Heat resistance was estimated coming from the number of heating-cooling cycles until the appearance of the first cracks and reaching a certain degree of cracking, i.e. the appearance of a net of fire cracks. Test results (mean values from 3–5 specimens of each type of deposited metal and kind of heat treatment) are given in Table 4.

Metal, deposited by the flux-cored wire PP-Np-Op-1, has the best characteristics of heat resistance, they are lower in metal, deposited by the wire PP-Np-Op-2, and the lowest characteristics are in metal, deposited by the wire PP-Np-Op-3. Here, the net of fire cracks in specimens, deposited by flux-cored wires PP-Np-Op-1 and PP-Np-Op-2, is much less developed than in specimens, deposited by the flux-cored wire PP-Np-Op-3.

Structure of specimen metal, deposited by the wire PP-Np-Op-3 after heat resistance tests (80 cycles) was investigated (Figure 2). The non-etched section has

numerous cracks, the maximum depth of which reaches $1500\ \mu\text{m}$ (Figure 2, a). After etching in nitric acid the surface decarburization of the last layer of deposited metal (Figure 2, b) for the depth of up to $250\ \mu\text{m}$ was observed. The decarburized layer has a microhardness $HV_{0.5}$ 1680 MPa, while the hardness of neighboring non-decarburized areas was $HV_{0.5}$ 3030–3680 MPa. Clusters of inclusions of dark grey color were formed in metal of test specimen (it is supposed to be graphite) which are located along the boundaries of ferrite grains and have hardness $HV_{0.5}$ 1480 MPa (Figure 2, c).

To define the causes of the earlier appearance of a net of fire cracks, the X-ray microanalysis of specimen, deposited by wire PP-Np-Op-3, was made after tests for heat resistance. The examinations were made at the depth of about $1.5\ \mu\text{m}$ from the surface of deposit in parallel to it in the automatic condition at $1.02\ \mu\text{m}$ interval along the front of fire crack (Figure 3).

It was found that near the fire crack the content of carbon, aluminium and calcium is abruptly increased. It allows assuming that the fire cracks are passed through the inclusions of free graphite, the appearance of which was contributed by modifying the deposited metal with aluminium and calcium. In the deposited metal in the zone of cracks the mass fraction of elements is varied within the following ranges, %: 0.2–9.6 C; 0.23–2.44 Al; 0.01–0.319 Ca; 1.48–1.99 Si; 0.137–0.66 Mn.

It was established that the metal, alloyed with 1.4–1.6 wt.% C and 1.5–2.0 wt.% Si, directly after surfacing has an optimum content of graphite inclusions and is characterized by high wear resistance in sliding friction of metal on metal at room temperature. The additional heat treatment for increasing the content of graphite inclusions to improve the wear resistance is, probably, not rational. As compared with a low-alloy steel 20KhGS the graphitized steels have the lower coefficient of friction. With higher content of inclusions of graphite in the steel structure, the coefficient of friction is lower. The investigations of heat resistance of deposited metal of a graphitized steel type showed that this metal should be used for strengthening the parts and tools, which are subjected to moderate cyclic, thermal and load effects.

1. Todorov, R.P., Nikolov, M.P. (1976) *Structure and properties of casts from graphitised steel*. Moscow: Metallurgiya.
2. Kondratiev, I.A., Ryabtsev, I.A., Bogajchuk, I.L. et al. (2008) Structure of deposited metal of the type of graphitized hypereutectoid steels. *The Paton Welding J.*, 7, 15–18.
3. Ryabtsev, I.I., Chernyak, Ya.P., Osin, V.V. (2004) Block-module unit for testing of deposited metal. *Svarshchik*, 1, 18–20.



CONDITIONS OF PROPAGATION OF THE SHS REACTION FRONT IN NANOLAYERED FOILS IN CONTACT WITH HEAT-CONDUCTING MATERIAL

T.V. ZAPOROZHETS¹, A.M. GUSAK¹ and A.I. USTINOV²

¹B. Khmelnytsky National University, Cherkassy, Ukraine

²E.O. Paton Electric Welding Institute, NASU, Kiev, Ukraine

The problem of propagation of the gas-free combustion (SHS reaction) front in nanolayered foils in thermal contact with the mating surfaces is considered. It is shown that dependence of the rate of propagation of the combustion front on the intensity of heat removal is of a threshold nature: there are critical values of the intensity of heat removal at which the combustion conditions in the nanolayered foil–heat-conducting material system are suppressed.

Keywords: *welding and brazing, multilayer foils, heat-conducting materials, mating surfaces, self-propagating high-temperature synthesis reaction, heat removal, threshold thickness, analytical estimation*

Materials in which the self-propagating high-temperature synthesis (SHS) reaction may occur between their components are regarded as good candidates for production of permanent joints by the welding or brazing methods [1–3]. Of special interest are multilayer foils (MF) consisting of layers based on intermetallic-forming components, in which under certain conditions the SHS reaction may take place with a high intensity of heat release. As thickness of the MF layers is decreased to the nanoscale level, the rate of propagation of the SHS reaction may amount to several metres per second, and the intensity of heat release may grow to 1–2 kW/cm². Location of such highly reactive foils between the mating surfaces with the SHS reaction initiated in them allows activation of the diffusion processes within the joining zone due to the heat release or melting of a filler metal during brazing. This makes it possible to form permanent joints in materials without their melting. Models allowing for the processes of diffusion interaction of components in MF and heat release under the conditions where there is no heat removal to the environment were developed to predict the rate of propagation of the SHS reaction front, temperature at the front and intensity of heat release [4–8].

To predict characteristics of occurrence of the SHS reaction under the conditions where MFs are in contact with the mating surfaces, it is necessary to allow for the reverse effect of heat removal on the reaction [9, 10]. In this case we might expect non-linearity in behaviour of the system and, in particular, existence of the combustion/extinction phase transition with a change of the heat removal parameters. Apparently, heating in the front at a very intensive heat removal may be insufficient for further occurrence of the reaction. So, the question is whether decrease in the

rate of occurrence of the SHS reaction with increase in heat removal is a gradual process or it stops upon reaching some threshold intensity of heat removal.

Studies [5–7] offer a simple model of occurrence of SHS in MF. A foil consisted of M alternating layers of components with multilayer spacing $4l$ (l is half of thickness of a layer of one component), allowing for a layer Δy_0 thick that reacted before the beginning of SHS. Along with a numerical solution of the model for one- and two-stage reactions, an analytical formula for estimation of the rate of movement of the front at the absence of external heat removal was offered and tested:

$$V = \sqrt{\frac{2a_{foil}^2 D_0 \Delta g T_0 (k_B T_f + Q)}{c(1-c)4l^2 - \Delta y_0^2 Q^2 (T_f - T_0)} \exp\left(-\frac{Q}{k_B T_f}\right)}, \quad (1)$$

where c is the mean concentration of a new phase with diffusion characteristics D_0 and Q , and thermodynamic formation stimulus per atom, Δg ; a_{foil}^2 is the thermal diffusivity of the foil; k_B is the Boltzmann constant; T_0 is the initial temperature of the foil; T_f is the maximal temperature at the front, which is determined by phase formation energy Δg multiplied by foil efficiency factor $f = 1 - \Delta y_0/2l$:

$$3k_B(T_f - T_0) = f\Delta g. \quad (2)$$

In study [6], this approach was specified with allowance for the final rate of relaxation of vacancies in metal foils, which substantially decreased predictable rates of the SHS reaction.

The present study considers occurrence of the SHS reaction in MF compressed between two heat-conducting plates (e.g. plates of brazing filler metal, which should be heated or melted by means of SHS). Then the heat removal may either inhibit the reaction or fully suppress it. As seen from formula (1), rate V of the reaction is determined, in the first turn, by front temperature T_f . Apparently, the heat removal should decrease heating of the foil. In this case, the degree of the decrease is determined by the rate: the slower



the reaction, the longer is the time of propagation of the front through a given point, the more heat is removed during the front propagation time, and the higher is the temperature drop. Therefore, there is a positive feedback between the decrease in rate and temperature drop, and this feedback may lead to escape from the steady-state condition, i.e. to extinction. To quantitatively estimate it, it is necessary to determine dependence of the degree of decrease in temperature on the rate of the SHS reaction. Consider the analytical estimation, and then specify it by means of numerical solution of the problem of unsteady heat transfer.

Analytical estimation. Density of the flow of heat removal, j_Q^\perp from the MF surface (Figure 1) is determined by characteristics of a contact material:

$$j_Q^\perp = -\kappa_p \frac{\partial T}{\partial y}, \quad (3)$$

where κ_p is the coefficient of thermal conductivity of contact plates; and η is the dimensionless coefficient of efficiency of the contact, which depends on the roughness of the contact surface and is defined by the efficient contact area to total area ratio ($0 < \eta \leq 1$).

To allow for the effect of heat removal on occurrence of the SHS reaction, it is enough to determine the heat flow at a given point only within time τ_f of propagation of the front through this point. By using standard solution of the one-dimensional problem, we can assume that the transverse temperature gradient that determines the heat removal has the Gaussian profile:

$$\frac{\partial T}{\partial y} \sim -\frac{T_c - T_0}{\sqrt{\pi a_{foil}^2 t}} e^{-y^2/(4a_{foil}^2 t)}, \quad (4)$$

where T_c is the temperature at the contact.

One of the approximations, i.e. formula (4), is made at a constant temperature on the surface. In our case this temperature changes with propagation of the front. Therefore, it is necessary to check the derived formulae by the numerical solution, where equation (4) is not used.

If temperature T_c at the contact during front propagation time τ_f increases from T_0 to the maximal value of T_f , the mean transverse temperature gradient can be estimated by replacing $T_c - T_0$ with $(T_f - T_0)/2$ and time t with τ_f in (4).

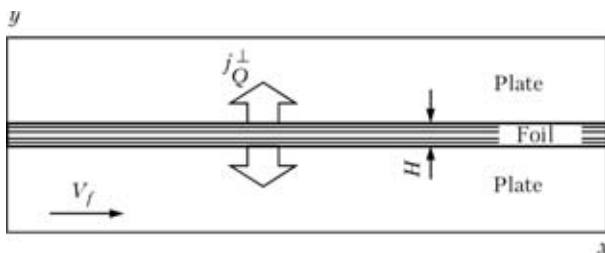


Figure 1. Schematic of heat removal in foil-plate system

Then we allow for the heat removed and, hence, for a change in temperature during the front propagation time (not after), as it is this fact that determines the intensity of the reaction, whereas cooling of the foil after the SHS reaction has practically no effect on the front propagation rate. Moreover, width of the front can be estimated in much the same way as width of the diffusion zone in diffusion, $L_f = \sqrt{a_{foil}^2 \tau_f}$. At the same time, front width is $L_f = V_f \tau_f$. Based on this fact, the mean transverse temperature gradient within the region of the SHS front can be described as $\frac{\partial T}{\partial y} \sim \frac{T_f - T_0}{2\sqrt{\pi}} \frac{1}{V_f \tau_f}$. Therefore, the heat flow density is inversely proportional to the rate of the front and its propagation time:

$$j_Q^\perp = \frac{\kappa_p \eta}{2\sqrt{\pi}} (T_f - T_0) \frac{1}{V_f \tau_f}. \quad (5)$$

Then the total amount of the heat removed through unit of the foil surface area is inversely proportional to the rate

$$j_Q^\perp \tau_f = \frac{\kappa_p \eta}{2\sqrt{\pi}} (T_f - T_0) \frac{1}{V_f}.$$

Allowing for a double-sided contact of the foil with the contact plates, heat removal from surface area S_0 of the foil is defined as $j_Q^\perp \tau_f 2S_0$. Assume that the heat is removed uniformly from each atom in a given cross section of the foil. This assumption is valid only for a sufficiently thin foil, if the time of levelling of the temperature across the section is much shorter than the time of propagation of the front through this section: $(H/2)^2/a^2 \ll a^2/V_f^2$, i.e. $H \ll 2a^2/V_f \approx 2L_f$. Simply speaking, thickness of the foil should be markedly smaller than width of the SHS front. Otherwise, it is necessary to calculate the temperature profile along the section of the foil. Area S_0 of the foil with thickness $H = M4l$ comprises $S_0 H/\Omega$ atoms (Ω is the atomic volume). Hence, the analytical estimation of heat removal per foil atom is

$$q_{an} = \frac{j_Q^\perp \tau_f 2}{H/\Omega} = \frac{\kappa_p \eta}{2\sqrt{\pi}} \frac{2\Omega}{H} (T_f - T_0) \frac{1}{V_f}. \quad (6)$$

Allowance for the heat removal leads to modification of formula (2):

$$3k_B(T_f - T_0) = f\Delta g - \frac{\kappa_p \eta}{2\sqrt{\pi}} \frac{2\Omega}{H} (T_f - T_0) \frac{1}{V_f}.$$

As a result, we obtain the required dependence of the front temperature as a function of the front propagation rate:

$$T_f = T_0 + \frac{f\Delta g}{3k_B(1 + U/V_f)}, \quad (7)$$



where $U = \frac{1}{3k_B} \frac{\kappa_p \eta}{2\sqrt{\pi}} \frac{2\Omega}{H}$ is the parameter which, allowing for the Dulong–Petit law, can be interpreted as a rate of heat removal (ratio of foil thickness $H/2$ to characteristic time of its cooling, $(H/2)^2/a_p^2$):

$$U = \frac{\eta}{\sqrt{\pi}} \frac{a_p^2}{H}, \quad (8)$$

where a_p^2 is the thermal diffusivity of the plate. Parameter U is the intensity of heat removal (in particular, $U = 0$ at its absence).

Numerical calculation of heat removal. To check and specify analytical estimation (7), the two-dimensional boundary problem was numerically solved to determine thermal conductivity in a rectangular plate adjoining the foil (Figure 2, *a*) at a preset temperature profile of SHS (Figure 2, *b*), which was used as a boundary condition at the foil–plate contact:

$$T(x, y = 0, t) = \begin{cases} T_f, & x < V_f t, \\ T_0 + (T_f - T_0) \exp\left(\frac{x - V_f t}{L_f}\right), & V_f t < x. \end{cases}$$

The boundary conditions at the remaining three sides of the region are trivial: $T(x, y = P_y, t) = T_0$, $\frac{\partial T}{\partial x}(x = 0, y, t) = 0$, $\frac{\partial T}{\partial x}(x = P_x, y, t) = 0$.

Heat flows released by the foil to the plate through the contact zone, $P_y = 0|P_y = 1$, up to the moment of reaching the maximal value of temperature T_f were summed up for each mesh point:

$$q_{num} = \kappa_p \eta \frac{\Omega}{H/2} \int_{\frac{x}{V_f} - \frac{2L_f}{V_f}}^{\frac{x}{V_f}} - \frac{\partial T(x, y)}{\partial y} \Big|_{y=0} d\theta.$$

The values of the heat flow were averaged by points of the contact zone.

As shown by numerical calculations, the rough analytical estimation (6) was proved to be accurate: $q_{an}/q_{num} = 1.023$ (at $\eta = 1$, $H = 20 \mu\text{m}$, $T_0 = 300 \text{ K}$, $T_f = 2000 \text{ K}$ and thermal conductivity for tin $\kappa_p = 65.7 \text{ J}/(\text{m}\cdot\text{s}\cdot\text{K})$).

Therefore, the analytical, inversely proportional dependence of heat removal on the front propagation rate is correct, and formulae (7) and (8) can be used for further analysis of the combustion and extinction conditions.

Self-consistent calculation of temperature and rate of the front. Formulae (1) and (7) realise the positive relationship between the front rate and decrease in temperature as a result of heat removal. By substituting formula (8) to (1), we obtain the transcendental equation for the SHS front rate as a function of characteristic heat removal rate U and foil efficiency f .

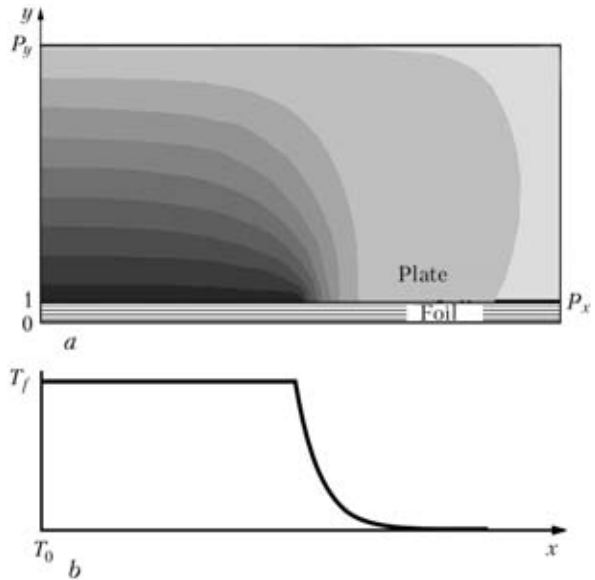


Figure 2. Propagation of heat in plate adjoining the foil surface as a result of propagation of SHS wave (*a*) with temperature profile (*b*)

As is evident from formula (8), the U value can be controlled by changing the contact efficiency and foil thickness. Figure 3, *a* and *b*, shows the maximal temperature and rate of the SHS reaction front depending on this or that parameter, the rest of characteristics of the system being constant. Both dependences have a jump corresponding to some critical value of the intensity of heat removal, U_{cr} , at which solution of the system of equations (1) and (7) transfers in a jump to $V_f = 0$ and $T_f = T_0$, i.e. the SHS reaction is probable at $U < U_{cr}$, and it is extinguished at $U > U_{cr}$.

Another factor of no small importance, which determines switching of the combustion / extinction conditions, is multilayer spacing $4l$. As shown in studies [4–6], the front propagation rate at the absence of heat removal is of a non-monotonous character at a change in the multilayer spacing (Figure 3, *c*): Δy_0 has a substantial effect at a small spacing, and diffusion activity of phase formation falls at a big spacing. Both factors decrease heating in the SHS reaction and, hence, the probability of its occurrence.

Moreover, it was experimentally proved that the combustion reaction may occur in low-reactivity multilayer foils at their insignificant heating before initiation of the reaction [11]. Increase of the ambient temperature leads to exponential growth of the diffusion coefficient and, hence, the rate of heat release to maintain the SHS condition.

Therefore, the probability of the SHS reaction in MF, which is in thermal contact with the mating surfaces, is determined by the following factors:

1) roughness or pressure on the contact of foils with plates – the lower the pressure, the worse is the thermal contact, the higher is the thermal resistance at the contact, and the closer is the heat removal coefficient to zero (see Figure 3, *a*);

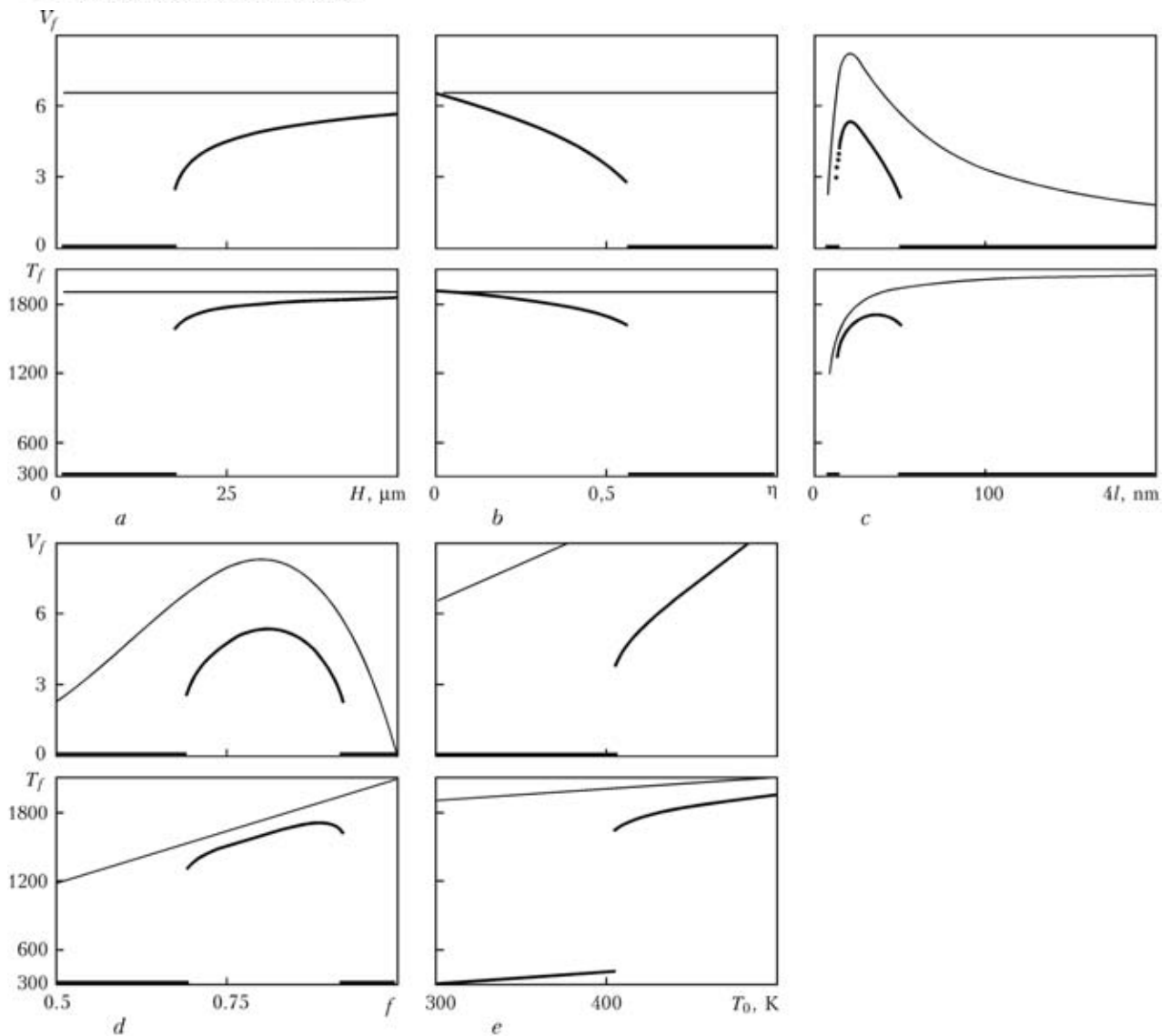


Figure 3. Dependence of rate V_f and maximal front temperature T_f on foil thickness H (a), contact efficiency coefficient η (b), multilayer spacing $4l$ (c), foil efficiency coefficient f (d) and initial temperature T_0 (e): thin and thick lines – SHS conditions without and with heat removal, respectively ($c = 0.5$, $D_0^2 = 1.5 \cdot 10^{-5}$, $Q = 1.7$ eV, $\Delta g = 0.46$ eV, $a_{\text{foil}}^2 = 7.42 \cdot 10^{-5}$ m²/s, $a_p^2 = 4 \cdot 10^{-5}$ m²/s, $\Delta y_0 = 2$ nm, $4l = 40$ nm, $f = 0.9$, $H = 20$ μm , $T_0 = 300$ K, $\eta = 0.5$); for Figure 3, e, $\eta = 1$

2) foil thickness H – the thicker the foil at a constant spacing, the more efficient is the heating, and the more difficult is suppression of the reaction (Figure 3, b);

3) spacing $4l$ and efficiency f of a MF multilayer – non-monotonous dependence $V_f(4l)$ is sensitive to heat removal at the multilayers that are too thin (f is low, as interlayer Δy_0 is always present), and at the thick layers (close to the systems of micron sizes) the extinction is absent only in a certain range of values of multilayer spacing $4l$ (Figure 3, c) or foil efficiency f (see Figure 3, d);

4) ambient temperature T_0 – the higher the initial temperature of the foil–plate system, the more efficient is the reaction diffusion, and the more difficult is suppression of the reaction (see Figure 3, e).

Whereas the third and fourth factors have an indirect effect on the heat removal by determining an insufficient local heating at a low rate of propagation

of the SHS wave, the first two factors directly determine the intensity of the heat removal (8).

It seems reasonable to re-write the ratio for the critical set of parameters, at which the combustion is probable, in the form of dependence $H(\eta, U)$. Then, the rest of the parameters being fixed, it is possible to add the critical value of thickness

$$H_{cr} = \frac{\eta}{\sqrt{\pi}} \frac{a_p^2}{U_{cr}} \quad (9)$$

Let us call parameter H_{cr} , above which the steady-state SHS condition is possible, the combustion threshold. Then condition $H > H_{cr}$ can be regarded as a combustion criterion at the fixed value of η . At the same time, at a constant thickness of the foil the combustion criterion can be the threshold value of

$$\eta_{cr} = \frac{\sqrt{\pi} H}{a_p^2} U_{cr} \quad (\text{the reaction occurs at } \eta < \eta_{cr}).$$



Dependence of critical foil thickness on phase formation energy and diffusion activation energy.

As the rate of the SHS front is determined primarily by reaction stimulus Δg and reaction activation energy Q , the extinction criterion depends on the same parameters. Solution of the system of equations (1) and (7) at different values of Δg , Q and η , and at fixed values of $4l$ and f , showed that dependence $H_{cr}(\Delta g, Q, \eta)$ can be well approximated by exponential function

$$H_{cr}(\Delta g, Q, \eta) = \eta H_0(\Delta g) \exp\left(\frac{Q}{Q^*(\Delta g)}\right), \quad (10)$$

where $Q^*(\Delta g) \approx b_Q \Delta g + Q_0$, $H_0(\Delta g) \approx b_H \ln(\Delta g / Q_0)$, coefficients b_Q and b_H depend on multilayer spacing $4l$ and foil efficiency f (the exact type of the dependences will be considered in a separate study).

CONCLUSIONS

1. It is shown that allowance for heat removal from the SHS reaction front propagating in a nanolayered foil in thermal contact with an environment may lead to its extinction under certain conditions.

2. Combustion is possible if the characteristic rate of heat removal determined by equation (8) is higher than the threshold value, which depends primarily on the diffusion activation energy, thermodynamic stimulus of intermetallic formation and temperature of the environment.

3. Extinction of the SHS reaction in the MF-heat-conducting material system can be avoided by increasing thickness of the foil, deteriorating thermal contact between the elements of the system, increasing temperature and reactivity of the foil (by selecting thickness of the layers which provides a higher rate of propagation of the SHS reaction front, and by decreasing thickness of intermetallic at interfaces between the layers).

4. Analytical approximation (10) of the threshold thickness is suggested for the combustion condition with regard to the activation energy and thermodynamic stimulus of the reaction.

The study was carried out with the support rendered by the Ministry of Education and Science of Ukraine under the integrated target basic research program of the HAS of Ukraine «Fundamental Problems of Nanostructured Systems, Nanomaterials and Nanotechnologies».

- (2003) *Concept of development of SHS as a field of scientific-technical progress*. Ed. by A.G. Merzhanov. Chernogolovka: Territoriya.
- Barzykin, V.V., Merzhanov, A.G., Strunina, A.G. (1990) Ignition of heterogeneous systems containing condensed reaction products. In: *Proc. of 23rd Int. Symp. on Combustion*. Pittsburgh: Combustion Institute, 1725–1731.
- Ustinov, A.I., Falchenko, Yu.V., Ishchenko, A.Ya. et al. (2008) Diffusion welding of γ -TiAl alloys through nanolayered foil of Ti/Al system. *Intermetallics*, **16**, 1043.
- Mann, B., Gavens, A.J., Reiss, M.E. et al. (1997) Modeling and characterizing the propagation velocity of exothermic reactions in multilayer foils. *J. Appl. Phys.*, **82**(3), 1178–1188.
- Zaporozhets, T.V., Gusak, A.M., Ustinov, A.I. (2010) Modeling of stationary condition of SHS reaction in nanolayered materials (phenomenological model). Pt 1: One-stage reaction. *Sovremen. Elektrometallurgiya*, **1**, 40–46.
- Zaporozhets, T.V., Gusak, A.M., Ustinov, A.I. (2010) SHS reactions in nanosized multilayers – analytic model versus numeric model. *Intern. J. Self Propagating High Temperature Synthesis*, **19**(4), 227–236.
- Zaporozhets, T.V. (2010) Modeling of stationary condition of SHS reaction in nanolayered materials (phenomenological model). Pt 2. Two-stage reaction. *Visnyk ChGU*, **171**, 16–30.
- Barron, S.C., Knepper, R., Walker, N. et al. (2011) Characterization of self-propagating reactions in Ni/Zr multilayer foils using reaction heats, velocities and temperature-time profiles. *J. Appl. Phys.*, **109**, 13–19.
- Wang, J., Besnoin, E., Duckham, A. et al. (2004) Joining of stainless steel specimens with nanostructured Al/Ni foils. *Ibid.*, **95**(1), 248.
- Wang, J., Besnoin, E., Knio, O.M. et al. (2005) Effects of physical properties of components on reactive nanolayer joining. *Ibid.*, **97**(11), 114–307.
- Grigoryan, A.E., Elistratov, N.G., Kovalev, D.Yu. et al. (2001) Autowave propagation of exothermic reactions in thin multilayer foils of Ti–Al system. *Doklady RAN*, **381**(3), 368–372.



PECULIARITIES OF TEMPERATURE DISTRIBUTION IN THIN-SHEET ALUMINIUM ALLOY AMg5M IN FRICTION STIR WELDING

A.G. POKLYATSKY

E.O. Paton Electric Welding Institute, NASU, Kiev, Ukraine

Influence of backing material, speed of welding and diameter of tool shoulder on the change in nature of temperature distribution in welded joint cross-section was studied. It was established that formation of permanent joints in friction stir welding takes place at the temperature of not higher than 450 °C.

Keywords: *friction stir welding, aluminium alloy AMg5M, thin sheet, butt joints, thermal cycle, distribution of temperatures*

During friction stir welding (FSW) the processes of deformation and moving along the complex path of material heated till plastic condition, mechanical refining of its components, recrystallisation of grains, diffusion of particles and intensive migration of dislocations, which results in formation of a permanent joint in a solid phase without melting of the base material. The efficiency of proceeding of these processes depends greatly on heat evolution in the places of contact of friction working surfaces of a tool with a metal being welded.

The distribution of temperature fields in the zone of a joint is considerably influenced by thermal physical characteristics of alloys to be welded and parameters of welding process. However, the analysis of results of experimental investigations and theoretic calculations, given in the foreign sources, show that in most cases in welding of aluminium alloys of medium thicknesses the formation of permanent joints takes place at maximal heating temperature of metal of not higher than 500 °C, which amounts about 70–80 % of melting temperature of these materials [1–5]. The metal in welding zone remains at increased temperature for a very short time, which considerably decreases its level of softening and physical-mechanical characteristics as compared to those in fusion welding [6–9].

During welding of thin-sheet semi-products the certain peculiarities arise predetermined by change in nature of heat removal both into backing, on which the formation of a permanent joint takes place, and also in longitudinal and transverse direction of a base material. Moreover, during rotary-onward movement of a working tool in the zones of contact of its working surfaces with the alloy being welded different thermo-deformational conditions arise both on the advancing side of a tool (where directions of vectors of its rotary and linear movement coincide), as well as on the its

retreating side (where they are moving in opposite directions).

The aim of this work is to investigate the peculiarities of distribution of temperatures in FS-welded butt joints of thin-sheet aluminium alloy AMg5M.

To conduct experimental investigations the aluminium alloy AMg5M widely applied in manufacturing of different welding structures was used. The FSW of sheets 2.8 mm thick was performed in the laboratory installation designed at the E.O. Paton Electric Welding Institute. Special tools with a shoulder of 12 and 14 mm diameter and a conical tip were used for producing butt joints. The rotation speed of tool was 2880 rpm, and the linear speed of its movement along the butt was 8–20 m/h. To compare thermal cycles, AMg5M alloy sheets were automatic TIG-welded in argon by the Fronius installation MW-450 (Austria) at the speed of 10 m/h at 160 A current using welding wire SvAMg5 as a filler material.

The temperature of metal in different zones of welded joints was measured using chromel-alumel thermocouples of 0.1 mm diameter. The results of measurements during welding were registered in the computer using the ICP DAS module of analogue input I-7018P applying EZ Data Logger v431 software. The module was connected to the computer using additional signal converter EX 9530 with the software DCON Utility v5.1.8.

The analysis of obtained results shows that the nature of changes in temperature of material being welded is predetermined by specific conditions of permanent joint formation in solid phase. At the initial stage of FSW process, when rotary tip of tool is gradually deepened into the butt, negligible increase in heat amount evolved as a result of friction occurs (Figure 1). During further deepening of working tool, when contact between end surface of its shoulder and material being welded (at the seventh second) occurs, the heating temperature of the latter begins growing sharply. It occurs unless the tool shoulder penetrates into metal being welded for about 0.1 mm, when between backing and working surfaces of tool the closed space is formed, inside which a plasticized material

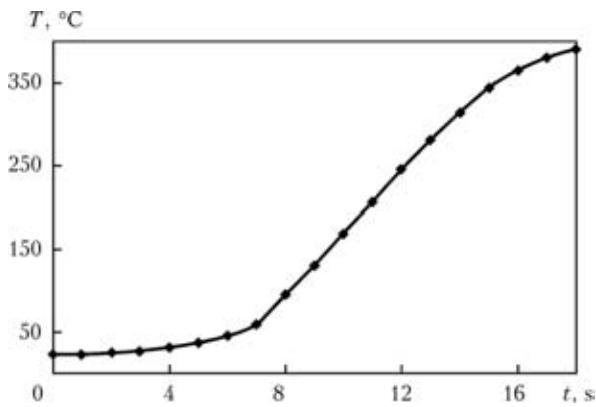


Figure 1. Distribution of temperature of heating of AMg5M alloy at the distance of 6 mm from the weld centre in FSW at $v_w = 8$ m/h at deepening of working tool with 12 mm diameter shoulder and tip of conical shape

being under high pressure is moving around by the rotary tool and forms a spot weld.

When except of rotary movement the tool starts onward movement along the butt to produce a linear weld, then in front of the advancing side of tool the zone of excessive pressure is formed, from which its working surfaces force out the material heated till plastic condition hindering their movement. This material due to reciprocate movement of tool is constantly moving to the zone releasing behind it. But during movement it forces its way under the high pressure near the tool on its retreating side, where plasticized metal is already present heated up to the same temperature. Obviously when friction appears between these volumes of material, negligible additional heat evolution takes place, which results in 10–15 °C higher temperature of metal in the zone of permanent joint formation always on the retreating side of tool as compared to that on its advancing side (Figure 2).

The heating of material being welded to the maximal temperatures takes place around the tool tip near its base in the zone of abutting the working surface of shoulder. However in welding of thin-sheet materials the tip of tool is very short. Therefore, considerable amount of heat evolved due to friction is spread to the backing where a permanent joint is formed. Consequently, one of the efficient methods to increase temperature of metal in welding zone is the use of backings manufactured of materials with low heat conductivity.

In the course of conducted experimental investigations it was established that when using the asbestos-cement backing instead of steel one in FSW of AMg5M alloy 2.8 mm thick, the temperature of metal near the edge of tool shoulder increases approximately by 20 % at the same condition parameters. Thus, the material being welded is heated up to 450 and 470 °C, respectively, on the advancing and retreating side of tool.

The measurements of temperatures at a different distance from the axis of weld on the retreating side of tool allowed establishing the regularities of con-

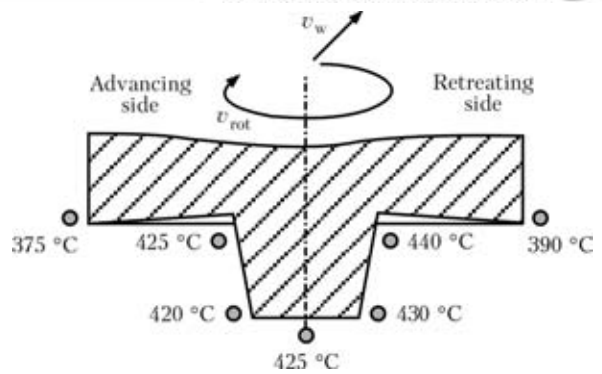


Figure 2. Temperature points of metal in the FS-welded joint on AMg5M alloy at $v_w = 8$ m/h

duction of a heat field in solid-phase welding of butt joints of thin-sheet aluminium alloys. The obtained results are evidence of the fact in FSW of AMg5M alloy at speed of 8 m/h at 6 mm distance from the axis of weld, the metal is heated up to 390 °C (Figure 3, a). The maximal value of the temperature is achieved not at the moment, when the tool is located opposite to the thermocouple, but after its further movement approximately by 2 mm. At the distance of 11 mm from the weld axis, the maximal temperature of heating of the metal (250 °C) is achieved during displacement of heating source from the thermocouple almost by 7 mm. With increase of distance from the weld axis up to 21 mm, the maximal heating temperature of metal decreases to 160 °C during displacement of heating source by 15 mm from the thermocouple. During further increase of distance from the weld axis

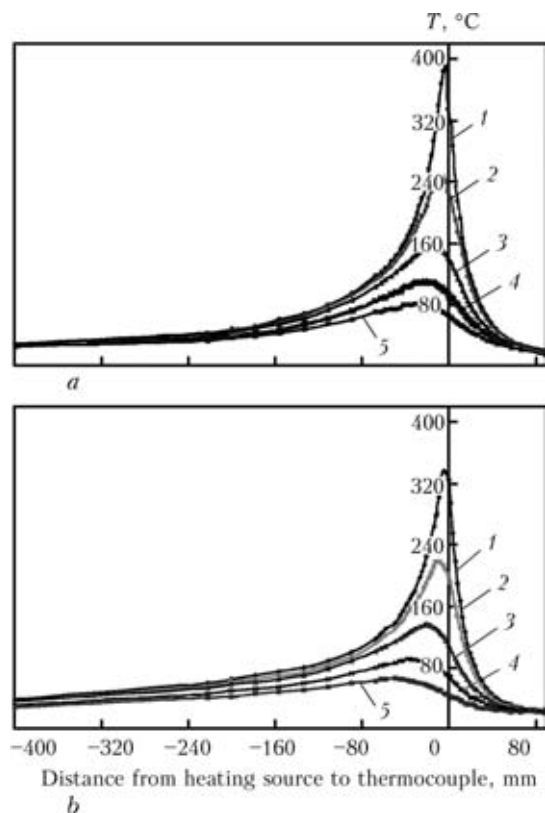


Figure 3. Distribution of temperature in FSW of AMg5M alloy butt joint at $v_w = 8$ (a) and 20 (b) m/h and different moving from the weld axis: 6 (1), 11 (2), 21 (3), 31 (4) and 40 (5) mm

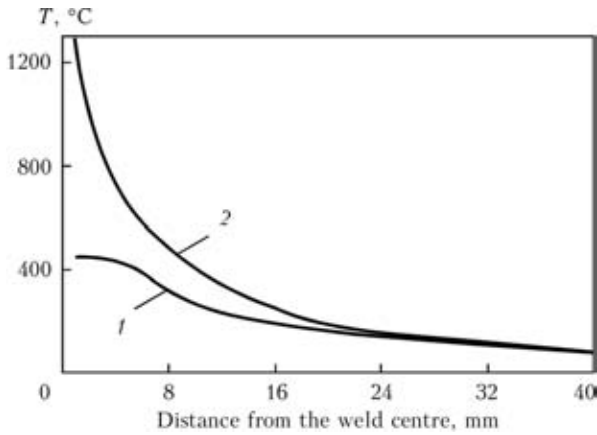


Figure 4. Distribution of temperature in transverse direction of butt joints of AMg5M alloy produced using FSW (1) and TIG welding (2)

to 31 and 40 mm, the maximal temperature of metal decreases accordingly to 110 and 80 °C. The obtained curves are evidence of rapid heat conduction in transverse and longitudinal directions from the axis of weld in FSW of thin-sheet semi-products of aluminium alloy AMg5M with a high heat conductivity. The segments of the curves corresponding to the processes of heating and cooling of metal bear a non-symmetric character. Thus, thermocouple located near the edge of shoulder shows that, if the tool is at the distance of 5 mm before it, then the metal in this zone is heated approximately to 270 °C and after displacement of the tool to the same distance beyond the thermocouple, the temperature of metal remains at the level of 380 °C, i.e. cooling of metal after welding is slower than its heating. However, the total time of metal being in the process of welding at the temperature higher than 200 °C does not exceed 15 s.

The increase of speed of linear movement of the tool along the butt sufficiently influences the temperature of heating of metal in the zone of welding. Thus, the increase of welding speed from 8 to 20 m/h leads to decrease of temperature of AMg5M alloy near the edge of shoulder on the retreating side of tool from 390 to 350 °C (Figure 3, b). Here, the maximal value of temperature of metal in that point is achieved at moving of tool from the thermocouple longer than

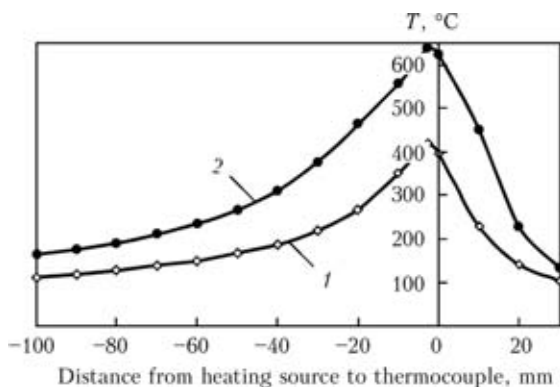


Figure 5. Distribution of temperature in longitudinal direction at the distance of 5 mm from the weld axis in FSW (1) and TIG welding (2) of butt joints of AMg5M alloy

4 mm. At displacement of the tool beyond the thermocouple almost by 10 mm at the distance from the weld axis of 11 mm, the maximal temperature of metal heating at the welding speed of 20 m/h is about 220 °C. With the increase of distance from the axis of weld to 21, 31 and 40 mm the maximal level of temperature of heating of the metal decreases to 140, 90 and 65 °C, respectively. However, the analysis of produced welded joints showed that at the temperature of heating of AMg5M alloy, which is achieved at welding speed of 20 m/h, the sufficient plasticity of material in the zone of formation of permanent joint is not provided due to which inner defects appear in the welds.

One of the ways to increase the amount of heat evolved in the welding zone is increase of diameter of the tool shoulder [10], that allows increasing the area of its edge surface contacted with a material being welded. In the course of carried out experimental investigations it was established that at the constant speed of welding of 8 m/h the application of the tool with 14 mm diameter shoulder allows increasing the temperature of heating of the metal at the base of tip on the retreating side of tool up to 470 °C. The proportional increase of temperature of metal is observed also in the rest characteristic zones around the working surfaces of tool. Thus, at 14 mm diameter of shoulder near its edge on the retreating side of tool, the metal is heated to 410 °C, which is 20 °C higher than that near the edge of shoulder of 12 mm diameter. The increase of temperature of metal in the zone of permanent joint formation leads to negligible decrease of its cooling rate and increase of time of its stay at increased temperatures.

The comparative analysis of temperature distribution in transverse (Figure 4) and longitudinal (Figure 5) directions of butt joints of AMg5M alloy is the evidence of existing distinction of level of the metal heating in TIG welding and FSW. In TIG welding in the zone of permanent joint formation the complete melting of material takes place. At the distance of 2 mm from the weld axis, the temperature of metal remains at the level of 1000 °C, and near the fusion zone of weld with the base metal at the distance of about 5 mm from the weld axis it approaches to 638 °C, i.e. to the temperature, at which solidification of AMg5M alloy only begins. Besides, heating of metal up to high temperatures during fusion welding pre-determines also a wider HAZ. Thus, until the temperatures higher than 200 °C the metal being welded is heated at the distance of 19 mm from the weld axis, while during solid-phase FSW the maximal temperature of heating of metal in the zone of a permanent joint formation does not exceed 450 °C, and at the distance of 5 mm from the weld axis it remains at the level of 410 °C. The heating of metal to the temperatures higher than 200 °C occurs only at the distance of 14 mm from the weld axis.



In the process of cooling of metal at removal of heating source from the place of welding, the gradual decrease of its temperature occurs. Therefore, in TIG welding the metal in the zone of fusion of weld with the base material has the temperature by 150 °C higher than that in FSW even during movement of heating source from this place by 30 mm. And if during solid-phase FSW the temperature of metal at the distance of 5 mm from the weld axis decreases to less than 200 °C at the removal of heating source by 35 mm, then in fusion TIG welding it is decreased at removal by 75 mm. Consequently, maximal temperature of metal heating in the zone of permanent joint formation and total time of stay of base material being welded at high temperatures are reduced, that results in decrease of probability of proceeding the irrevocable physical-chemical processes leading to significant deterioration of mechanical properties of welded joints and causing their deformation.

In conclusion it should be noted that quality formation of welds in FSW of butt joints of aluminium alloy AMg5M 2.8 mm thick is provided at heating of metal in the zone of welding up to 450 °C, which amounts 79 % of temperature of beginning of its melting. Here, at the distance of 5 mm from the weld axis the metal is heated only to the temperature of 410 °C, while in TIG welding still it remains in molten state at 638 °C, i.e. at the temperature of solidification beginning. The decrease of maximal temperature of

heating of the zone of welding and reduction of time of stay of material being welded at increased temperatures will have a positive effect on properties of welded joints produced using FSW.

1. Lambrakos, S.G., Fonda, R.W., Milewski, J.O. et al. (2003) Analysis of friction stir welds using thermocouple measurements. *Sci. and Techn. of Welding and Joining*, **5**, 385–390.
2. Shercliff, H., Russel, M., Taylor, A. et al. (2005) Microstructural modeling in friction stir welding of 2000 series aluminium alloys. *Mechanics and Industries*, **6**, 25–35.
3. Kokubo, M., Takayama, Y., Kazui, S. et al. (2007) Temperature analysis in friction stir welding of ADC12/5052 dissimilar aluminium alloys. *J. Japan Institute of Light Metals*, **11**, 511–517.
4. Colegrove, P.A., Shercliff, H.R. (2003) Experimental and numerical analysis of aluminium alloy 7075-T7351 friction stir welds. *Sci. and Techn. of Welding and Joining*, **5**, 360–368.
5. Khandkar, M.H., Khan, J.A., Reynolds, A.P. (2003) Prediction of temperature distribution and thermal history during friction stir welding: input torque based model. *Ibid.*, **3**, 165–174.
6. Cederqvist, L., Reynolds, A.P. (2001) Factors affecting the properties of friction stir welding aluminum lap joints. *Welding J.*, **12**, 281–287.
7. Hassan, A.A., Prangnell, P.B., Norman, A.F. et al. (2003) Effect of welding parameters on nugget zone microstructure and properties in high strength aluminium alloy friction stir welds. *Sci. and Techn. of Welding and Joining*, **4**, 257–268.
8. Sato, Y. (2002) Relationship between mechanical properties and microstructure in friction stir welded Al alloys. *J. JWS*, **8**, 33–36.
9. Chao, Y., Wang, Y., Miller, K. (2001) Effect of friction stir welding on dynamic properties of AA2024-T3 and AA7075-T7351. *Welding J.*, **8**, 196–200.
10. Okamura, H. (2003) Point of application for ESW. *Welding Technology*, **15**, 60–69.

XII INTERNATIONAL SCIENTIFIC-PRACTICAL CONFERENCE «RENEWABLE POWER GENERATION OF THE XXI CENTURY»

September 12–16, 2011

Crimea, Ukraine,
Nikolaevka, «Energetik» Holiday

Organizers: Institute of Renewable Power Generation of the NAS of Ukraine, ISTC of Wind Power Engineering of the NAS of Ukraine.

Conference topics: complex DEP systems, wind power generation, solar power engineering, biomass energy, hydro-power engineering, geothermal power generation, hydrogen power engineering, environmental energy, intelligent networks, energy parks.

Contact address: nikolaevka2010@gmail.com



DEVELOPMENT OF THE METHODS FOR ELIMINATION OF DEFORMATION OF CRANKSHAFTS IN WIDE-LAYER HARDFACING

S.Yu. KRIVCHIKOV

E.O. Paton Electric Welding Institute, NASU, Kiev, Ukraine

Methods were developed for elimination of deformation of crankshafts of car engines caused by wide-layer hardfacing at their reconditioning. It is established that an effective method to eliminate deformations is preheating of hardfaced bearings and (or) application of axial tensile load to the crankshaft during hardfacing.

Keywords: arc wide-layer hardfacing, crankshafts, deformation, measures of elimination

Different methods of arc hardfacing are widely used for reconditioning of worn crankshafts of the car engines. According to the practice, wide-layer hardfacing with self-shielding flux-cored wire [1] is the most perspective among them. It differs by high efficiency, stable quality of obtained results and provides operating live time of reconditioned crankshaft on a level of new one. Along with it, significant heating [2] of working surfaces (main and crank bearings) takes place during wide-layer hardfacing, that results in deformation occurrence, i.e. change of initial length of the crankshaft. Most of crankshaft types are characterized by basic length l_0 , which according to design documentation can be changed only in the narrow ranges (± 0.3 mm). Therefore, if linear deformation Δl exceeds specified limits as a result of hardfacing, this promotes appearance of increased end-play and creates problems during setting of reconditioned crankshaft in the engine.

Present study is devoted to development of the methods for elimination of linear deformation (shortening) of the crankshafts by wide-layer hardfacing.

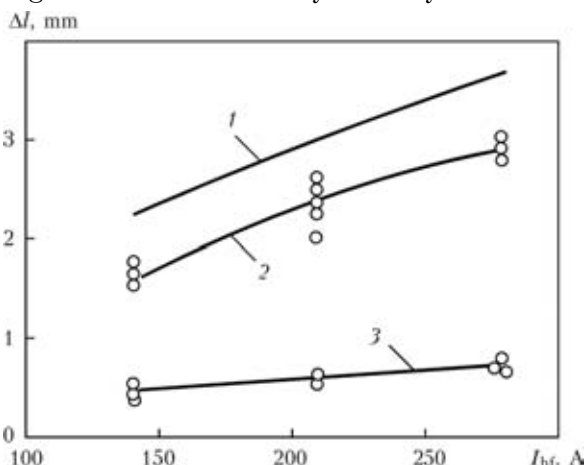


Figure 1. Influence of current of wide-layer hardfacing on change of length of the crankshaft and its structural elements: 1 – $\Sigma\Delta l$; 2 – Δl_c ; 3 – Δl_m

Five-bearing crankshaft representing itself crank consisting of five main and four crank bearings was selected as an object for investigation. Such a structure of the crankshaft is widely used in many engines of present cars of domestic and foreign manufacture and differs only by geometry and chemical composition of the base metal (medium alloyed carbon steel or high-strength pearlite cast iron). Corresponding cylinder specimen-imitators were manufactured for determining shortening of separate structural elements of the crankshaft (main and crank bearings). Error of measurement of all linear dimensions made ± 0.05 mm.

Figure 1 shows an influence of wide-layer hardfacing mode on total length of main Δl_m and crank Δl_c groups of bearings as well as on general length of the crankshaft $\Sigma\Delta l$ ($\Sigma\Delta l = \Delta l_m + \Delta l_c$) after hardfacing and cooling of the crankshaft to room temperature. As can be seen from the Figure, increase of current of hardfacing I_{hf} rises difference of lengths Δl before and after hardfacing of all structural elements and crankshaft in whole, and allowable limits, specified for basic length l_0 are significantly exceeded at maximum efficiency of hardfacing process. Besides, shortening of the main bearings Δl_m after hardfacing has insignificant dependence on I_{hf} . At the same time Δl_c is significantly higher than Δl_m and rises proportionally to increase of I_{hf} at similar currents of hardfacing. At that, input of Δl_c in $\Sigma\Delta l$ makes 73–80 %. Different influence of I_{hf} on Δl_m and Δl_c is related with the fact that the crank bearings are manufactured hollow in contrast to main bearings thereby temperature of their heating is significantly higher in the process of hardfacing. As a result, favorable conditions for more complete passing of shrinkage are developed in solidified weld pool and base metal of the crank bearing.

Application of repair rings. Setting of the repair rings (Figure 2) (before hardfacing) is one of the most simple and allowable methods of elimination of crankshaft shortening caused by hardfacing. At that thickness of each ring should be 0.5–1.0 mm higher of $\Sigma\Delta l$, determined from Figure 1. Finally, basic length of the crankshaft is regulated by mechanical treatment after hardfacing. The main disadvantage of specified



method is that compensation of total shortening of the crankshaft is performed only with regard to first main bearing. Thus, axial displacement of the holes of oil channels for all groups of bearings relatively to fixed supply of lubrication in the engine oil system takes place. This, depending on $\Sigma\Delta l$ value, can result in partial or full overlapping of section of the hole of oil channel and breakdown of lubricant supply to wear surfaces. Practice shows that specified method can be successfully used in wide-layer hardfacing of the crankshafts of relatively small dimensions (for example, crankshafts of car engines of VAZ family, «Tavriya» etc.) where $\Sigma\Delta l$, as a rule, does not exceed 1.5 mm.

Application of preheating. Formation of relatively narrow weld pool over the whole length of hardfaced bearing virtually simultaneously with beginning of the hardfacing process is one the characteristic peculiarities of wide-layer hardfacing. Further, hardfacing rate (speed of rotation of hardfaced bearing) determines movement of a weld pool front and its solidification. As a result, whole surface of the bearing after hardfacing becomes covered by layer of deposited metal, the width of which equal to bearing length. Elongation Δl_t of the specimen at heating is determined by dependence $\Delta l_t = k l_i \alpha_{av} \Delta T$ (here, k – factor of proportionality; l_i – initial length of the specimen; α_{av} – average value of coefficient of linear expansion of specimen metal in considered temperature range; ΔT – difference between heating temperature and initial temperature of the specimen) according to general theory of deformation. Following it, if a bearing of the crankshaft of l_i length is preheated (before hardfacing) up to specific determined temperature $T_{preheat}$ than wide-layer hardfacing will already be performed on a bearing of $l_i + \Delta l_t$ length, where Δl_t is the increment of bearing length caused by heating. At that, length of the weld pool is also increased per Δl_t due to peculiarities of wide-layer hardfacing. As a result, it can be assumed that Δl_t value compensates shortening of Δl_c bearing at properly selected $T_{preheat}$ since wider solidified layer of the deposited metal prevents more complete passing of the shrinkage processes in the base metal during bearing cooling.

Wide-layer hardfacing of the specimen-imitators of corresponding bearings was carried out on optimum mode ($I_{hf} = 250$ A) at different preheating temperatures for studying the influence of $T_{preheat}$ on linear dimensions of the main and crank bearings. Obtained results (average value on two-three specimens) are given in the Table. It can be seen from data provided that an increase of $T_{preheat}$ promotes monotone decrease of residual linear deformation of the crank as well as main bearing and the latter becomes approximately equal zero at $T_{preheat} \approx 300$ °C. Higher temperatures of preheating result in that the basic length of hard-

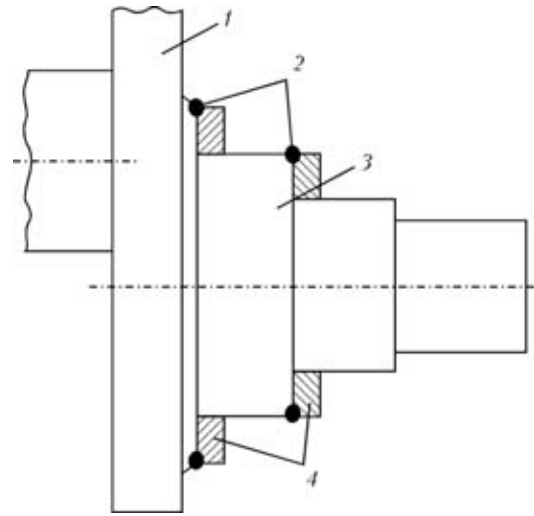


Figure 2. Scheme for setting of repair rings on the first main bearing for eliminating shortening of hardfaced crankshaft: 1 – bearing; 2 – tacks; 3 – first main bearing; 4 – repair rings

faced crankshaft will be more than in the initial one (before hardfacing).

It should be noted that in spite of the fact that introduction of additional operation of preheating in the technological process of hardfacing makes it more energy- and labor-consuming, such an operation is useful for some dimension-types of crankshafts and being necessary measure, reducing formation of cracks in the deposited and base metals for cast iron crankshafts. Moreover, it should be considered that application of preheating increases the danger of draining of liquid weld pool from cylinder surface in the process of wide-layer hardfacing. Therefore, usage of specified method for elimination of deformations is possible only in those cases when diameter of bearings of the crankshaft exceeds 50 mm.

Application of tensile loads in the process of hardfacing. It is well-known fact that medium-carbon steels differ by sufficiently high deformation ability ($\delta > 10$ %) at normal temperature. If pearlite high-strength cast iron (for example, VCh 50-2) is a material of the crankshaft than it will be low-plastic ($\delta \approx 2$ %) at normal temperature. However, its elongation can achieve 12 % with temperature increase and tensile and yield strengths reduce per order. Deformation of heated samples from high-strength cast iron occurs at relatively small (6–7 MPa) tensile loads [3] under welding process conditions. Base metal of bearings of the crankshaft depending on their dimensions, hard-

Influence of temperature of preheating on change of dimensions of the main and crank bearings

Parameter	$T_{preheat}, ^\circ\text{C}$					
	20	100	200	300	400	500
Δl_c	-2.88	-2.42	-1.92	-0.54	0.25	1.04
Δl_m	-0.68	-0.44	-0.35	0.42	0.76	0.82

Note. Negative value – shortening, positive – elongation of the bearing as compared to initial dimensions.

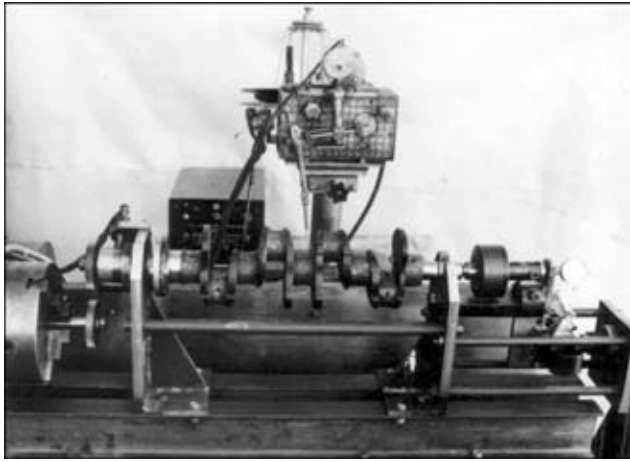


Figure 3. Appearance of device for applying and regulating of axial tensile load to crankshaft in the process of hardfacing

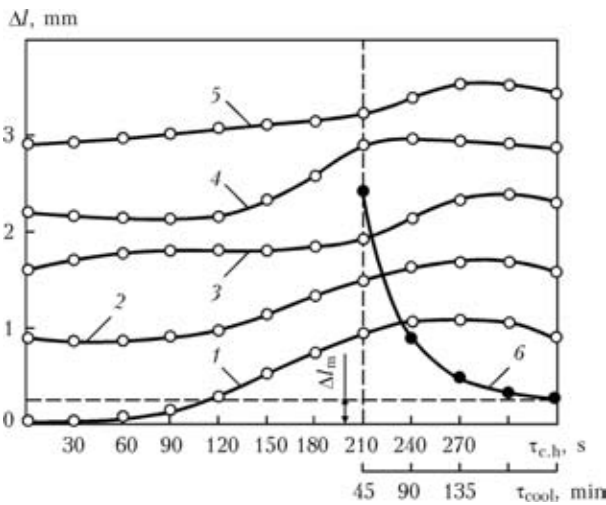


Figure 4. Dynamic curves of change of length of the crankshaft in the process of wide-layer hardfacing of main bearings (1–5) and in the process of its cooling (6) under effect of axial tensile load

facing mode and location of heating source can heat up to 800–1150 °C due to thermal cycle of wide-layer hardfacing.

Investigations of influence of axial tensile loads on length of the crankshaft under conditions of real thermodeformation cycle of wide-layer hardfacing were carried out based on that. The investigations were performed using specially manufactured device (Figure 3) allowing carrying out wide-layer hardfacing of the crankshaft at simultaneous application of tensile load to it. The device consists of metal body with fastened to it clamping mechanisms (left and right), providing fixing of the crankshaft in necessary position as well as its rotation and possibility of axial elongation under tensile load effect. The latter is applied to the crankshaft with the help of screw-jack through measuring resilient member, i.e. shrinkage dynamometer DOSM 3-3 and leverage system. The device body is fixed on a base of universal hardfacing machine UD-209. Rotation of the crankshaft with regulated speed is performed from spindle of UD-209 machine through gear drive. The device allows regulating tensile load in the ranges from 0 to 30 kN.

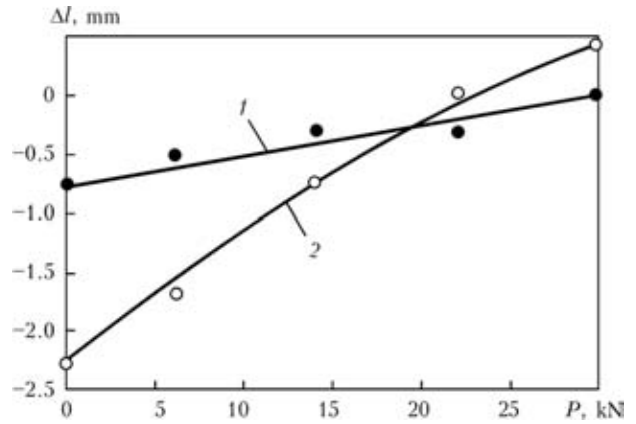


Figure 5. Effect of axial tensile load on change of length of main Δl_m (1) and crank Δl_c (2) bearings of the crankshaft in wide-layer hardfacing

Wide-layer hardfacing was performed on optimum mode ($I_{hf} = 220\text{--}250$ A) for considered type of the crankshaft. Figure 4 shows dynamic curves of change of crankshaft length in the process of hardfacing of the main bearings ($\Delta l - \tau_{c,h}$) and in the process of its cooling ($\Delta l - \tau_{cool}$) under effect of constant tensile load $P = 30$ kN. A time of cycle of hardening $\tau_{c,h}$ includes time used for bearing hardfacing (300 s) and time for setting of hardfacing machine for hardfacing of the next bearing.

A conclusion can be done according to obtained data that the length of crankshaft increases as a result of thermal elongation as well as plastic deformation caused by effect of tensile load in the process of bearing hardfacing. Then, the length of shaft reduces due to passing of shrinkage process in the base and deposited metals during cooling. At room temperature Δl achieves a constant value equal Δl_m characterizing actual elongation ($\Delta l_m > 0$) of the crankshaft, occurring under effect of axial tensile load.

It is seen from Figure 5 that Δl changes in sign as well as value depending on axial load. Moreover, shortening of the crankshaft as a result of hardfacing of crank Δl_c and main Δl_m bearings is different and depends on tensile load. It is obvious that additional application of preheating of the bearings allows reducing optimum value of tensile load.

It should be noted that the latter method for control of residual deformations can be considered universal since it is applicable to any type of the crankshaft independent on its geometry, shape and chemical composition of the base metal.

1. Zhudra, A.P., Krivchikov, S.Yu., Petrov, V.V. (2010) Technology for wide-layer hardfacing of crankshafts. *The Paton Welding J.*, **2**, 32–35.
2. Krivchikov, S.Yu., Zhudra, A.P., Petrov, V.V. et al. (1998) Thermal cycle of wide-layer hardfacing of cylindrical cast iron parts with self-shielded flux-cored wire. *Avtomatich. Svarka*, **4**, 49–50.
3. Gretskey, Yu.Ya., Novikova, D.P., Kroshina, G.M. (1986) Influence of thermal cycle on resistance of cast irons to cracking in welding without preheating. *Ibid.*, **4**, 1–4, 13.



SEMINAR OF THE SOCIETY OF WELDERS OF UKRAINE

On June 16–17, 2011 seminar-meeting on «Welding Fabrication of Ukraine: Status and Prospects» was held in Knyazhichi village of Kiev district in the Technology Center of «Fronius Ukraina» Ltd. The event was organized by the Council of the Society of Welders of Ukraine (SWU), E.O. Paton Electric Welding Institute and «Fronius Ukraina» Ltd.

More than 50 specialists participated in the seminar, representing the majority of regional branches of SWU, including chief welders, technical directors of enterprises, university lecturers, heads of welding laboratories. PWI leading specialists also took part in the seminar.

Seminar was opened by Dr. V.G. Fartushny, SWU President, who noted the importance of such meetings of specialists, allowing exchange of current information on the problems of welding fabrication in the regions, discussion of priority directions in SWU activity, outlining the ways to improve its activity. Special attention should certainly be given to the issues of improvement of product quality, increasing its competitiveness. Dr. Fartushny read the greetings from Prof. Boris E. Paton, PWI Director, to seminar participants with wishes of strengthening the contacts of specialists, improvement of the efficiency of their activity for the benefit of Ukraine.

Then A.I. Komissar, General Manager of «Fronius Ukraina» welcomed the participants and gave brief information on establishment and development of the affiliate of «Fronius» in Ukraine. Now that the Company already is 20 years old, its products are being prepared for certification for «European level» criterion, that will allow widening the product market. Mr. A.I. Komissar wished fruitful work to the seminar.

Dr. V.M. Ilyushenko, SWU Executive Director, thanked the management of «Fronius Ukraina» for excellent working conditions for the seminar, and presented to the participants the first issue of information-technical journal «Visnyk Tovarystva Zvarnykiv Ukrainy», publication of which was timed to this seminar.

Then Dr. A.A. Mazur, Head of Department of PWI, Executive Director of the PWI Technology Park, made a presentation on «Welding Fabrication of Ukraine in 1990–2010». He analyzed the dynamics and causes for a decline in manufacturing of welding equipment and consumables, and welded structure fabrication in Ukraine during the years of restructuring. He noted that annual statistical reporting of enterprises still has not been organized. There are problems related to quality of training of welding production specialists. At present optimization of the balance in «quality + price» categories is urgent for production. In this connection, SWU should increase its role

in reduction of the scope of coated-electrode arc welding application and widening the application of gas-shielded welding (cost of one meter of weld, made by manual arc welding, is 3–4 times higher than when MAG welding is used). PWI Department of Economic Studies is ready to render services to enterprises on optimization of selection of the welding process, calculation of cost effectiveness, etc.

In the paper of V.L. Bondarenko, Marketing Director of «Fronius Ukraina», entitled «Fronius Ukraina» — Today» Ltd. a historical overview of establishment and development of «Fronius» known in the welding community, as well as its affiliate in Ukraine, was made. The speaker gave a detailed presentation of new developments of «Fronius» over the last years, making it a prominent technological leader in the world.

V.I. Okul, Technical Manager of OJSC «KZESO», in his presentation focused on the main directions of development and improvement of equipment manufactured by the Plant. This, first of all, is equipment for flash-butt welding of rails under stationary and track conditions, new generation of ESW equipment with modern systems of process control and monitoring.

N.A. Korol, Director of «Svarkontakt» Ltd., spoke about inverter power sources for arc welding produced by the enterprise. Most of the users now have a clear understanding of the merits and advantages of inverters. The enterprise is continuously searching for new possibilities: equipment samples are being developed for application for underwater welding, plasma welding and cutting, and stud welding. Together with PWI, a new specialized block was developed, the application of which essentially widens the technological capabilities of arc welding with any rectifier. Welding without spatter is achieved with arc shielding by carbon dioxide gas.





N.V. Vysokolyan, Chief Welder of OJSC «Kryukovsky Vagonzavod», described the requirements of new standards in car-building. He noted the high demand for freight cars. Increasing requirements on safety and production monitoring necessitated the introduction of international standards of welding production in railway transportation. They include the systems of design and management and should be introduced at the end of 2013. The enterprise is mastering the technology of manufacturing passenger cars with a body of stainless steel of 18-10 type. For a number of years the enterprise has successfully used welding equipment supplied by «Fronius Ukraina» and «Svarkontakt» Ltd.

Presentation by Dr. B.P. Budzan, Director of Consultative Center on Management, on «Role of enterprise leader in the current economic conditions», generated a lot of interest. He highlighted those traits of modern production manager, which guarantee successful performance of an enterprise under changing conditions.

A.Ya. Ishchenko, Corresp.-Member of NASU, Head of PWI Department of Welding Nonferrous Metals, gave a brief overview of the capabilities of Department, and positive experience of co-operation with «Fronius Ukraina» and invited the audience to place contracts with the Department.

V.P. Slyuta, Manager of Marketing Department of «Fronius Ukraina», described in detail a number of technologies and equipment, developed by «Fronius» over the last 15 years: welding and surfacing with cold metal transfer (CMT), laser hybrid welding, resistance spot welding of thin metals, including zinc-plated metals and metals of different thickness, new design of Contec (durable contact tip for welding wire feed), Trans Steel Yard apparatus for MAG welding of steels with digital program control and connecting hose-pack of up to 40 m for ship-building, etc.

Detailed paper by Yu.A. Didus, Director General of «Binzel Ukraina GmbH», was devoted to welding torches manufactured by «Abicor Binzel»: design features, main types, ergonomics, medical certificates, fields and experience of application. A number of samples of commercial torches were demonstrated. Contact lubricant for cleaning and wetting of welding

wire, as well as a device for accurate positioning of the torch are presented.

V.A. Belinsky, Chief Welder of «NKMZ» Company (Kramatorsk), spoke about a unique installation for electroslag welding of large-sized thick-walled products developed and operating at «NKMZ» starting from 2002.

V.V. Maksimchuk, Chief Technologist of «ZhZMK» Ltd. (Zhitomir), described the technologies and equipment applied at the plant in fabrication of building metal structures, as well as product quality assurance system.

Problems of introduction of quality control system in welded structure fabrication, based on DSTU ISO 9001:2009 were considered in the paper presented by Dr. Yu.K. Bondarenko, Head of PWI Department.

Dr. P.P. Protsenko, Director of PWI ITCC, presented two documents, developed and approved in Ukraine, which describe the integrated profession of «Welder» and program of vocational training complying with international standards.

Prof. A.A. Kajdalov, Vice-President of SWU, described in detail the welders' competitions conducted by the Society in Ukraine, as well as participation of Ukrainian welders in the competitions conducted in other countries as methods to promote the profession of a welder.

This was followed by discussion of a number of subjects raised in the seminar, and seminar resolutions were passed:

- Note the need for actualization of the normative base in the field of welding fabrication in some branches of industry of Ukraine. It is believed to be expedient, following SWU advice, to promote more active efforts on updating the normative documents, indicated by seminar participants;

- Note that the procedure of document submission by developers of technologies, materials and equipment for participation in the tenders is imperfect and creates difficulties for organizing the work. Request SWU Council to study the issue for possible application to higher organs;

- It expedient for SWU to study the question of its participation in the activities of the Commission on State-Public Cooperation at the Cabinet of Ministers of Ukraine;

- Approve the publication of the SWU bulletin;
- Take notice of the information on introduction of integrated profession of «welder» and on creation of a new program of vocational training in the field of welding in Ukraine. These two documents should be published in the journal «Visnyk Tovarystva Zvarnykiv Ukrainy»

- Conduct seminar-meeting of leading specialists of welding fabrication of Ukraine on an annual basis.

Prof. V.N. Lipodaev, PWI
Prof. A.A. Kajdalov, SWU

UKRAINIAN-POLISH SCIENTIFIC-TECHNICAL CONFERENCE

From June 29 to July 1, 2011 the International Scientific-Technical Conference on «Development of Advanced Technologies and Equipment for Welding Railway Rails in Preparation of Ukraine and Poland to EURO-2012» was held in the conference-hall of Lviv hotel «Sykhiv». The Conference was organized by State Administration of Railway Transportation of Ukraine «Ukrzaliznytsa», Chief Administration of Railway Equipment of «Ukrzaliznytsa», SA «Lvovskaya Zheleznaya Doroga», company «Polski Linii Kolijowe», PWI, OJSC «KZESO».

About 50 specialists from Ukraine, Poland, Germany, involved in development and manufacturing of equipment for welding rails, railway track equipment, as well as construction, service and repair of railway tracks, participated in the Conference activities.

Less than a year is left till the moment, when the starting whistle of the first match of European football championship 2012 will be blown. Today the host countries still have quite a lot of work related to development of both hotel-tourist services, and road transport networks, as the motor-roads and railways are a kind of visiting card. That is why their sound upgrading is one of the goals of the entire euro preparation (the more so, since this will be beneficial not only for the present, but also after the football forum is over).

In Ukraine tens of kilometers of motor-roads are laid every year. This, however, is a tiny fraction compared to the work conducted in «Ukrzaliznytsa», as the annual scope of upgrading of the railway bed here reaches four thousand kilometers. «This causes not only surprise, but also white envy» — these were exactly the words, by which R. Fronchek, Director of Rail Track Administration of Polish Railways, who actively participated in the Conference, described the sound upgrading of the Ukrainian track.

According to Ya. Mikitin, Chairman of Administration of «KZESO», the need for such a Conference is dictated by time, as the two countries are preparing for EURO-2012, and both here and over there it is necessary to make rail transportation faster and more comfortable. The more so, since Poland is lagging behind in some respects as regards rail welding. The current requirements to rail welding are on a totally different technical level, and each welded butt joint should have its own certificate, electronic record of welding modes. All this requires more modern technologies and other machines. And the equipment, included into the fleet of Polish Railways, does not meet the current requirements. V. Yakovlev, Chief Engi-



neer of Central Directorate of the Track of «Ukrzaliznytsa», noted that this Conference is not just exchange of experience, but also good schooling for the railroaders of the two neighbouring countries.

The following presentations were made in the Conference: S.I. Kuchuk-Yatsenko and A.V. Didkovsky (PWI) «Modern technologies and equipment for rail welding under the stationary and field conditions»; Ya.I. Mikitin, A.V. Motry, S.V. Dukh («KZESO») «Rail-welding and track machines manufactured by Kakhovka Plant of Electric Welding Equipments»; E. Podymnyak-Fijolek (Railway Bureau, «Polski Linii Kolijowe») «Rails in service in the roads of «Polski Linii Kolijowe»; I. Yasinsky (Diagnostic Center, «Polski Linii Kolijowe») «Requirements for obtaining permission for welding operations performance in Polish railways»; V.A. Yakovlev («Ukrzaliznytsa») «Experience of operations performance in the railways of Ukraine».

Presentations were also made by companies «Rapid», official distributor of Lincoln GmbH (Ger-



many), «Dnepropetrovsky Strelchyny Zavod» (Ukraine), GRAW (Poland), «Spetskran» (Ukraine).

Conference participants were familiarized with the operation of track machines in the main tracks of Lvov Railway. Particularly impressive was demonstration of track welding machines (in Sknyliv station of Lvov main line) manufactured by «KZESO», which is the real proof of effective experience of cooperation of science and production in Ukraine («KZESO» has been working side by side with PWI for more than 50 years). It was exactly where one could see under working conditions one of the most advanced developments of patonovites and Kakhovka Plant staff – K922 machine, which applies tension to rail sections during welding without using 600 m loop, inducing the specified stress level in them with drive upsetting force of 120 t. «Use of such equipment», – Ya. Mikitin maintains, – «enables a cardinal improvement of the technology of construction and reconstruction of the railway tracks, increase of its efficiency, lowering

of operation cost, and, most importantly, ensuring production in Ukraine of continuous welded, so-called velvet rail track. The demonstration has made a lot of impressions also on Polish colleagues, because, as stated by R. Fronchek: «It is not easy to certify a full set of functional equipment having driven it to the Polish railway, as this is extremely expensive. And the process of welding with «KZESO» machines that we saw, is very convincing. I can confidently say that we became interested in it. The more so, as there is still not a single track machine on the roads of Polish railways».

Thus, the main result of the three day scientific-technical Conference is establishment of close cooperation between the railways and enterprises of Poland and Ukraine, which, in its turn, will promote laying a velvet track between the two countries.

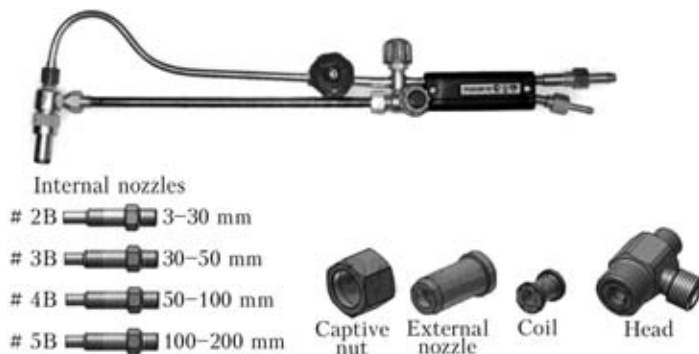
*Ya.M. Mikitin, KZESO,
A.V. Didkovsky, PWI*

NEWS

HAND LIQUID-FUEL CUTTER

Autogenous Equipment Factory «Donmet» (Kramatorsk, Ukraine) offers new Bobukha RK200 hand liquid-fuel cutter (gasoline blow torch) «Vognyk» 182. The novelty is intended for severing of low-carbon steel from 3 to 200 mm thick.

- gasoline of A-76, A-80, AI-91, A-92, A-95 and other grades designed for engines (GOST 2084-77), and gasoline of «Regulyator-91» and «Normal-80» (GOST 51105-97) grades can be used as fuel;
- operation even at a frost of -25°C is possible;



Characteristic features of RK200 cutter «Vognyk» 182:

- absence of asbestos cord and of separate heating flame for evaporation of liquid fuel (gasoline);

- complete combustion of fuel;
- 100 % resistance to back kick;
- reaching the working parameters during 15-30 s;
- length – not more than 555 mm;
- weight – not more than 840 g.